Characterization of NADPH Oxidases in Uterine Smooth Muscle during Pregnancy

A Thesis Submitted to the College of

Graduate and Postdoctoral Studies

For the Degree of Master of Science

Department of Veterinary Biomedical Sciences

University of Saskatchewan

Saskatoon

By

MIKAYLA DAWN WARD WALLER

Permission to Use

In presenting this thesis in partial fulfillment of the requirements for a postgraduate degree from the University of Saskatchewan, I agree that the Libraries of this University may make it freely available for inspection. I further agree that permission for copying of this thesis in any manner, in whole or in part, for scholarly purposes may be granted by the professor or professors who supervised my thesis work or, in their absence, by the Head of the Department or the Dean of the College in which my thesis work was done. It is understood that any copying or publication or use of this thesis or parts thereof for financial gain shall not be allowed without my written permission. It is also understood that due recognition shall be given to me and to the University of Saskatchewan in any scholarly use which may be made of any material in my thesis.

Requests for permission to copy or to make other uses of materials in this thesis in whole or part should be addressed to:

Head of Veterinary Biomedical Sciences
Western College of Veterinary Medicine
52 Campus Drive
Saskatoon, Saskatchewan S7N 5B4 Canada

OR

Dean
College of Graduate and Postdoctoral Studies
University of Saskatchewan
116 Thorvaldson Building, 110 Science Place
Saskatoon, Saskatchewan S7N 5C9 Canada

Abstract

During gestation, the uterine smooth muscle, or myometrium, transforms from a quiescent tissue to a contractile muscle required for parturition. Immune system activation is a crucial precursor to labour during which the myometrium is infiltrated by immune cells. Immune and myocyte activation rely on signal transduction via oxidation-reduction reactions and generation of reactive oxygen species (ROS). Nicotinamide adenine dinucleotide phosphate oxidases (Nox) are proteins responsible for the transport of electrons across biological membranes. It was hypothesized that Nox proteins and their regulatory subunits would be readily expressed in the rat myometrium during pregnancy to help prepare the tissue for parturition. Using rat myometrial tissue collected from pregnant rats throughout gestation, an immortalized human myometrial cell line, as well as immunoblot and immunofluorescence analyses, the spatial and/or temporal expression pattern of Nox1, Nox4, as well as their regulatory subunits NoxO1, NoxA1 and p22phox were examined, including possible regulation by uterine distension and inflammation. Nox1 was prominently localized to myocyte cytoplasm, with some plasma membrane association, and significantly expressed during the contractile and labour phases. NoxO1 was similarly expressed during these periods and was observed to have a general cytoplasmic staining pattern in situ. Nox4 was prominently localized in peri-nuclear regions, again with some plasma membrane association, and significantly expressed during the proliferative and synthetic phases. p22phox was similarly expressed during both phases while NoxA1 expression was only elevated during the proliferative phase. Stimulation of inflammation in hTERT-HM cells using the pro-inflammatory cytokine IL-1β only induced Nox1 expression in hTERT-HM cells while uterine distension did not significantly affect expression of any Nox enzyme or subunit examined. It is speculated that Nox1 could form signaling platforms during late pregnancy and labour at caveolae to help prime the uterine contractile apparatus prior to labour while Nox4 could participate in cellular signaling events that lead to myometrial proliferation during early pregnancy. This study was the first to methodically characterize the expression of Nox1 and Nox4 enzymes as well as their regulatory subunits in the rat myometrium throughout gestation. The results highlight the potential importance of these proteins in the myometrium for pregnancy and parturition.

Acknowledgements

Firstly, I would like to thank my supervisor and mentor Dr. Daniel MacPhee for the opportunity to participate in the ongoing research conducted by the MacPhee lab to uncover the mechanisms behind preterm labour. I would also like to thank him for sharing his academic expertise as well as his guidance and support over the past two years. Thank you for keeping me track and not letting my procrastination get the best of me! Thank you to Dr. Ewa Miskiewicz for teaching me proper laboratory techniques as well as your assistance with numerous experiments. You were an invaluable source of knowledge regarding all things lab related.

I am thankful to have been able to share this experience with my labmate and friend, Georgia Bailey. You were always there to help with experiments, share teaching responsibilities or go grab a coffee. The past two years would have been much more difficult without you by my side! Thank you to my graduate committee Dr. Ali Honaramooz, Dr. Suraj Unniappan and Dr. Carlos Carvalho for your ideas, feedback and time contributed to my studies. Thank you to Cindy Pollard for all your help with everything admin related as well as for your excellent planning and organizational skills.

Thank you to my fellow graduate students for the good times shared both on and off campus as well as the opportunity to assist with your individual research projects. I met many new people throughout my degree and am thankful for the friendships gained. Thank you to the College of Graduate and Postdoctoral Studies for the scholarly assistance. Thank you to the Western College of Veterinary Medicine, the Department of Veterinary Biomedical Sciences as well as the Department of Biology for the teaching opportunities. And last but not least, a huge thank you to my family and friends for the endless love and support throughout my educational career.

Table of Contents

List of Tables

List of Figures

List of Abbreviations

Ang II - angiotensin II
AT_1R - G protein-coupled angiotensin II type 1 receptor
Bcl-2 - B-cell lymphoma-2
BLAST - basic local alignment search tool
BM - basement membrane
BrdU - bromodeoxyuridine
CAPs - contractile-associated proteins
CASP - caspase
Cat # - catalogue number
CM - circular muscle
CYBA - cytochrome B-245 alpha chain
Cx - connexin
D - day
DAPI - 4′,6-diamidino-2-phenylindole
Duox - dual oxidase
E - endometrium
EC - enzyme commission
ECM - extracellular matrix
EDTA - ethylenediaminetetraacetic acid
EGFR - epidermal growth factor receptor
ER - endoplasmic reticulum
FA - focal adhesions
FAD/H_2 - flavin adenine dinucleotide
FAK - focal adhesion kinase
FITC - fluorescein isothiocyanate
FBS - fetal bovine serum
G - gravid
GAPDH - glyceraldehyde 3-phosphate dehydrogenase
GP - glycoprotein
GPCRs - G protein-coupled receptors
Hic-5 - hydrogen peroxide inducible clone-5
HPA - hypothalamic-pituitary-adrenal
HRP - horseradish peroxidase
HSA - human serum albumin
hTERT-HM - human telomerase reverse transcriptase-human myometrial cells
IGF - insulin-like growth factor
IGFBP - insulin-like growth factor binding protein
IB - immunoblot
IF - immunofluorescence
IL - interleukin
KOX - zinc finger protein
L - lumen
LM - longitudinal muscle
LPS - lipopolysaccharide

M - myometrium
MCP-1 - monocyte chemoattractant protein-1
MOX - mitogenic oxidase subunit
NADPH - nicotinamide adenine dinucleotide phosphate
NG - non-gravid
NK - natural killer
NOH - NADPH oxidase homolog
Nox - NADPH oxidase
NoxA1 - Nox activator 1
NoxO1 - Nox organizer 1
NP - non-pregnant
O - ovary
Ovd - oviduct
P/S - penicillin/streptomycin
PBS - phosphate-buffered saline
Phox - phagocytic NADPH oxidase
PM - plasma membrane
Poldip2 - polymerase (DNA-directed) delta interacting protein 2
PP - 1-day post-partum
PPROM - preterm premature rupture of the membranes
PR - progesterone receptor
PRR - proline rich region
PTB - preterm birth
qPCR - quantitative polymerase chain reaction
Redox - oxidation-reduction
RENox - recombinant human Nox
RIPA - radio-immunoprecipitation assay
ROK - rho-associated kinase
ROS - reactive oxygen species
RRX - rhodamine-red-X
RT-PCR - reverse transcriptase polymerase chain reaction
S - serosa
SDS - sodium dodecyl sulfate
SDS-PAGE - sodium dodecyl sulfate-polyacrylamide gel electrophoresis
SGA - small for gestational age
SH3 - Src homology 3
SNX - sorting nexin-28.
TBST - tris-buffered saline plus Tween
TGF - transforming growth factor
TNF-α - tumor necrosis factor-α
TPR - tetratricopeptide repeats
TUNEL - terminal deoxynucleotidyl transferase dUTP nick end labeling
UB - uterine body
UH - uterine horn(s)
VSMC - vascular smooth muscle cells

1. Introduction

1.1. Preterm Birth

The World Health Organization defines preterm birth (PTB) as delivery of an infant prior to 37 weeks of gestation. Preterm birth can be further divided into three sub-categories based on gestational age: extremely preterm (<28 weeks), very preterm (28-32 weeks) and moderate to late preterm (32-37 weeks) (WHO, 1977). In 2014, 8% of pregnancies in Canada resulted in PTB, with most babies being delivered between 32 and 36 weeks (PHAC, 2017). Most preterm infants are born being small for gestational age (SGA), meaning they weigh less than 90% of babies of the same gestational age and sex, leaving them at a higher risk for mortality and morbidity (Lim et al. 2009). Preterm and SGA babies require special postnatal care and monitoring, and on average, remain in hospital for longer than full-term infants. Additionally, preterm babies require the use of more hospital resources such as specialized equipment (monitors, respirators, dialysis pumps) and highly trained healthcare personnel resulting in increased healthcare costs (Cuevas et al. 2005). PTB alone was estimated to cost the Canadian health care system over $8 billion per year (Lim et al. 2009).

PTB is a multifactorial syndrome which can be categorized into three broad groups: (1) Spontaneous: PTB following spontaneous preterm labour with intact membranes, (2) PPROM: PTB following preterm premature rupture of the membranes (PPROM), and (3) Indicated: provider-initiated PTB for maternal or fetal indications (Tucker et al. 1991). Approximately 40-45% of PTB are spontaneous, 25-30% are due to PPROM and the remaining 30-35% are indicated (Goldenberg et al. 2008). These rates vary between countries and may be influenced by many factors including maternal demographic, ethnicity, pregnancy history and nutritional status.

The onset of labour is a precisely controlled mechanism that is still poorly understood but requires the initiation of two separate but integrated pathways to induce activation, and thus contractility, of the myometrium. In approximately half of all spontaneous PTB cases, the exact cause of myometrial activation is unknown (Menon, 2008). There are many well established risk factors of PTB including individual and family history of PTB, maternal nutritional status, body-mass index, age, reduced pregnancy intervals (>6 months), multiple pregnancy, uterine, cervical and placental abnormalities, and maternal infection (Tamura et al, 1992; Smith et al. 2003;

Hendler et al, 2005; Goldenberg et al. 2008). However, the role that each risk factor may play or how multiple factors may compound a woman's risk for PTB remains unknown. As further research is conducted on PTB and PPROM, additional risk factors continue to be identified.

The determination of risk factors and potential biochemical markers associated with PTB is important not only for the health of mother and baby but also for the medical community. The benefit of defining PTB risk factors and markers would be threefold, as discussed by Goldenberg et al. (2005). Firstly, defining risk factors or biochemical markers may highlight mechanisms involved in PTB. Secondly, properly identifying at-risk women may provide the opportunity to study PTB intervention techniques and lastly, identifying at-risk women early would allow physicians to implement a treatment plan unique to the risk of each patient. Despite the numerous risk factors already identified, the mechanisms underlying PTB remain largely unknown. A limitation in identifying PTB risk factors is the large overlap with risk factors associated with pregnancy itself and other common side effects such as hypertension, preeclampsia and gestational diabetes.

The search for a biochemical marker which may predict PTB has proven to be a challenge for researchers. Many biological samples have been tested such as cervical and vaginal fluids, amniotic fluid, plasma, saliva and urine (Goldenberg et al. 1996; Gray et al. 1992; McLean et al. 1999; Andrews et al. 2000; Ramsey and Andrews, 2003). Each sample has its own advantages and disadvantages with regards to collection and efficacy of PTB prediction with no one sample presiding over the others (Goldenberg et al. 2005). For example, saliva samples are easy to collect with minimal risk and discomfort to the patient, but levels of putative biochemical markers, such as estriol, may fluctuate over time and may interact with concurrent medications (McGregor et al, 1999). Additionally, there is limited clinical utility for a PTB prediction marker as there are no current treatments to prevent PTB.

1.2. Challenges of Labour in Rural Settings

Canada is the world's second largest country, geographically, covering more than 9.9 million square kilometers (Statistics Canada, 2009b). Despite the large land mass that Canada boasts, the majority of Canadians reside within urban areas with only 18% of the population living in rural settings defined by Statistics Canada (2009a) as a population of less than 10,000 persons. Since urban areas host most of the population, the majority of professional services, such as medical

clinics and hospitals, are also located in these areas. Regionalization of essential medical services leaves rural areas with little to no access; thus, rural residents have to travel great distances to gain access to medical professionals. In most health regions across Canada, more than 20% of hospital births involve women living in rural areas with a greater percentage (>60%) of births by rural women occurring in central and northern Canada (Figure 1.1). In 2013, the four provinces with the highest percentage of births involving rural women were Nunavut (where there are no areas considered urban) Newfoundland and Labrador, Saskatchewan and Manitoba (CIHI, 2013).

The ability of rural women to deliver in facilities close to home is largely dependent on the services and facilities available as well as the number of staff with obstetric training. In communities where medical services are available, most facilities can handle low-risk pregnancies, but if complications arise the patients must be transferred elsewhere. Most rural women (67%) deliver in urban hospitals and must travel great distances prior to delivery, with some women travelling more than 2 hours (17%) and 40.5% of women travelling more than one hour (CIHI, 2013). This travel time is vastly different from most urban women (90%) who travelled 30 minutes or less to their birthing destination (CIHI, 2013). Long distance travel to urban hospitals has both financial and emotional impacts on women and their families. Some travel costs may not be covered by provincial health care plans, pre- and postnatal complications may lengthen time spent away from family, and women must often travel alone to a foreign place during an already stressful period of time. Thus, a biochemical marker capable of predicting impending PTB and/or normal parturition within an accurate and more specific timeframe would be a significant advance for women's health, particularly in rural settings where physiological, psychological, economical, and social burdens are often high. Such a marker would also give physician teams ample notice to prepare for the arrival of a term or preterm infant and would lessen the risk of neonatal health problems associated with delay of care.

Figure 1.1 A geographical map of Canada representing rural deliveries as a percentage of all deliveries. Data are presented by Health Region and selected provinces/territories. Data excludes Quebec and was collected between 2007-2008 and 2011-2012. Figure used with permission from CIHI, 2013, see Appendix A.

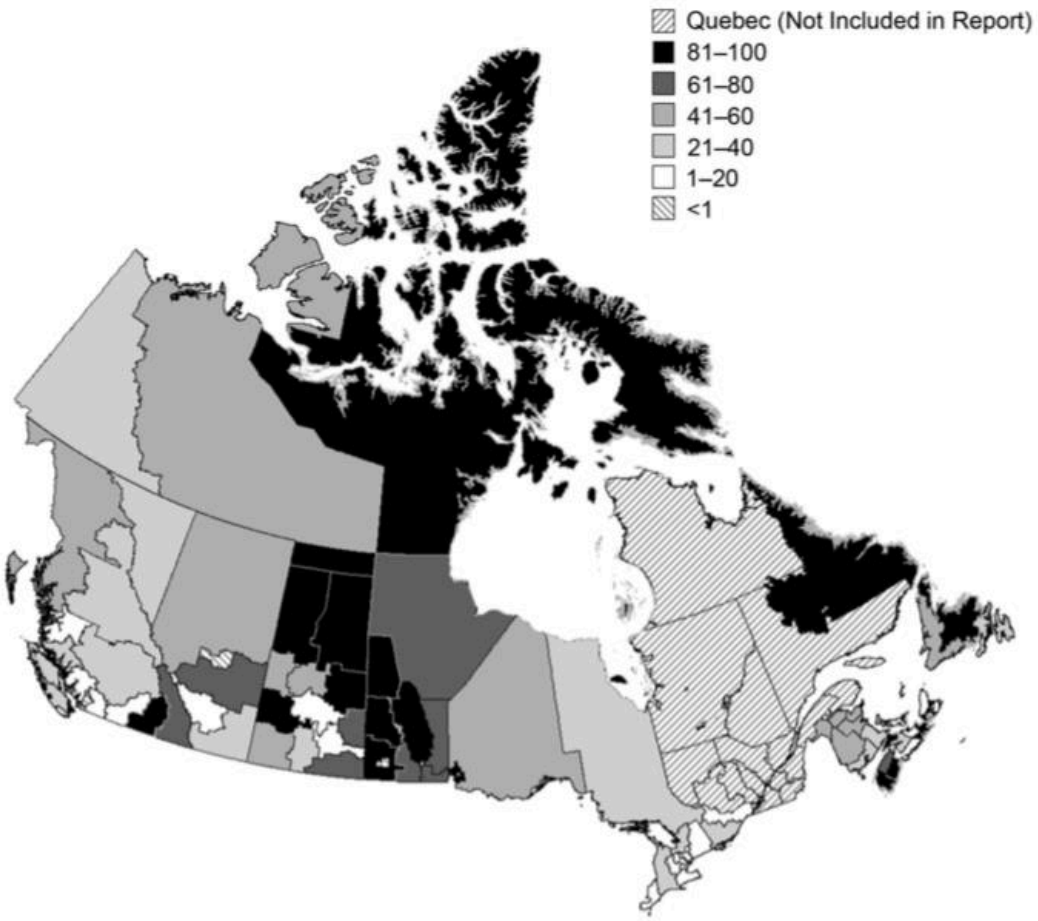
Quebec (Not Included in Report)
81–100
61–80
41–60
21–40
1–20
<1

The exact integrated mechanisms underlying normal parturition and PTB remain poorly understood and pose many clinical, investigative and economic challenges for doctors, researchers and families around the world. This information highlights why it is important to understand the basic mechanisms of normal pregnancy and labour and to build the scientific knowledge foundation necessary for discovering a reliable predictor of labour and PTB and ways to therapeutically treat the latter syndrome.

1.3. Uterine Anatomy

Human females have a pear-shaped simplex uterus that is derived from the paramesonephric (Müllerian) ducts *in utero* (Gondos, 1985; Figure 1.2). Uterine size can vary between individuals based on hormonal status, age, previous pregnancies and the presence of leiomyomata or uterine fibroids (Verguts et al. 2013). A single cervix protrudes into the vagina with prominent anterior and posterior fornices. The human myometrium consists of interwoven bundles of smooth muscle supported by dense connective tissue containing fibroblasts and interstitial telocytes (Cretoiu et al. 2013; Figure 1.3). The smooth muscle of the myometrium is spontaneously active and is able to produce synchronous contractions without nervous input (Wray and Arrowsmith, 2012). This syncytium is possible through the linking of myocytes via gap junctions which allow the passage of action potentials to adjacent cells (Young, 2007). Externally, the myometrium is surrounded by the perimetrium, a layer of serosa/adventitia. Internal to the myometrium lies the endometrium, consisting of three layers: stratum compactum, stratum spongiosum and stratum basalis. It is this layer, the endometrium, that undergoes a series of histological changes during the menstrual cycle to prepare for the potential implantation of an embryo (Dallenbach-Hellweg, 1981).

Due to the limitations of human studies, animal models are often implemented to replicate human physiology. Rats and mice have been widely accepted as models for reproductive science studies related to humans due to the similarities observed in placentation strategies (Soares et al. 2012). These rodent species are easy to maintain, offer short growth and gestational periods, and have genetics that are easily manipulated (e.g. knockout mice), making them an ideal animal model for studying pregnancy with relevance to human reproduction (Bezold et al. 2013). While these animals do share many similarities to humans, there are a few key anatomical differences that must be considered when comparing rats to humans.

Figure 1.2. Schematic diagrams of the human and rat uterus. UB, uterine body; UH, uterine horn(s), O, ovary; Ovd, oviduct.

Human

Rat

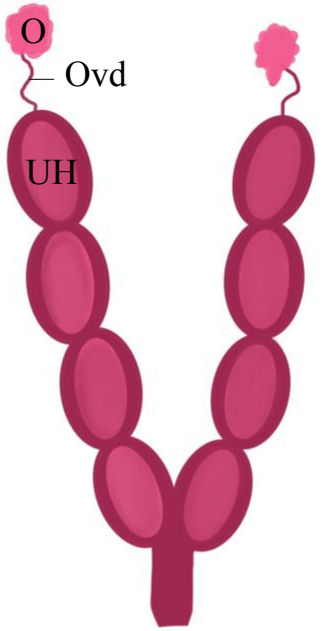

Figure 1.3. Schematic cross-sectional diagrams of human and rat uteri. S, serosa; M, myometrium; LM, longitudinal muscle; CM, circular muscle; E, endometrium; L, lumen.

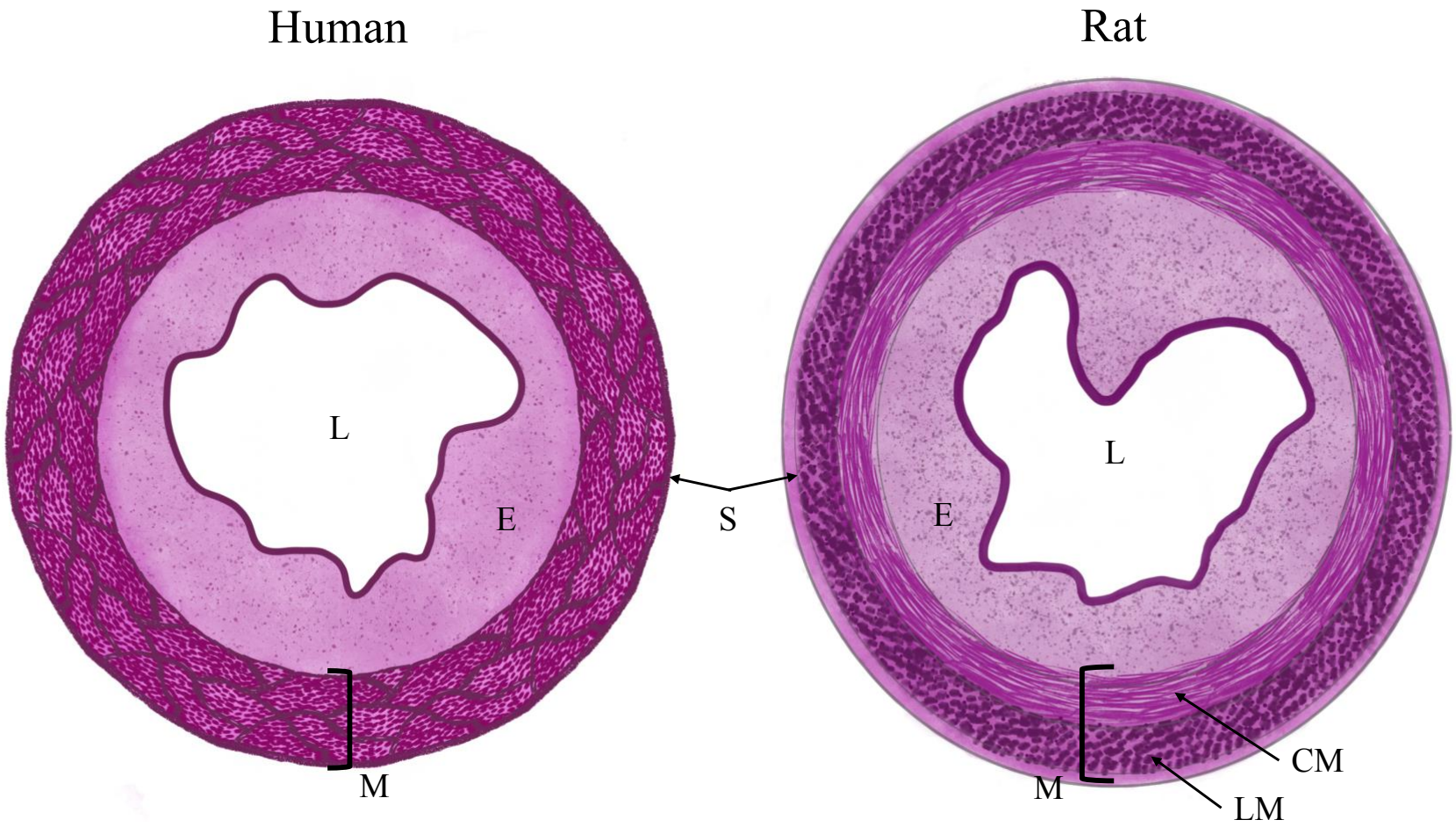
Human
Rat
L
E
M
S
L
E
M
CM
LM

Rats have a bicornuate uterus with two separate lateral horns which are partially fused caudally (Figure 1.2). Due to the partial fusion of the uterine horns, rats do not have a true uterine body. A single cervix protrudes into the uterus with two distinct canals for each uterine horn. The walls of the cervix and vagina are continuous both dorsally and ventrally but extend laterally to form deep fornices on either side. Rodent myometrium is composed of an inner circular layer and an outer longitudinal layer of smooth muscle separated by loose connective tissue of fibroblasts, telocytes and blood vessels called the stratum vasculosum (Bengtsson et al. 1984; Figure 1.3). The morphology of the endometrium changes depending on the stage of the estrous cycle; however, not as drastically as observed in humans.

1.4. Myometrial Programming

During pregnancy, the uterus undergoes substantial physical and biochemical changes (Shynlova et al. 2009a). The myometrium must transform from a rather quiescent tissue to a responsive, contractile muscle required for labor and parturition. This transformation has been well defined in the pregnant rat model and occurs in five distinct phases: four throughout gestation and one post-partum (Figure 1.4).

The first phase of myometrial differentiation is the proliferative phase, occurring from day (D) 1 (designated by observation of vaginal plug) to D14 in the rat. Implantation of the embryo(s) and maternal recognition of pregnancy are essential for continuation of the pregnancy and are the hallmark beginning of this phase. Insulin-like growth factor-I (IGF-I) plays a central role during this implantation window and alterations in IGF-I expression may contribute to early embryonic loss (Katagiri et al. 1996). The proliferative phase is characterized by hyperplastic growth of uterine myocytes. Such growth was detectable through Bromodeoxyuridine (BrdU) immunostaining of myometrial tissue with the highest rate of BrdU incorporation, indicative of cellular growth, occurring at D6 (Shynlova et al. 2006). The rate at which the circular and longitudinal muscular layers proliferate is not the same, and BrdU incorporation in myocyte nuclei within these layers determined that the longitudinal layer was more proliferative during this time (Shynlova et al. 2006). Quantitative polymerase chain reaction (qPCR) analysis of IGF ligands was conducted to determine the role these genes may play in myometrial proliferation and differentiation (Jones and Clemmons, 1995). Increased mRNA levels of IGF-I and its binding protein, IGF binding protein-1 (IGFBP-1), were found during this phase with levels

Figure 1.4 The preprogrammed pattern of myometrial phenotypic transformation seen throughout gestation. This cycle of transformation includes (1) a proliferative phase involving myocyte hyperplasia, (2) a synthetic phase involving myocyte hypertrophy, (3) a contractile/labour phase involving myometrial activation, and (4) a post-partum involution phase associated with apoptosis and wound repair.

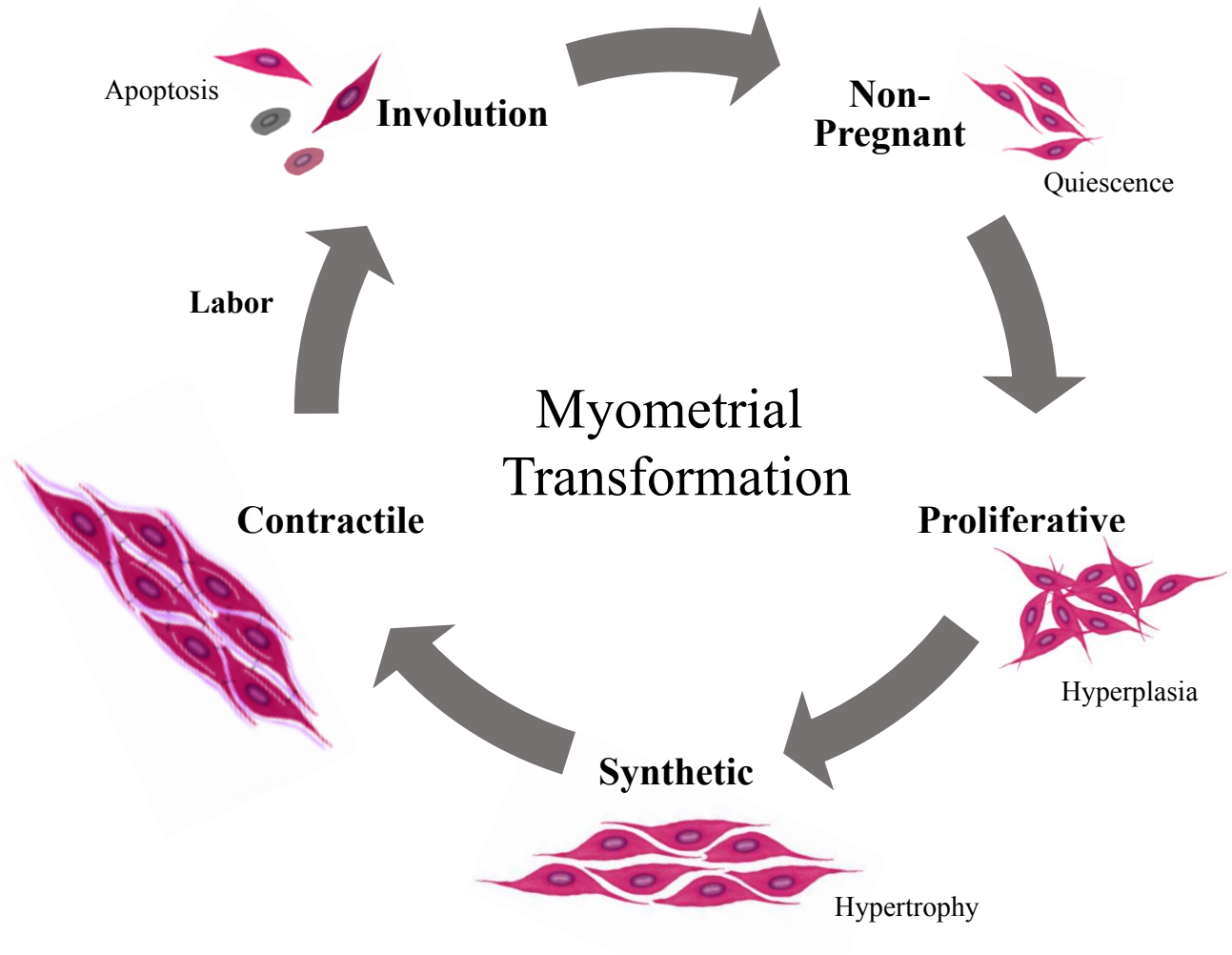
Myometrial Transformation
Apoptosis
Involution
Non-Pregnant
Quiescence
Proliferative
Hyperplasia
Synthetic
Hypertrophy
Contractile
Labor

peaking at D12 (Shynlova et al. 2007). In superovulated rats, levels of IGF-I were elevated and levels of IGFBP-1 were diminished from D0-3 of gestation resulting in a hostile uterine environment and increased early embryonic loss, suggesting these proteins influence the proliferation of uterine myocytes, but also may impact the uterine environment (Katagiri et al. 1996). The uterine IGF system contributes to the overall proliferation of uterine myocytes during this phase along with increased expression of other anti-apoptotic factors. Immunoblot analysis of rat myometrial lysates showed increased expression of apoptosis-regulating protein B-cell lymphoma (Bcl-2) as well as cell replication marker proliferating cell nuclear antigen during the proliferative phase (Shynlova et al. 2006).

During the transition from the proliferation phase to the following synthetic phase, a switch in myometrial phenotype occurs. After D15 of gestation, myometrial cells switch from hyperplastic growth to hypertrophic growth. Hypertrophy can be characterized by an increase in DNA:protein ratio, a commonly used biological marker (Winick and Noble, 1965). Enlargement of individual myocytes accounts for most of the growth seen, with some growth occurring in the nucleus and within organelles, such as mitochondria (Gabella, 1990). There is also evidence that a stress-induced, intrinsic apoptosis cascade is activated during the transition from proliferative to synthetic phases. Transient induction of the Caspase (CASP) 9 pathway and its downstream caspases, CASP3, CASP6 and CASP7, was confirmed by Western blot analysis of myometrial lysates from D12-15 of gestation; however, upregulation of Bcl2-like, a potent anti-apoptotic protein, also took place during this time and TUNEL assays confirmed no myometrial apoptosis was occurring (Shynlova et al. 2006). Shynlova and colleagues (2006) hypothesized that the stress-induced apoptotic pathway did not stimulate programmed cell death but rather halted myometrial proliferation and promoted differentiation required later for synchronized uterine contractions.

In addition to hypertrophic growth of individual myocytes, there is also increased synthesis and deposition of extracellular matrix (ECM) components during the synthetic phase (Shynlova et al. 2009a). Increased expression of ECM proteins such as elastin, procollagen I, procollagen II and fibronectin aid in formation of the interstitial matrix (Shynlova et al. 2004). Growing myocytes remain connected to the ECM through structures called focal adhesions (FA). These clusters of integrin receptors lie within the cell membrane and facilitate muscle-ECM connections that promote myometrial growth and development of mechanotransduction

(MacPhee and Lye, 2000). For muscle-ECM connections to remain viable during this period of growth, significant FA remodelling must take place. Remodelling of muscle-ECM connections is indicated by increased expression of focal adhesion kinase (FAK), an enzyme known for its role in FA turnover, from D15 of gestation until parturition (MacPhee and Lye, 2000). Altered expression of integrin subunits in the myometrium is also seen during gestation. A significant increase in mRNA expression of subunits $\alpha 1$ and $\beta 1$ was seen throughout gestation, D6-23, and increased mRNA expression of subunits $\alpha 3$ and $\alpha 5$ was observed after D14 and D17, respectively (Williams et al. 2005; Williams et al. 2010).

This adaptation of the uterus is influenced by two different mechanisms: firstly, by the hormonal profile of pregnancy and secondly by the mechanical distension from the growing fetuses. Progesterone is the major hormone involved in maintaining pregnancy through the suppression of inflammatory pathways which promotes uterine quiescence (Keelan, 2016). Additionally, progesterone promotes uterine growth and matrix synthesis (Shynlova et al, 2009a). A decrease in progesterone during gestation, either endogenously (ie systemically) at term in rats or through the administration of progesterone receptor agonist, RU486, on D19 resulted in decreased expression of ECM proteins (Shynlova et al, 2004). The mechanical distention caused by growing fetuses also plays a role in regulating uterine growth and ECM formation. Shynlova et al. (2004) compared uterine horns in unilaterally pregnant rats and observed no myocyte hypertrophy and significantly reduced expression of elastin, procollagen I and II, in non-gravid uterine horns compared to gravid horns, despite being under the same hormonal control.

Following the synthetic phase is a relatively short contractile phase from D21-23. During this period, synthesis of interstitial matrix components slows and increased synthesis of basement membrane (BM) components begins (Shynlova et al. 2009a). This switch in matrix protein synthesis is attributed to falling circulating levels of progesterone in rats as labour nears term. Shynlova et al. (2004) found that the administration of RU486, a progesterone receptor antagonist, on D19 induced a premature switch from interstitial ECM to BM components and induced preterm labour within 24 hours. Preventing the fall in circulating progesterone levels, by exogenous hormone injection, also prevented the switch in matrix protein synthesis and subsequent labour on D23 (Shynlova et al. 2004). Uterine distension also regulates the expression of BM components with increased expression of laminin $\beta 2$ and collagen IV,

confirmed via immunoblot analysis, only occurring in gravid uterine horns (Shynlova et al. 2009b). Additionally, decreased expression of activated FAK late during this phase suggests that myocyte-ECM adhesions become stabilized in preparation for labour (MacPhee and Lye, 2000).

During the final phase of gestation, the myometrium once again switches its phenotype; this secondary switch has been termed activation. Myometrial activation occurs as the result of increased expression of contractile-associated proteins (CAPs) and requires the triggering of a mechanical pathway and an endocrine cascade (Challis et al. 2002). Although separate, these two pathways integrate at FA sites (MacPhee and Lye, 2000). Focal adhesions serve as organizational hubs for regulatory and structural proteins, including integrins, FAK and paxillin, to orchestrate complex cellular functions and facilitate signal transduction required for coordinated contractions (Ushio-Fukai, 2009). Integrin subunits $\alpha 1$, $\alpha 3$, $\alpha 5$ and $\beta 1$ localize to myocyte membranes and exhibit increased mRNA expression during this time, likely contributing to the development of a mechanical syncytium (Williams et al. 2005; Williams et al. 2010).

The activation of both the endocrine and mechanical pathways are thought to be triggered by the fetal genome (Gibb et al. 2006). The maturation of the fetal hypothalamic-pituitary-adrenal (HPA) axis near term results in increased fetal adrenal cortisol production which stimulates the endocrine cascade and the fully-grown fetus causes uterine tension which activates the mechanical pathway (Gibb et al. 2006). Increased fetal HPA function results in maternal endocrine alterations, such that previously high levels of circulating progesterone begin to fall and estrogen levels, especially 17ß-estradiol, being to rise (Lye at al. 1993). The fall in progesterone removes the quiescent block that was in place and the rise in 17ß-estradiol promotes the expression of CAPs, both contributing to myometrial activation (Neulen and Breckwoldt, 1994). These hormonal changes are seen in most mammalian species, with the exception of humans. Human studies have reported high levels of circulating progesterone during late gestation and into labour (Boroditsky et al. 1978). The initiation of parturition in humans occurs through a functional progesterone withdrawal as opposed to the systemic withdrawal characteristic of other animals, including rodents (Golightly et al. 2011; Menon et al. 2016). As human gestation near term, there is a switch in the expression of progesterone receptor (PR) isoforms, specifically an increase in the expression of PR type A relative to PR type B (Mesiano et al. 2002). This alteration in PRs has a refractory effect on the myometrium and

suppresses the “pro-gestation” effects of progesterone (Mesiano et al. 2002; Mesiano et al. 2011).

Rising 17ß-estradiol levels promote synchronous uterine contractions through increased expression of CAPs, such as connexin (Cx)-43, oxytocin receptors, and prostaglandin receptors as well as prepares the uterus to respond to uterotonins such as prostaglandins and oxytocin (Lye et al. 1993; Ou et al. 1998; Al-Matubsi et al. 2001; Challis et al. 2002; Golightly et al. 2011). The formation of gap junctions is only observed just prior to, during and immediately after labour and connects individual myocytes both electrically and chemically, allowing the uterus to contract as a single unit for successful parturition (Garfield et al. 1978). Uterine stretch also influences the expression of CAPs, with significantly increased expression of Cx-43, Cx-26 and oxytocin receptors only seen in gravid horns of unilaterally pregnant rats (Ou et al. 1997; Ou et al. 1998). Once again, human gestation does not follow this hormonal pattern. Estrogen levels remain high throughout gestation with no significant differences prior to or during active labour (Boroditsky et al. 1978). The pro-labour effects of estrogens such as 17β may be initiated through a functional estrogen activation, similar to that seen with progesterone (Golightly et al. 2011). In labouring human myometrium, expression of estrogen receptor-α is elevated as compared to non-labouring myometrium samples (Mesiano et al. 2002).

Post-partum involution is the fifth and final phase of myometrial differentiation. Upon shedding of the placenta, the uterus must once again transform to return to the non-pregnant state and complete the reproductive cycle. Involution is a process similar to wound healing that includes tissue reorganization, ECM degradation and apoptosis (Shynlova et al. 2009a). Immediately following parturition, expression levels of IGF-I and IGFBP-5 rise, as determined by real time-qPCR (Shynlova et al. 2007). These growth factors have been implicated in the involution of other tissues, including mammary glands, and are thought to promote mitogenesis (Hakuno and Takahashi, 2018). Tissue infiltration by immune cells is another marker of involution. Increased post-partum expression of monocyte chemoattractant protein-1 (MCP-1), a proinflammatory cytokine, aids in attracting immune cells such as monocytes, leukocytes and macrophages where they participate in decidual breakdown (Shynlova et al. 2008). Uterine immune cells are not only important for post-partum involution but also during menses where they facilitate breakdown and shedding of the endometrium (Salamonsen and Lathbury, 2000).

1.5. Immunological Transformation

It has long been thought that pregnancy is a time of maternal immunological weakness, where a suppressed maternal immune system leaves the mother at high risk of infectious diseases; however, pregnancy is arguably the most important life stage for the survival of a species and it is crucial that both mother and baby are protected (Mor et al. 2011). Thus, pregnancy represents a unique immune condition where the maternal immune system is modulated, not suppressed, and continues to prevent damage and infection to both mother and fetus (Mor et al. 2011). During gestation, the maternal immune system is characterized by a reinforced network of communication and repair as well as by modified responses to the environment due to the developing fetal immune system (Cardenas et al. 2010).

Similar to the transformation seen in the myometrium during pregnancy, the immune system also transforms throughout gestation. Shynlova and colleagues (2013a) found that the phases of immunological transformation occur in parallel to the changes seen in myometrial phenotype. Immunological transformation occurs in four distinct phases, three throughout gestation and one post-partum (Figure 1.5). The first phase of immunological transformation, termed initiation, begins during implantation and placentation/decidualization. Embryo implantation is the first critical process of pregnancy establishment and can only occur in a receptive uterus. In humans, the uterus becomes receptive during the mid-secretory phase (D12-24) of the menstrual cycle and in rodents the uterus becomes receptive four days after mating (Navot et al, 1991). For successful implantation, the blastocyst must break the epithelial lining of the uterus, invade the endometrial tissue and replace maternal endothelium with trophoblast cells (Dekel et al. 2010). Implantation resembles an 'open wound' and requires a strong proinflammatory response. Invading trophoblast cells are able to initiate an inflammatory response through a three-stage process: 1) attraction, 2) education and 3) response (Mor and Koga, 2008). During placentation, there is a high number of uterine natural killer (NK) cells present (Williams et al. 2009). These NK cells regulate trophoblast invasion and the induced inflammatory response through the secretion of select cytokines, such as interleukin (IL)-8 and interferon-inducible protein-10 (Hanna et al. 2006). Secretion of these cytokines, as well as IL-6, tumor necrosis factor-α (TNF-α), and chemokines, growth-related oncogene-α and MCP-1 from NK and trophoblast cells attract monocytes to the implantation site (Fest et al. 2007).

Figure 1.5. Phases of maternal immunological transformation throughout gestation. This transformation includes (1) an initiation phase involving implantation, placentation and a pro-inflammatory response with increased expression of cytokines IL-6, IL-8, TNF-α and MCP-1, (2) a tolerance phase where mother, fetus and placenta are symbiotic, (3) an activation/labour phase involving immune cell influx and localized inflammation caused by dropping levels of progesterone and increased expression of IL-6, IL-8, TNF-α, MCP-1 and IL-1β, and (4) a pro-inflammatory involution phase characterized by increased expression of IL-3, IL-4, IL-12, TNF-α, MCP-1 and IL-1β. IL, interleukin; MCP-1, monocyte chemoattractant protein-1; TNF-α, tumor necrosis factor α.

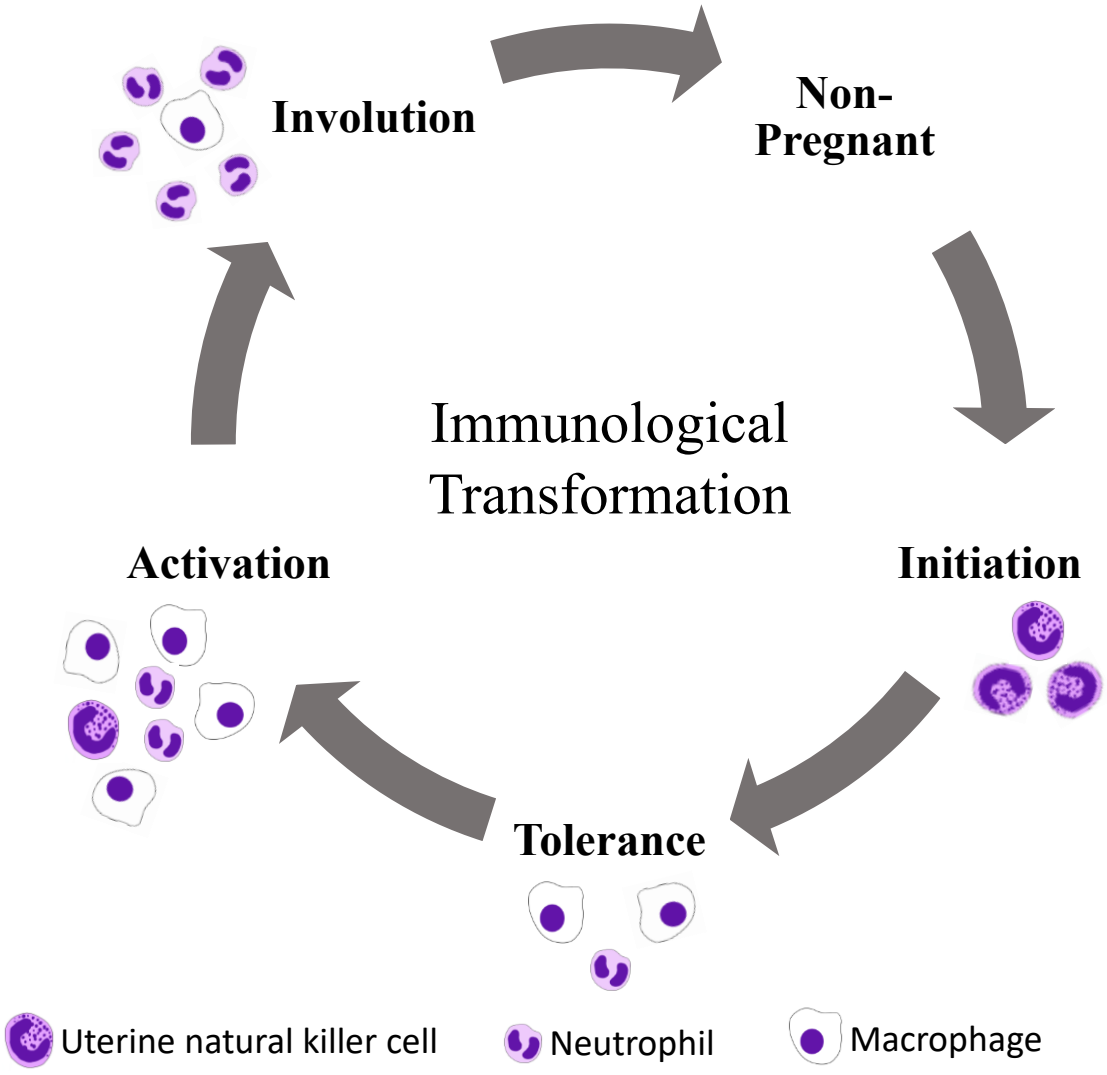
Involution
Non-
Pregnant
Immunological
Transformation
Activation
Initiation
Tolerance
Uterine natural killer cell
Neutrophil
Macrophage

Newly attracted monocytes promote further secretion of IL-6 and MCP-1, from trophoblasts and NK cells, and these regulatory cytokines modulate the evolution of monocytes into macrophages, or the so-called education stage (Fest et al. 2007). Finally, during the response stage, decidual-differentiated macrophages secrete IL-6 and TNF-α which promotes trophoblast growth and completes maternal immune response (Mor and Koga, 2008). Uterine NK cells secrete angiogenic factors, vascular endothelial growth factor and placental growth factor, that promote vascular growth in the decidua to support the growing trophoblast cells (Hanna et al. 2006).

The second phase of immunological transformation is the tolerance phase. This phase is characterized by rapid fetal growth and corresponds with the synthetic phase of myometrial differentiation. The pro-inflammatory response seen during the initiation phase fades and the uterus enters an anti-inflammatory state, allowing the mother, fetus and placenta to act as one symbiotic being. During this time, uterine quiescence is maintained through PR-B mediated anti-inflammatory actions (Tan et al. 2012). Immune cells such as leukocytes and macrophages remove apoptotic and damaged cells as the myocytes undergo hypertrophy and significant uterine remodelling occurs to keep up with the rapidly expanding fetus (Shynlova et al. 2013b; Yang et al. 2019).

During the final phase of gestation, the immune system switches back to an inflammatory response; this phase has been termed immunological activation. Typically, the fetus has developed to term and induction of labour ensues. The timing of labour onset and progression to delivery is the result of a complex process involving inflammatory and hormonal inputs from mother, fetal and placental tissues (Shynlova et al. 2013b). Progesterone is known to regulate uterine quiescence through repressing expression of CAP genes and promoting expression of relaxin (Mesiano et al. 2011). Pregnant rats treated with a progesterone antagonist exhibited preterm labour (Shynlova et al. 2008); thus, a drop in circulating progesterone levels may initiate the labour cascade in rats.

Much like the pro-inflammatory response seen during implantation, the onset of labour is triggered by a localized inflammatory process. The drop in circulating progesterone levels that occurs during late gestation in rats and mice, allows for increased expression of cytokines such as TNF-α, IL-1β, IL-6, IL-12 and MCP-1 in the myometrium (Shynlova et al. 2008; Shynlova et al. 2013a). In humans, increased expression of cytokines IL-6, IL-8 and MCP-1 occurs in the

cervix at term and during spontaneous PTB, despite progesterone concentrations remaining high (Tornblom et al. 2005). Expression of these chemoattractant proteins as well as increased mechanical tension promotes the influx of immune cells, predominantly neutrophils and macrophages, into the myometrium (Romero et al. 2006). Maternal immune cells also infiltrate fetal membranes with increased levels of IL-1β, IL-6 and TNF-α found in the amniotic fluid in women at term labour (Halgunset et al. 1994).

Parturition can be described as a highly orchestrated inflammatory event where both maternal and fetal tissues respond to and produce pro-inflammatory signals (Shynlova et al. 2020). The immunological activation phase corresponds with myometrial activation to achieve successful delivery of the fetus and detachment of the placenta. Myometrial activation ensures myocytes are firmly anchored to the ECM and are able to generate powerful, synchronous uterine contractions (Shynlova et al. 2009b). Adverse labour outcomes, such as PTB are often the result of pre-term activation of either the inflammatory response or myometrial contractions. Increased systemic inflammation is caused by many of the risk factors for PTB and may be a potential explanation for the increased number of PTBs (Goldenberg and Culhane, 2005). Researchers are currently looking into targeting the inflammatory cascade as a novel approach to prevent PTB.

Post-partum restoration is the fourth and final phase of immunological transformation. This phase corresponds with the involution phase of myometrial differentiation and has very similar characteristics. High levels of cytokine and chemokine expression in the myometrium promotes immune cell invasion to produce a localized inflammatory response (Shynlova et al. 2013b). The cytokine expression prolife of post-partum involution is similar to that seen during labour and includes increased expression of TNF-α, IL-1β, IL-12, IL-3, IL-4 and MCP-1 (Shynlova et al. 2013a). It is clear that pregnancy is not a time of immune weakness but rather, a dynamic period where the immune system must swing between pro- and anti-inflammatory phases to ensure survival for both mother and baby.

1.6. NAPDH Oxidases

1.6.1. Form and Function

Nicotinamide adenine dinucleotide phosphate (NADPH) oxidases (Nox) are proteins which are responsible for the transport of electrons across biological membranes. Seven Nox

proteins have been identified in mammals, Nox1 through Nox5 as well as dual oxidase (Duox)1 and Duox2, with Nox5 absent in rats and mice (Holterman et al. 2014). These transmembrane proteins share a similar structure consisting of 1) an NADPH-binding site, 2) a flavin adenine dinucleotide (FAD)-binding region, 3) six transmembrane domains, and 4) four conserved heme-binding histidine residues (Figure 1.6; Bedard and Krause, 2007). Nox5 as well as Duox 1 and 2 have an additional calcium-binding domain located at their N-terminus (Bedard and Krause, 2007). Although the Nox family of enzymes are similar in structure, they differ in their mechanisms of activation. Nox1 though 4 require co-localization with transmembrane protein p22 phagocyte NADPH oxidase (p22phox; CYBA), and various cytosolic subunits, discussed below, while Nox5 and Duox1/2 are activated by Ca^{2+} and do not appear to require cytosolic subunits (Table 1.1; Bedard and Krause, 2007).

Nox proteins are considered one of the two main sources of reactive oxygen species (ROS) generation within the cell, with the other source being the mitochondrial electron transport chain (Roy et al. 2015). To produce ROS, Nox enzymes must first be activated. This activation is achieved through binding of the Nox enzyme to its respective cytosolic subunits and subsequent formation of an active oxidase complex (Petry et al. 2010). Once activated, FAD is reduced to $FADH_2$ via the transfer of an electron from NADPH (Block and Gorin, 2012). An electron from $FADH_2$ is then transferred to the inner heme domain of the Nox enzyme. The heme binding domains are only capable of binding one electron at a time; thus, the first electron must be transferred from the inner heme to the outer heme domain before the second electron can be accepted from FADH (Bedard and Krause, 2007). The donated electrons are used to reduce molecular oxygen, bound to the outer heme, creating a superoxide anion. Superoxide is the main ROS product of Nox1, Nox2, Nox3 and Nox5 (Brown and Griendling, 2009). However, this molecule is unstable in low pH environments and often undergoes dismutation where one superoxide molecule donates its electron to another superoxide molecule, mediated by superoxide dismutase, forming H_2O_2 and O_2 (Day and Suzuki, 2005). Hydrogen peroxide is the ROS product of Nox4, Duox1 and Duox2 (Brown and Griendling, 2009). Block and Gorin (2012) hypothesize that these Nox enzymes are not actually producing H_2O_2 but rather acting as enhancers of the spontaneous dismutation of superoxide to form subsequent H_2O_2.

Figure 1.6. Generalized structure of the core region of NAPDH oxidase (Nox) enzymes. No crystal structures of Nox enzymes are currently available. I-VI, transmembrane domains; FAD, flavin adenine dinucleotide; Fe, iron, NADPH, nicotinamide adenine dinucleotide phosphate. Used with permission from Bedard and Krause, 2007, see Appendix B.

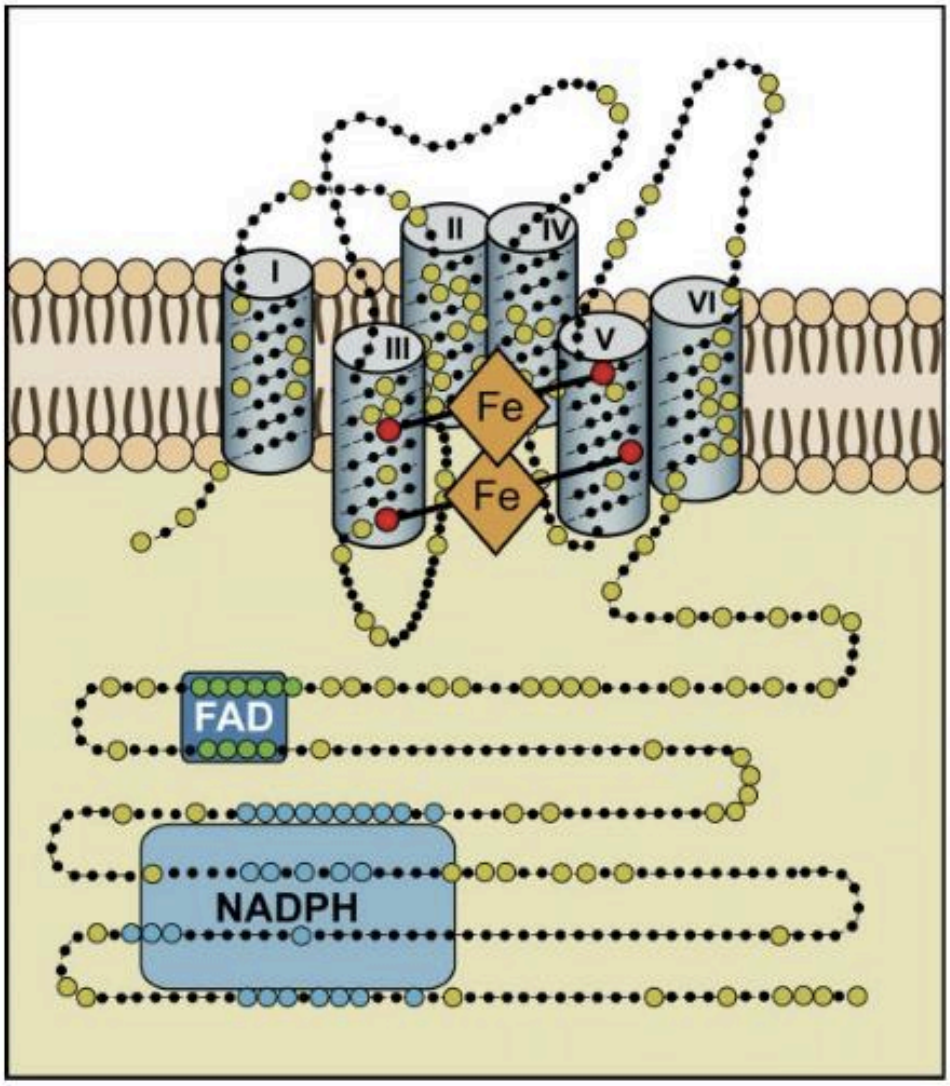
I
II
III
IV
V
VI
Fe
Fe
FAD
NADPH

Table 1.1. General characteristics of Nox family proteins including select tissue expression. Phox, phagocytic NADPH oxidase; VSMC, vascular smooth muscle cells. ? indicates requirement unknown.

	Protein Size	Activation Requirements	Tissue Expression
Nox1	~ 70 kDa ~ 50 kDa	NoxA1, NoxO1, p22phox, Rac1	VSMC, uterus (Suh et al. 1999), placenta (Cui et al.2006)
Nox2	~ 70-90 kDa	p40, p47, p67, p22phox, Rac1	Ovary, placenta, testis (Cheng et al. 2001), skeletal muscle myocytes (Javesghani et al. 2002)
Nox3	~ 64 kDa	NoxA1?, NoxO1, p22phox, Rac1?	Inner ear (Banfi et al. 2004), fetal tissues (Cheng et al. 2001)
Nox4	~67 kDa ~ 65 kDa	p22phox	VSMC (Ellmark et al. 2005), placenta, ovary, skeletal muscle (Cheng et al. 2001)
Nox5	~ 85 kDa	Ca^{2+}	VSMC (Furmanik et al. 2020), uterus, placenta, ovary (Cheng et al. 2001)
Duox1/2	160 kDa	Ca^{2+}	Thyroid (De Deken et al. 2000)

1.6.2. Nox1

Nox1 was the second Nox homolog to be described and is believed to be the product of a recent gene duplication due to the similarity (~60%) to the first discovered Nox, Nox2 (Bedard and Krause, 2007). The Nox1 gene is located on the X chromosome in both humans (Xq22.1) and rats (Xq32; Table 1.2) and contains 14 and 13 exons, respectively. BLAST analysis revealed that human and rat Nox1 proteins share 83% amino acid identity (Appendix C). Western blot analysis of vascular smooth muscle cells (VSMC) identified Nox1 as having two distinct molecular weights, a primary species at 65 kDa and a second at 50 kDa (Hilenski et al. 2004). The secondary band may be due to alternative splicing and several variants have been described in the mouse (Arakawa et al. 2006). Most abundantly expressed in the colon, Nox1 has also been localized to VSMC, uterus, placenta and endothelial cells (Suh et al. 1999; Ago et al. 2005; Cui et al. 2006). Nox1 localizes on the cell surface and requires three subunits: Nox organizer 1 (NoxO1), Nox activator 1 (NoxA1), and p22phox as well as the small GTPase Rac for activation and subsequent superoxide generation (Banfi et al. 2003; Hilenski et al. 2004). Cheng et al. (2006) discovered that Rac form Rac1-GTP (Rac1) significantly induced Nox1 ROS production and in Rac1 inhibited cells, ROS production was reduced by 50% confirming the role of Rac1 as a required activator of Nox1. Best studied in VSMC, Nox1 is growth promoting and expression is upregulated by growth factors such as angiotensin II (Ang II) and platelet-derived growth factor (Lassegue et al. 2001). In Nox1-deficient mice, Ang II-induced proliferation of vascular smooth muscle was conserved but with decreased accumulation of ECM proteins (Gavazzi et al. 2005).

1.6.3. Nox4

Nox4 does not appear to be as highly conserved as its homologue Nox1 and shares only ~39% similarity to Nox2 (Bedard and Krause, 2007). In humans, Nox4 is located on chromosome 11 (11q14.3) and contains 29 exons, while in rats Nox4 is located on chromosome 1 (1q32) and contains 22 exons (Table 1.2). Despite the largely different gene locations, BLAST analysis confirmed that human and rat Nox4 proteins are 90% identical (Appendix D). Western blot analysis of VSMC identified Nox4 as a species at ~65 kDa (Hilenski et al. 2004). Nox4 likely undergoes post-translational glycosylation as Nox4 contains four putative *N*-glycosylation sites (Bedard and Krause, 2007). Nox4 has been identified in tissue types throughout the body

Table 1.2. Alternative names and chromosomal locations for Nox enzymes in humans (*Homo sapiens*) and in rats (*Rattus norvegicus*). EC, enzyme commission; GP, glycoprotein; KOX, zinc finger protein; MOX, mitogenic oxidase subunit; NOH, NADPH oxidase homolog; RENox, recombinant human Nox.

Gene Name	**Other Names**	**Chromosome Location**	
		H. sapiens	*R. norvegicus*
Nox1	*NOH-1, MOX1 GP91-2*	Xq22.1	Xq32
Nox4	*RENox, KOX-1, EC1.6.3*	11q14.3	1q32
Nox5		15q23	-

including endothelial cells, VSMC, and neurons, with the highest levels of expression found in the kidney (Geiszt et al. 2000; Ellmark et al. 2005; Vallet et al. 2005; Van Buul et al. 2005). Nox4 ROS production relies on the colocalization of Nox4 with its subunit, p22phox, and in the absence of this subunit ROS production ceases (Martyn et al. 2006). In VSMC, Nox4 and p22phox are known to co-localize with vinculin, a FA marker (Hilenski et al. 2004). In transfected cells, Nox4 had a reticular staining pattern that was similar to that of tyrosine phosphatase PTP1B, a protein that is known to localize to the exterior of endoplasmic reticulum (ER) membranes, suggesting localization on these intracellular membranes (Martyn et al. 2006). In smooth muscle cells, Nox4 expression is upregulated upon transforming growth factor (TGF)-β1 and TNF-α stimulation (Sturrock et al. 2005; Moe et al. 2006). A study conducted by Schroder et al. (2012) suggested a potential protective action of Nox4 on vascular function where Nox4 deficient mice exhibited increased inflammation, hypertrophy and endothelial dysfunction following oxidative stress and had reduced endothelial nitric oxide synthase expression and nitric oxide production, resulting in increased apoptosis.

1.6.4. Nox5

Of the Nox proteins of interest, Nox5 is the furthest branched homolog in terms of phylogenetics (Figure 1.7) containing an intracellular NH_2 terminus with a loop-helix-loop structure, called an EF-hand domain, that binds Ca^{2+} which is not present in either Nox1 or 4 (Bedard and Krause, 2007). In humans the Nox5 gene is located on chromosome 15 (15q23) and contains 18 exons. The Nox5 gene is absent in the rat.

Figure 1.7. A phylogenetic tree comparing the lineage of Nox1, Nox4 and Nox5 between *Homo sapiens* (human), *Pan troglodytes* (chimpanzee), *Mus musculus* (house mouse), and *Rattus norvegicus* (rat). Protein sequences were obtained using HomoloGene and the phylogenetic tree was drawn by inserting the FASTA protein sequence into Phylo.io software.

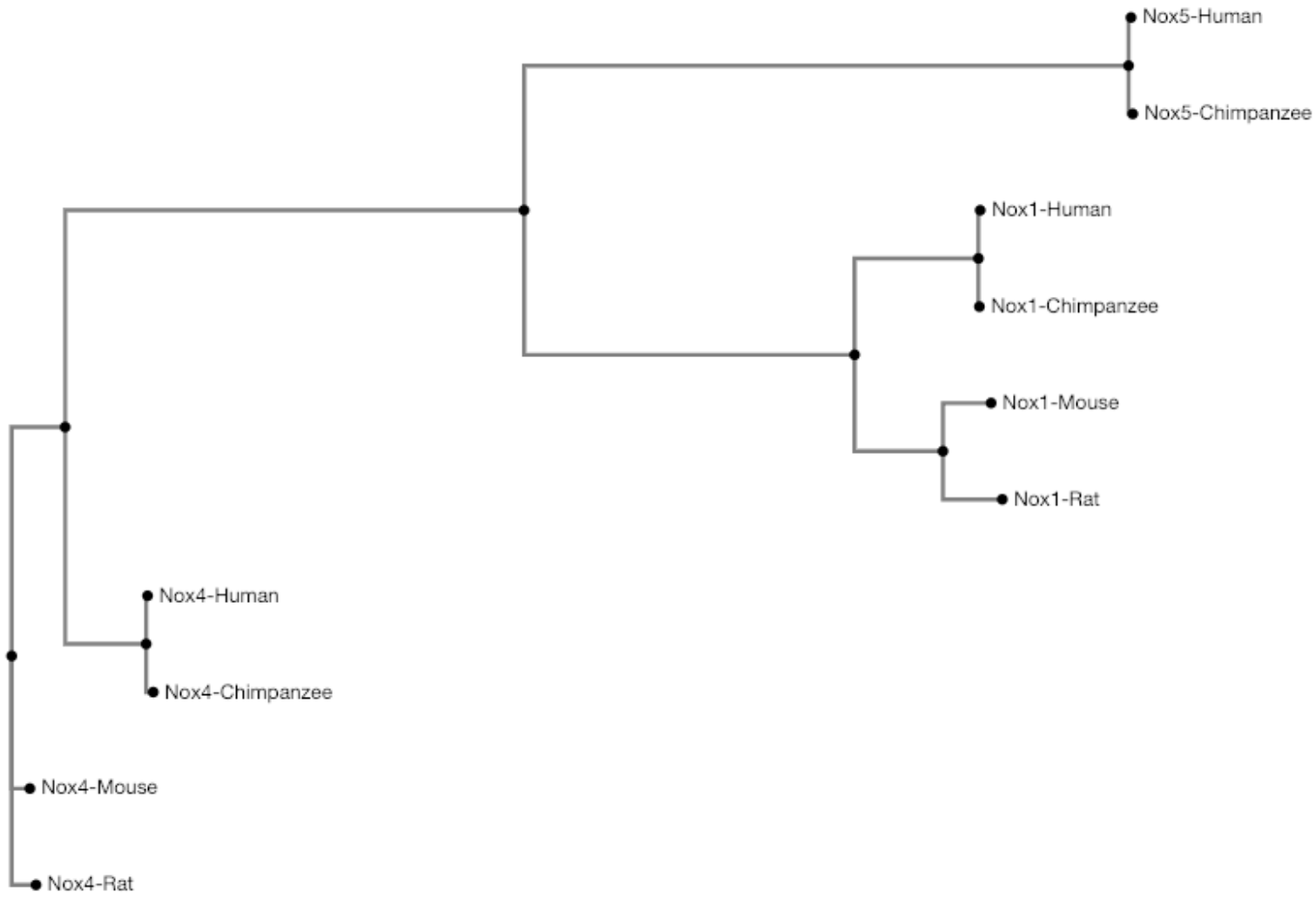
Nox5-Human
Nox5-Chimpanzee
Nox1-Human
Nox1-Chimpanzee
Nox1-Mouse
Nox1-Rat
Nox4-Human
Nox4-Chimpanzee
Nox4-Mouse
Nox4-Rat

1.6.5. Regulatory Subunits

It is well known that Nox enzymes rely on additional cytosolic components for proper assembly and activation (Bedard and Krause, 2007). There are currently seven known regulatory components that interact with the Nox family of enzymes: organizer subunits NoxO1 and p47phox; activator subunits NoxA1 and p67phox, cytochrome b component p22phox, p40phox and the small GTPase Rac. The regulatory components for Nox1 and Nox4, in rodents, are NoxO1, NoxA1 and p22phox. In human systems, activation of Nox1 may utilize NoxO1 and NoxA1 or p47phox and p67phox or a combination of the two systems (Bedard and Krause, 2007). Chromosomal location of NoxO1, NoxA1 and p22phox in humans (*Homo sapiens)* and rats (*Rattus norvegicus)* are summarized in Table 1.3. The Nox subunits of interest were also compared using HomoloGene analysis to determine phylogenetic lineage between select mammalian species (Figure 1.8).

Table 1.3. Alternative names and chromosomal locations of Nox subunits in humans (H*omo sapiens*) and in rats (*Rattus norvegicus*). CYBA, cytochrome B-245 alpha chain; phox, phagocytic NADPH oxidase; SNX, sorting nexin-28.

Gene Name	**Other Names**	**Chromosome Location**	
		H. sapiens	*R. norvegicus*
NoxA1	*p51Nox, p67phox-like factor*	9q34.3	3p13
NoxO1	*p41Nox, SNX28*	16p13.3	10q12
p22phox	*CYBA, phox*	16q24.2	19q12

Figure 1.8. A phylogenetic tree comparing the lineage of NoxO1, NoxA1 and p22phox between *Homo sapiens* (human), *Pan troglodytes* (chimpanzee), *Mus musculus* (house mouse), and *Rattus norvegicus* (rat). Protein sequences were obtained using HomoloGene and the phylogenetic tree was drawn by inserting the FASTA protein sequence into Phylo.io software.

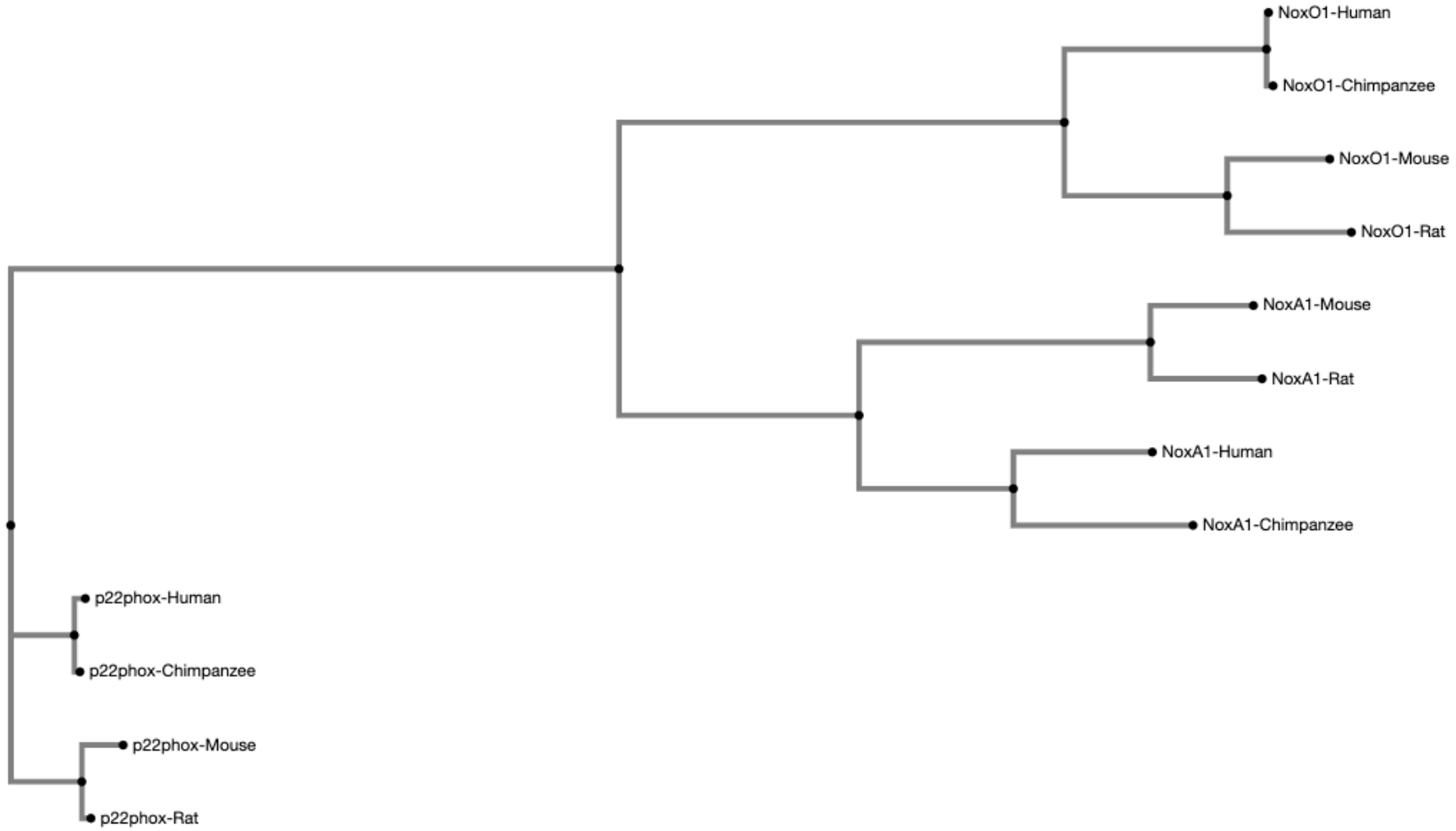
NoxO1-Human
NoxO1-Chimpanzee
NoxO1-Mouse
NoxO1-Rat
NoxA1-Mouse
NoxA1-Rat
NoxA1-Human
NoxA1-Chimpanzee
p22phox-Human
p22phox-Chimpanzee
p22phox-Mouse
p22phox-Rat

1.6.5.1. NoxO1

Organizer subunit, NoxO1, was discovered in humans as a novel homologue of p47phox, sharing ~25% sequence identity and having similar functional domains (Takeya et al. 2003). As such, NoxO1 and p47phox can interchangeably bind with Nox1 and Nox2; however, the degree of activation varies with subunit combinations (Takeya et al. 2003). This 40 kDa subunit is responsible for the translocation of required subunits to the plasma membrane (PM) and has previously been identified in the colon, small intestine and in the uterus (Banfi et al. 2004; Cheng and Lambeth, 2005). Homologue p47phox shares the same functionality, but its expression is reportedly restricted to other cell types and tissues including endothelial cells, testis and the inner ear (Jones et al. 1996; Cheng and Lambeth, 2005). In humans, the NoxO1 gene is located on chromosome 16 (16p13.3) and contains 9 exons while in the rat, the gene is located on chromosome 10 (10q12) and contains 8 exons. BLAST analysis revealed that the rat and human proteins share 71% amino acid identity (Appendix E). Four splice variants (α, β, δ, γ) of NoxO1 have been described in humans (Cheng and Lambeth, 2005; Schroder et al. 2017). NoxO1 contains three distinct domains that allow protein-protein interactions required for Nox1 assembly: 1) a phox domain, 2) two Src homology 3 (SH3) domains, and 3) a proline rich region (PRR) located at the COOH terminal (Bedard and Krause, 2007). NoxO1 interacts with phosphoinositide groups of membrane lipids via the phox domain (Bedard and Krause, 2007). Interactions of NoxO1 and p22phox occur through the SH3 domains which bind to the COOH terminal PRR of p22phox (Cheng and Lambeth, 2004). And lastly, interactions of NoxO1 and NoxA1 occur via the PRR (Miyano et al. 2006). Unlike its homologue p47phox, NoxO1 lacks an autoinhibitory domain and constitutively interacts with NoxA1 and p22phox (Schroder et al. 2017). In NoxO1 knockout mice, otoconia formation, a component of the inner ear formed in utero that allows vertebrates to perceive acceleration, is affected resulting in a severe balance deficit such that mice were unable to orient themselves with respect to gravitational forces and had a phenotypic head tilt (Kiss et al. 2006).

1.6.5.2. NoxA1

Activator subunit, NoxA1, was discovered in humans as a novel homologue of p67phox, sharing ~28% sequence identity and a similar domain structure (Takeya et al. 2003). Aptly named, this subunit is responsible for Nox activation following assembly and translocation of all

required subunits to the PM and has been identified in the colon, small intestine, uterus and VSMC (Banfi et al. 2004; Nauseef, 2004; Ambasta et al. 2006). Functionality of p67phox remains the same, but expression differs with p67phox reportedly detectable in endothelial cells, phagocytes and in the kidney (Leto et al. 1990; Jones et al. 1996; Chabrashvili et al. 2002). In humans, the NoxA1 gene is located on chromosome 9 (9q34.3) and contains 15 exons. In rats, the NoxA1 gene is located on chromosome 3 (3p13) and contains 12 exons. BLAST analysis revealed the two homologues share 58% amino acid identity (Appendix F). NoxA1 has a molecular mass of 50 kDa and contains three distinct domains that allow binding to Nox1 as well as the other regulatory subunits. The tetratricopeptide repeats (TPR) domain lies at the NH_2 terminus and interacts with Rac (Miyano et al. 2006). The activation domain of NoxA1 allows direct interaction with Nox enzymes and interaction with NoxO1 occurs via the SH3 domain (Miyano et al. 2006). Mice lacking NoxA1 are viable, fertile and have no apparent phenotypic abnormalities; however, no further studies have been conducted examining Nox function and/or ROS generation in these animals (Flaherty et al. 2010).

1.6.5.3. p22phox

The subunit p22phox is the alpha component of cytochrome b and has a molecular mass of 22 kDa (Bedard and Krause, 2007). In humans, the p22phox gene is located on chromosome 16 (16q24.2) and contains 7 exons. In rats, the gene is located on chromosome 19 (19q12) and contains 6 exons. BLAST analysis revealed the two proteins share 89% amino acid identity (Appendix G). The interaction of p22phox with Nox1 (Takeya et al. 2003) and Nox4 has been confirmed using fluorescent resonance energy transfer and by immunoprecipitation (Ambasta et al. 2004). In general, p22phox has two functions: 1) to provide stability to the Nox complex and 2) provide a binding site for NoxO1 (Bedard and Krause, 2007). A PRR on the COOH terminus of p22phox interacts with NoxO1 and mutations to this domain lead to a loss of Nox1 activation but have no effect on Nox4 activation (Leto et al. 1994; Kawahara et al. 2005). Additionally, downregulation of p22phox leads to a decrease in function of Nox1 and Nox4 (Kawahara et al. 2005). Subcellular distribution of p22phox is dependent upon Nox function within a given cell type as p22phox is only stable when combined with a Nox enzyme to form a heterodimer (Bedard and Krause, 2007). Mice lacking p22phox have a severe balance deficit caused by altered development of the inner ear, similar to that seen in NoxO1 knockout animals (Nakano et

al. 2008). Additionally, p22phox deficiency leads to chronic granulomatous disease-like immune defects, similar to the immune disorder seen in humans with hereditary inactivation of p22phox (Nakano et al. 2008).

1.7. Oxidation- Reduction Signaling

Electron transfer by Nox homologs is the primary source of ROS in vascular tissues. ROS, including superoxide, hydrogen peroxide and hydroxyl radical, exert toxic effects on cells when present in excessive amounts, but function as key signaling molecules when present at physiological levels (Ushio-Fukai, 2009). Oxidation-reduction (redox) signaling within the cell is mediated through Nox-generated ROS. Because ROS are short-lived, with hydroxyl radicals having a half-life of 10^{-9}s, production in specific subcellular locations is necessary for targeted activation of downstream pathways (Pryor, 1986; Ushio-Fukai, 2009). These signaling molecules participate in various cellular responses based on their localization within the cell, including FA formation and anchorage dependant growth, Ang II-induced hypertrophy and reorganization of the actin cytoskeleton to facilitate cell migration (Ikeda et al. 2005; Zuo et al. 2005; Taddei et al. 2007).

It is hypothesized that Nox homologues participate in redox reactions through forming redox signaling platforms with FA and caveolae (Ushio-Fukai, 2009). Caveolae are a subset of lipid-rafts that possess caveolin-1 as their major structural protein (Harder and Simons, 1997). Lipid-rafts are low-density plasma membrane domains that are rich in both cholesterol and sphingolipids and function as docking stations for signaling molecules. Signaling molecules that are known to concentrate in caveolae include G protein–coupled receptors (GPCRs), Src family kinases and Nox subunits (Li et al. 1996; Insel et al. 2005; Callera et al. 2007). In fact, the ability of Nox enzymes to assemble, and subsequently produce ROS, is dependent on caveolae as these PM sites are where subunits gp91phox, p47phox and Rac assemble prior to Nox activation (Callera et al. 2007).

The renin-angiotensin system is known to stimulate hypertrophy in VSMC. These effects are dependent upon Ang II stimulation and subsequent binding to G-protein–coupled Ang II type 1 receptor (AT_1R) leading to tyrosine phosphorylation of the epidermal growth factor receptor (EGFR) (Ushio-Fukai et al. 2001). Downstream targets, such as tyrosine kinases and protein kinase B, are then activated by EGFR to elicit a hypertrophic response (Ushio-Fukai et al. 2001).

Immunofluorescence analysis of VSMC detected co-localization of Nox1 to caveolin-1 within caveolae under normal conditions (Hilenski et al. 2004). Stimulation of VSMC with Ang II stimulated upregulation of Nox1 expression and promoted trafficking of AT_1R to caveolin-1 containing caveolae and binding of AT_1R to caveolin-1 (Lassegue et al. 2001; Zuo et al. 2005). Transactivation of EGFR is dependent on ROS production via Rac translocation to caveolae and subsequent Nox1 activation, also stimulated by Ang II (Zuo et al. 2004). Large signaling platforms are formed (Figure 1.9) by phosphorylated EGFR and caveolin-1 localizing to FA where they interact with Nox4 and paxillin, known FA-associated proteins (Ushio-Fukai, 2009).

1.8. Cell-ECM Remodelling during Gestation

The uterine mechanotransduction that is required for parturition is facilitated through the development of FAs. The major transmembrane components of FAs are integrins, a large family of glycoprotein $\alpha\beta$ heterodimer receptors with extracellular, transmembrane and cytoplasmic domains (Hynes, 1992). These structures lie at the terminal ends of actin stress fibers where they facilitate reversible adhesion of the cell to its ECM and transmit mechanical signals responsible for cellular processes such as migration and proliferation (Hanks and Polte, 1997). FAs also include scaffolding molecules, GTPases and signaling molecules. The exact number of proteins which participate in these structures is constantly growing, making FAs one of the most complex structures formed in the cell (Zamir and Geiger, 2001). Immunofluorescence analysis of α_1, α_3 and β_1 integrin subunits revealed localization to rat myometrial myocyte PM by late pregnancy and labour and immunocytochemistry of α_5 integrin subunit exhibited the same PM localization pattern from D15-23 as well as 1-D post-partum (Williams et al. 2005; Williams et al. 2010). Expression of integrin proteins has also been confirmed in human myometrial lysates with increased protein expression of α_5, α_7, α_v and β_3 subunits observed during gestation (Burkin et al. 2013).

Clustering of integrins at FA sites promotes the activation and recruitment of the FA adapter protein, FAK. FAK is a 125-kDa cytoplasmic tyrosine kinase, belonging to the protein-tyrosine kinase family, known for its role in regulating FA reorganization (Schaller et al. 1992). Once at a FA site, FAK interacts with a host of additional FA proteins to integrate signals into downstream effects (Mitra et al. 2005). Of particular interest is the interaction between FAK and hydrogen peroxide inducible clone-5 (Hic-5) observed during late pregnancy and labour. Hic-5, a

Figure 1.9. Redox signaling complex formation with caveolae and focal adhesions. Angiotensin-II stimulation promotes localization of AT_1R into caveolae where binding with caveolin-1 occurs. This binding promotes localized ROS production and ROS-dependent transactivation of EGFR. Activated EGFR and caveloin-1 then localize to FA, where a redox signaling complex can be formed. Used with permission from Ushio-Fukai, 2009, see Appendix H. AT_1R, G protein-coupled angiotensin II type 1 receptor; EGFR, epidermal growth factor receptor; FA, focal adhesions; ROS, reactive oxygen species.

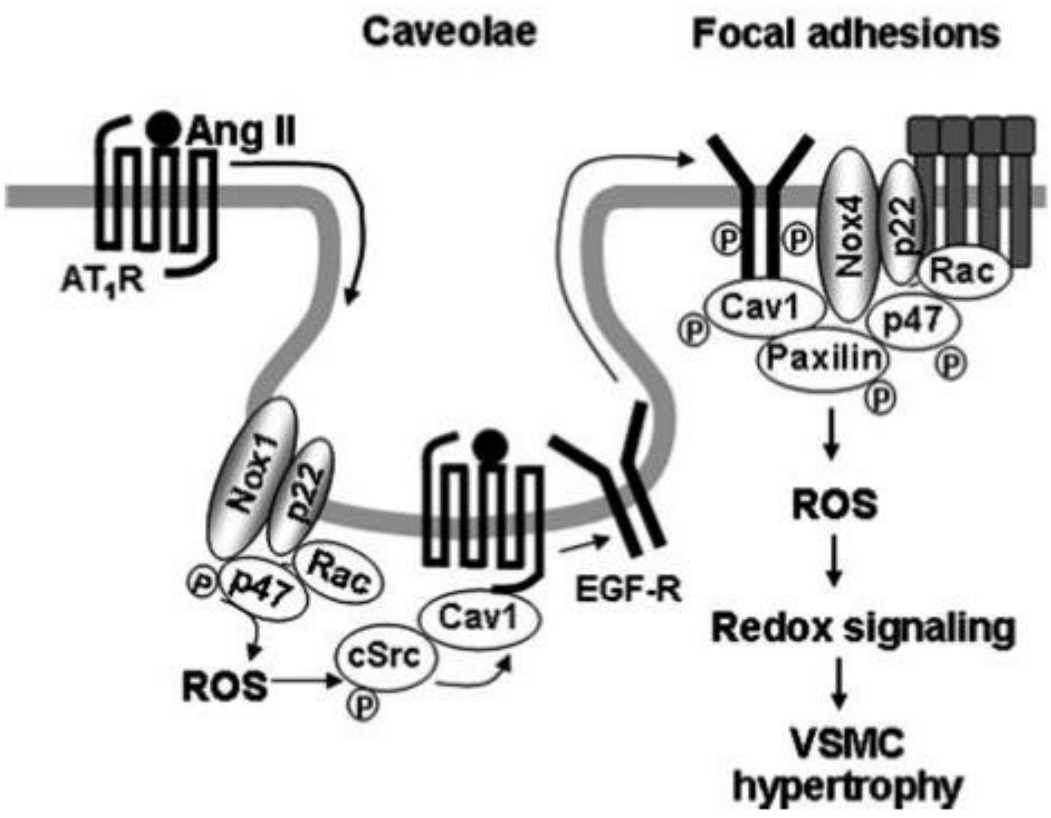
Caveolae
Focal adhesions
Ang II
AT1R
Nox1
p22
p47
Rac
ROS
cSrc
Cav1
EGF-R
Nox4
p22
Rac
Cav1
p47
Paxilin
ROS
Redox signaling
VSMC
hypertrophy

member of the Paxillin family of adapter proteins, is a FA scaffolding protein that mediates numerous protein-protein interactions including integrin-mediated signaling (Croke et al. 2007). Hic-5 is mediated through downstream effects of Nox4 and has been shown to co-localize with FAK at the cell membrane in the longitudinal muscle layer of rat myometrium (Croke et al. 2007; Fernandez et al. 2015). It is postulated that these protein interactions occurring at FA sites act as an important signaling mechanism for the development of a mechanical syncytium, through their connection to cytoskeletal elements, for coordinated powerful labour contractions required for parturition.

The formation and maintenance of FAs relies on Nox4 expression. Hilenski et al. (2004) found Nox4 and its subunit, p22phox to localize to FAs and stress fibers in VSMC. Within these sites, Nox4 localization is mediated via binding of polymerase (DNA-directed) delta interacting protein 2 (Poldip2) to p22phox, as in the absence of Poldip2 Nox4 and p22phox no longer localize to FAs (Lyle et al. 2009). Additionally, Poldip2 increases Nox4 ROS production leading to cytoskeletal remodelling and in the absence of either Poldip2 or Nox4, there is a reduction in the number of FAs (Lyle et al. 2009). ROS produced by Nox4 are crucial for expression and maintenance of the VSMC contractile phenotype (Clempus et al. 2007).

1.9. Oxidative Stress during Pregnancy

Oxidative stress is the result of imbalanced ROS production and antioxidant scavenging ability. Increased ROS production and/or decreased antioxidant capacity may lead to ROS-induced cellular damage. Increased oxidative stress during pregnancy is especially damaging and may play a role in reproductive-related disorders such as recurrent pregnancy loss, preeclampsia, PPROM, PTB and fetal death (Gupta et al 2007; Moore et al. 2018). During early pregnancy, the placenta and fetus survive in a hypoxic environment (Jauniaux et al. 2000). After trophoblast invasion, a burst of oxidative stress is exhibited as maternal blood flow is established and the placenta and fetus are reperfused (Jauniaux et al. 2000). If maternal blood flow is established too early, the trophoblast cannot withstand the oxidative insult and the pregnancy is often lost (Jauniaux et al. 2003). Nox1 expression has been identified in placental homogenates from pregnant women and immunohistochemistry confirms localization to syncytiotrophoblasts (Cui et al. 2006). In patients with preeclampsia, a condition arising from increased oxidative stress,

western blot analysis revealed significantly increased Nox1 expression in the placenta as compared to control patients (Cui et al. 2006).

As the pregnancy nears term, the maternal immune system is once again activated, and a localized inflammatory response begins the labour process. This inflammatory response induces a second period of oxidative stress with levels of urinary 8-hydroxydeoxyguanosine, a biochemical marker of oxidative stress, significantly higher in women at 35 weeks of gestation as compared to 10 and 20 weeks of gestation (Ferguson et al. 2015). In addition to the complications that may arise throughout gestation, the combination of inflammation and increased oxidative stress near term may also contribute to PPROM and PTB (Moore et al. 2018). Samples from fetal membranes with PPROM had lower levels of antioxidant enzymes peroxiredoxin and superoxide dismutase-1 and higher levels of oxidative stress marker 3-nitrotyrosine as compared to samples from PTB infants (Dutta et al. 2016). Expression of Nox2, 3 and 4 has been detected in fetal membranes from term, PPROM and preterm deliveries with Nox2 expression highest in PTB and Nox3 expression highest in PPROM deliveries (Polettini et al. 2014). Thus, ROS produced by Nox enzymes, both in maternal and fetal tissues, may play a role in the oxidative stress induced pathophysiologic pathways of PTB and PPROM.

1.10. Rationale for the Study

Although Canada's rate of PTB has remained relatively steady since 2005 at ~8% (PHAC, 2017), it is estimated to cost the Canadian health care system upwards of $8 billion per year (Lim et al. 2009). Preterm babies remain in hospital longer and require more hospital resources as compared to full term babies (Cuevas et al. 2005). Additionally, preterm infants have increased rates of mortality and morbidity, with cardiovascular, metabolic and neurologic disorders often following the infant into adulthood (Saigal and Doyle, 2008). Extended time in hospital and mother-child separation places additional strain on the physical, psychological and social connections between mother and child as well as increases the overall economic burden of childbearing. This is particularly true for rural women whom often have to travel for longer than one hour to reach the nearest medical facility (CIHI, 2013). Unfortunately, not enough information is yet known about how the myometrium becomes a powerful contractile tissue at term. Only through persistent basic research on myometrial programming and inflammation will the scientific foundation of knowledge be created to identify candidate molecules that could

eventually be used to successfully and effectively predict, prevent or therapeutically treat PTB. A biochemical marker capable of predicting impending PTB and/or normal parturition would be a significant advance for women's health, particularly in rural settings where physiological, psychological, economical, and social burdens are often high.

Of the seven Nox family members, Nox1, Nox4 and Nox5 have previously been found in human leiomyoma derived myometrial tissue (Cui et al. 2010). Within the cell, ROS mediate various responses including cellular proliferation, differentiation and modification of the ECM and are a critical component of inflammation (Griendling et al. 2000). However, when and where these Nox enzymes are expressed in myometrium throughout pregnancy remains unknown. As such, Nox1, Nox4 and their regulatory subunits have been chosen as the proteins of interest for this study.

1.10.1. Hypothesis and Objectives

Nox1 and Nox4 are known to be growth promoting proteins that are upregulated by growth factors such as Ang II (Lassegue et al. 2001). Furthermore, inflammation is associated with oxidative stress and this process is integral to parturition. Thus, it was hypothesized that Nox1 and Nox4 will be highly expressed in the myometrium during gestation as myometrial growth and inflammation occur.

Objective 1: Determine where and when NADPH oxidases are found in rat myometrium during gestation.

Objective 2: To examine where and when Nox subunits NoxO1, NoxA1 and p22phox are expressed in the myometrium as potential regulators of Nox1 and Nox4 function.

2. Materials and Methods

2.1. Animals

Sprague Dawley rats were used for all experiments and were acquired from the Mount Scio Vivarium (Memorial University of Newfoundland). All experimental protocols were approved by the Institutional Animal Care Committee under 08-02-DM to 11-02-DM. Animals were cared for in the Animal Care Unit at the Health Sciences Centre (Memorial University of Newfoundland, St. John's, NL, CA) and maintained under standard environmental conditions (12:12-h light-dark cycle). Rats were individually housed, with *ad libitum* access to water, and fed LabDiet Prolab RMH 3000 (PMI Nutrition International, Brentwood, MO, US).

2.2. Tissue Collection

2.2.1. Gestational Timecourse Experiments

For gestational timecourse experiments, previously prepared rat uterus and myometrium tissue banks were utilized from the MacPhee laboratory. Briefly, virgin female rats (220-250g) were mated with stud males. D1 of the gestation period was determined by observation of a vaginal plug the morning after mating. Following this time scheme, the gestation period was 23D. Animals were euthanized by carbon dioxide induced asphyxiation prior to sample collection. For timecourse experiments, samples were collected from non-pregnant (NP) animals and from pregnant animals at eight time points: D6, D12, D15, D17, D19, D21, D22, D23 (labour) as well as 1-D post-partum (PP).

For immunofluorescence detection, a portion of the uterine horn was fixed in 4% paraformaldehyde in phosphate-buffered saline (PBS; pH 7.4) overnight. Tissues were processed and paraffin embedded by the Histology Unit of Memorial University of Newfoundland School of Medicine. When required, five micrometer thick tissue sections were prepared by the MacPhee lab using a Leica RM2135 microtome and sections were mounted on glass slides previously treated with silane (2% (3-aminopropyl) triethoxysilane in acetone, Cat#: A3648; Sigma-Aldrich, St. Louis, MO, US). Cross sections of the uterine horn utilized for experiments included both longitudinal and circular muscle layers of the myometrium.

For immunoblot analysis, uterine horns were removed and opened longitudinally. Fetuses and placentae were discarded, and uterine tissue was placed in ice-cold PBS. To isolate the myometrium, a scalpel blade was used to gently scrape away the endometrial layer, as previous

described by White et al. (2005). All myometrial samples were flash-frozen in liquid nitrogen and stored at -80°C until utilized for experiments.

2.2.2. Unilaterally Pregnant Rat Model

For examination of the effect of uterine distension on spatiotemporal protein expression, a previously produced tissue bank in the MacPhee lab was utilized. Briefly, anesthetized virgin female rats were subjected to unilateral tubal ligations though bilateral flank incisions as described by White and MacPhee (2011). Animals were monitored and allowed to recover for ~5D before matings were attempted. Samples of gravid and non-gravid horns were collected on D19 and D23 of gestation for use in immunofluorescence and immunoblot analyses as described above.

2.3. Cell Culture

All cell culture experiments used to generate cell lysates for analyses in this thesis were largely conducted by past trainees in the MacPhee laboratory (Ms. Georgia Bailey and Mr. Logan Hahn) and utilized an immortalized human myometrial cell line (hTERT-HM) that was obtained from Dr. Ruth Word at the University of Texas South Western Medical Center (Dallas, TX, US). Uterine samples from healthy women undergoing hysterectomies was used to establish a primary cell culture which was then used to acquire the cell line. Cells were then stably transfected with expression vectors containing human telomerase reverse transcriptase (hTERT) which immortalized the cells by maintaining telomere length (Condon et al. 2002).

For propagation, hTERT-HM cells were cultured in DMEM/F12 media (Cat#: 11330032; ThermoFisher Scientific, Ottawa, ON, CA) containing 10% fetal bovine serum (FBS; Cat#: 12483020; ThermoFisher Scientific) and 1% penicillin/streptomycin (P/S) (Cat#: 15140122; ThermoFisher Scientific). To limit the accumulation of metabolites and cellular debris, media was changed daily. Upon cell culture reaching 90% confluency, passaging was conducted using a trypsin-ethylenediaminetetraacetic acid (EDTA) solution (0.05% v/v trypsin in EDTA, Cat#: 15400-054; ThermoFisher Scientific). Cell number and viability were routinely assessed using a Bio-Rad TC20- cell counter and trypan blue dye (Cat#: 1450013; Bio-Rad, Mississauga, ON, CA).

2.3.1. Stimulation of Pro-Inflammatory Conditions

Two approaches were used by the MacPhee lab to generate pro-inflammatory conditions in the hTERT-HM cells: addition of lipopolysaccharide (LPS; Hahn, 2018) or IL-1β (Bailey, 2020) to the culture media.

2.3.1.1. LPS Experiments

Briefly, preceding experiments, six-well tissue culture plates were seeded with hTERT-HM cells (0.35 x 10_6 cells/well) and propagated under serum reduced conditions: DMEM/F12 media containing 5% FBS and 1% P/S. On the day of the experiment, cells were briefly washed and subsequently cultured in DMEM/F12 media containing either 100ng/mL LPS (*E.coli* serotype 0111:B4; Cat#: 14011; Cell Signaling Technology, Danvers, MA, US) or PBS (0 ng/ml) (Cat#: 20012027; Thermo Fisher Scientific) vehicle control for 0.5h, 1h, 3h and 6h (n=3 per timepoint). Cell culture supernatants were collected at 3h and 6 h timepoints to subsequently verify inflammatory conditions (i.e. production of pro-inflammatory cytokines) using ELISA (Hahn, 2018). Cell lysates were collected at all timepoints by adding radio-immunoprecipitation assay (RIPA) lysis buffer (50mM Tris-HCl [pH 7.5], 150mM NaCl, 1% Triton X-100, 1% sodium deoxycholate, 0.1% sodium dodecyl sulfate (SDS)) containing protease and phosphatase inhibitors (Complete Mini, Cat#: 04693159001; PhosSTOP, Cat#: 04906845001; Roche Diagnostics, Laval, QC, CA) to cells and physically removing the cell monolayer using a cell scraper. Lysates were subsequently homogenized using 1.4mm ceramic beads and a MINILYS Bead Mill (Bertin Corporation, Rockville, MD, US). The homogenized mixture was centrifuged for 15 min at 12,000 x g at 4°C, lysates were collected and subsequently used for SDS-polyacrylamide gel electrophoresis (SDS-PAGE) analysis as described below.

2.3.1.2. IL-1β Experiments

Briefly, preceding experiments, six-well tissue culture plates were seeded with hTERT-HM cells (0.35 x 10_6 cells/well) and propagated under serum reduced conditions: DMEM/F12 media containing 5% FBS and 1% P/S. On the day of the experiment, cells were briefly washed and subsequently cultured in DMEM/F12 media (5% FBS; 1% P/S) containing either 1 ng/mL IL-1β (Cat#: H6291; Sigma-Aldrich) or 0.1% human serum albumin (HSA) (Cat#: A9731; Sigma-Aldrich) vehicle control for 0.5h, 1h, 3h and 6h (n=3 per timepoint). Cell culture

supernatants were collected, as described above, for subsequent verification of pro-inflammatory conditions (i.e. production of pro-inflammatory cytokines) using ELISA (Bailey, 2020). Cell lysates were also collected as described above and supernatants were used for SDS-PAGE analysis as described below.

2.4. Sodium Dodecyl Sulfate-Polyacrylamide Gel Electrophoresis

Myometrial tissue samples were pulverized with a mortar and pestle under liquid nitrogen and then homogenized in RIPA lysis buffer plus protease and phosphatase inhibitor tablets using 1.4mm ceramic beads and a MINILYS Bead Mill. Lysates were then centrifuged at 12,000 x g for 15 mins, supernatants were collected in an Eppendorf tube and stored at -80°C.

Myometrial tissue and hTERT-HM cell protein concentrations were determined using the Bio-Rad Protein Assay Kit according to the manufacturer's instructions (Cat#: 500-0002; Bio-Rad). Briefly, protein sample concentrations were determined from a standard curve of 7 BSA standard protein concentrations (0 to 0.6 mg/ml) using an Eppendorf Biophotometer Plus. Protein samples for SDS-PAGE (10 or 20μg/lane for myometrial tissue; 12μg/lane for hTERT-HM cell lysates) were then prepared by mixing with 2x loading dye (100 mM Tris-HCl, pH 6.8, 10% β-mercaptoethanol, 4% SDS, 0.2% bromophenol blue, 20% glycerol). Samples were then stored at -80°C for subsequent analysis. Protein samples were electrophoretically separated under reducing conditions in 10% SDS-polyacrylamide gels. Following separation, samples were electroblotted onto 0.2μm nitrocellulose membranes (Cat#: 162-0097; Bio-Rad).

To verify the protein transfer, membranes were stained for 30 s using a Memcode Reversible Protein Stain Kit (Cat#: 24580; ThermoFisher Scientific) followed by washes in Destain solution. Membranes were then digitally scanned for future reference and the reversible stain removed by a wash in Stain Eraser solution.

2.5. Immunoblot Analysis

Immunoblot analysis was performed on four independent myometrial sample sets collected from normal rat gestation (n=4 per timepoint). Membranes were blocked in 5% non-fat dry milk (w/v) in Tris-buffered saline plus Tween 20 (TBST; 20mM Tris-HCl [pH 7.6], 150mM NaCl, 0.1% Tween 20) followed by incubation overnight at 4°C with the appropriate primary antisera (Table 2.1) diluted in blocking solution. Blots were subsequently washed three times in

Table 2.1. Antibodies utilized for immunoblot and immunofluorescence analysis. IB, immunoblot; IF, immunofluorescence; HRP, horseradish peroxidase; FITC, fluorescein isothiocyanate; RRX, rhodamine-Red-X. *Matched to concentration of primary antisera utilized.

Antibody	Supplier	Catalog Number	Procedure / Dilution
Anti-NoxA1 (Mouse Monoclonal)	Santa Cruz Biotechnology, Dallas, TX, US	Sc-398873	IB: 1:5,000 IF: 1:50
Anti-NoxO1 (Rabbit Polyclonal)	Abcam, Cambridge, MA, US	Ab34761	IB: 1:10,000 IF: 1:100
Anti-Nox1 (Rabbit Polyclonal)	Sigma-Aldrich, St. Louis, MO, US	SAB4200227	IB: 1:40,000 IF: 1:500
Anti-Nox4 (Rabbit Monoclonal)	Abcam	Ab133303	IB: 1:20,000
Anti-Nox4 (Rabbit Polyclonal)	Sigma-Aldrich	HPA015475	IF: 1:50
Anti-p22phox (Mouse Monoclonal)	Santa Cruz	Sc-130551	IB: 1:2,000
GAPDH (Rabbit Polyclonal)	Abcam	Ab9485	IB: 1:30,000
Anti-Rabbit HRP	Promega, Madison, WI, US	W4011	IB: 1:10,000
Anti-Rabbit IgG FITC	Sigma-Aldrich	F7512	IF: 1:250
ChromePure Rabbit IgG	Jackson ImmunoResearch Laboratories, West Grove, PA, US	011-000-003	IF: N/A*
Anti-Mouse HRP	Promega	W4021	IB: 1:10,000
Anti-Mouse IgG RRX	Jackson ImmunoResearch	715-295-150	IF: 1:150
ChromePure Mouse IgG	Jackson ImmunoResearch	015-000-003	IF: N/A*

TBST followed by incubation at room temperature for 1h with the appropriate horseradish peroxidase (HRP)-conjugated secondary antibodies diluted in blocking solution (Table 2.1). Membranes were then washed an additional four times in TBST before development. Blots were developed using the SuperSignal West Pico Plus chemiluminescence substrate detection system (Cat#: 34580; Thermo Fisher Scientific) according to the manufacturer's instructions. Multiple images were generated using a Bio-Rad ChemiDoc MP digital imaging system to ensure the linearity of the exposures. All blots were additionally probed for glyceraldehyde 3-phosphate dehydrogenase (GAPDH) expression, which served as a loading control, using a GAPDH-specific antibody (Table 2.1) diluted in blocking solution.

2.6. Immunofluorescence Analysis

Immunofluorescence analysis was performed on three independent sets of rat uterine tissue samples from normal gestation (n=3 for each timepoint analyzed). Tissue sections were deparaffinized in xylene three times for 5 min each and rehydrated using a descending series of ethanol solutions for 3 min at each concentration (100%, 95%, 90%, 80%, 70%, and 50%). Heat-induced epitope retrieval was performed by placing slides in boiling 10 mM sodium citrate buffer [pH 6.0] for 20 min. Slides were allowed to cool in the same buffer for an additional 20 mins before being washed in ice-cold PBS. Tissue sections were circled using an ImmEdge Pen (Cat#: H-4000, Vector Laboratories, Burlingame, CA, US). Enzyme-induced epitope retrieval was subsequently performed using a 1 mg/mL trypsin solution (Cat#: T7168; Sigma-Aldrich) at room temperature for 10 mins followed by two washes in PBS. Tissues were then blocked with 5% normal goat serum/1% normal horse serum/1% FBS, washed with ice-cold PBS, and incubated overnight at 4^{0}C with appropriate primary antisera (Table 2.1) diluted in blocking solution. To serve as a negative control, separate tissue sections from the same timepoints were incubated with non-specific rabbit or mouse IgG (Table 2.1), used at the same concentration as the primary antisera. Following two washes in ice-cold PBS, all slides were incubated with the appropriate secondary antisera (Table 2.1) at room temperature for 1h. For double-immunofluorescence analysis, slides were washed three times in ice cold PBS and blocked using 5% normal goat serum/1% normal horse serum/1% FBS. A second antibody combination was utilized after the latter washes, following the same procedure as above.

Slides were washed three times in ice-cold PBS plus 0.1 % Tween 20 before coverslip mounting with ProLong Diamond Anti-Fade Reagent containing 4′,6-diamidino-2-phenylindole (DAPI) (Cat#: P36971, ThermoFisher Scientific). Once mounting media was cured for 24h, coverslips were sealed with nail polish.

Slides were imaged using an Olympus IX83 microscope equipped for widefield epifluorescence with an Andor Zyla 4.2 sCMOS camera containing a 2048 x 2048 pixel array (Andor USA, Concord, MA) and CellSens software (Olympus, Richmond Hill, ON, CA). Select tissue sections of interest were further examined in some instances by collecting a z-series of optical images (7 images; each 0.25 μm thick). Images were then processed post acquisition with the CellSens Differential Contrast Enhancement plugin (Olympus).

2.7. Data Analysis

Densitometric analysis was performed on all immunoblot data using Image Lab software (version 5.02; Bio-Rad). All analyses of target proteins were analyzed and normalized to densitometric measurements of GAPDH. Statistical analysis was performed using GraphPad Prism 8.0 for MacOS (GraphPad Software, San Diego, CA, USA, www.graphpad.com). Data from normal gestational profiles were subjected to a One-way Analysis of Variance and Tukey multiple comparisons tests. Data from unilaterally pregnant rat models were subjected to a t-test. Data from pro-inflammatory experiments with hTERT-HM cells were subjected to a Two-way Analysis of Variance followed by Tukey multiple comparisons tests. Values with a $P<0.05$ were considered to be significantly different.

3. Results

3.1. Expression of Nox1 and Nox4 protein in Pregnant Rat Myometrium

Immunoblot analysis for expression of Nox1 in myometrium demonstrated that Nox1 was detectable at ~70 kDa in NP tissue, at all timepoints throughout pregnancy and PP (Figure 3.1). However, expression on D23 was significantly greater ($P<0.05$) compared to D6, D12, D17 and D19 (*) and expression on D22 was significantly higher than expression on D6 (**). Immunoblot analysis also showed that Nox4 in myometrium was detectable at ~65 kDa and constitutively expressed in NP tissue as well as throughout gestation and 1-D post-partum (Figure 3.2). However, expression of Nox4 was significantly greater at NP, D6, D12, D15 and D22 compared to PP (*), while expression on D12 was significantly higher than expression on D21 (**).

3.2. Spatial localization of Nox1 and Nox4 in Pregnant Rat Myometrium

The spatial localization of Nox1 in rat myometrium was assessed throughout gestation by immunofluorescence analysis. Nox1 was detectable at all timepoints assessed (NP-PP) in both muscle layers. In the longitudinal muscle layer (Figures 3.3, 3.4), Nox1 immunostaining was detected throughout the entire myocyte, including the cytoplasm and associated with the plasma membrane, but was not present in myocyte nuclei throughout gestation. An increase in detection was observed at D23 and PP and immunostaining at PP was often observed to be concentrated in specific myocytes within the muscle bundles. In the circular muscle layer (Figures 3.5, 3.6), Nox1 was detected in the myocyte cytoplasm and associated with plasma membranes. Similar to the longitudinal muscle layer, there was no detection of Nox1 in the myocyte nuclei in the circular muscle layer. Relative to the smooth muscle bundles of both myometrium layers, where Nox1 was highly detectable, Nox1 was virtually undetectable in the surrounding interstitium (Figures 3.3-3.6).

Immunofluorescence analysis of Nox4 in rat myometrium demonstrated that detection of this protein increased during gestation with maximal detection observed mid-late gestation (D12-D19). In the longitudinal muscle layer (Figures 3.7, 3.8), Nox4 expression was progressively more pronounced, particularly in perinuclear regions, as gestation progressed. A similar detection pattern was observed in the circular muscle layer of the myometrium (Figures 3.9,

Figure 3.1. Immunoblot analysis of Nox1 expression in rat myometrium throughout gestation. Representative immunoblots are shown above the densitometric analysis. Expression levels were determined in non-pregnant rat tissue (NP) and tissue from day (D) 6, D12, D15, D17, D19, D21, D22, D23 (active labour) and 1-day post-partum (PP). *Expression on D23 was significantly higher than expression on D6, D12, D17 and D19. **Expression at D22 was significantly higher than at D6. Expression levels were considered significantly different when $P<0.05$. Glyceraldehyde 3-Phosphate Dehydrogenase (GAPDH) protein expression was used as a normalization control for densitometric analysis. Densitometric data are from 4 independent experiments (n=4 per timepoint).

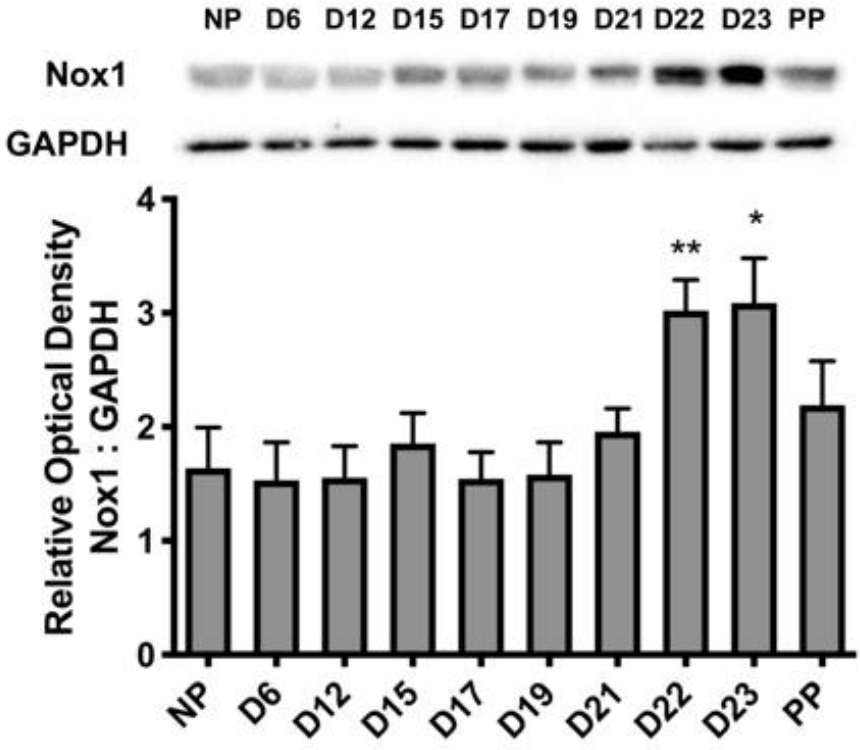
NP D6 D12 D15 D17 D19 D21 D22 D23 PP
Nox1
GAPDH
Relative Optical Density
Nox1 : GAPDH
0
1
2
3
4
**
*
NP
D6
D12
D15
D17
D19
D21
D22
D23
PP

Figure 3.2. Immunoblot analysis of Nox4 expression in rat myometrium throughout gestation. Representative immunoblots are shown above the densitometric analysis. Expression levels were determined in non-pregnant rat tissue (NP) and in tissue from day (D) 6, D12, D15, D17, D19, D21, D22, D23 (active labour) and 1-day post-partum (PP). *Expression at NP, D6, D12, D15 and D22 was significantly higher than at PP ($P<0.05$). ** Expression at D12 was significantly higher than at D21 ($P<0.05$). Glyceraldehyde 3-Phosphate Dehydrogenase (GAPDH) protein expression was used as a normalization control for densitometric analysis. Densitometric data are from 4 independent experiments (n=4 per timepoint).

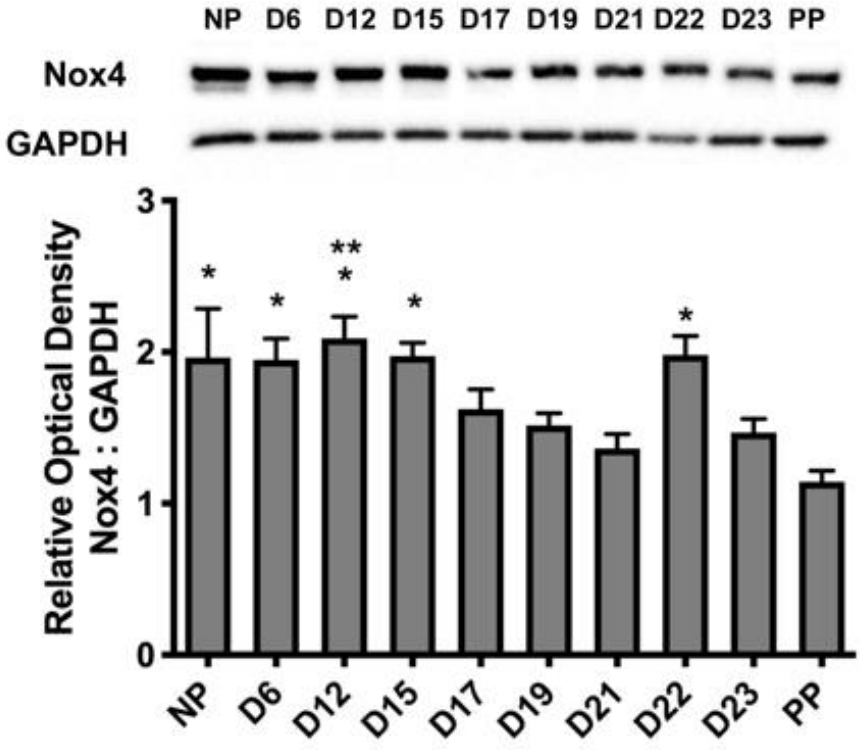
NP D6 D12 D15 D17 D19 D21 D22 D23 PP
Nox4
GAPDH
Relative Optical Density
Nox4 : GAPDH
3
2
1
0
*
*
**
*
*
*
NP D6 D12 D15 D17 D19 D21 D22 D23 PP

Figure 3.3. Immunofluorescence detection of Nox1 in longitudinal uterine smooth muscle layers from non-pregnant (NP) rats and pregnant rat uterine horns at day (D) 6, D12, D15, D17 and D19 of gestation. Representative images are shown for each timepoint. Expression was detected using a rabbit polyclonal anti-Nox1 antibody followed by an anti-rabbit FITC conjugated antibody. Detection of Nox1 was observed in the myocyte cytoplasm and associated with plasma membrane and virtually undetectable in the interstitium relative to the smooth muscle. Scale bar = 50μm.

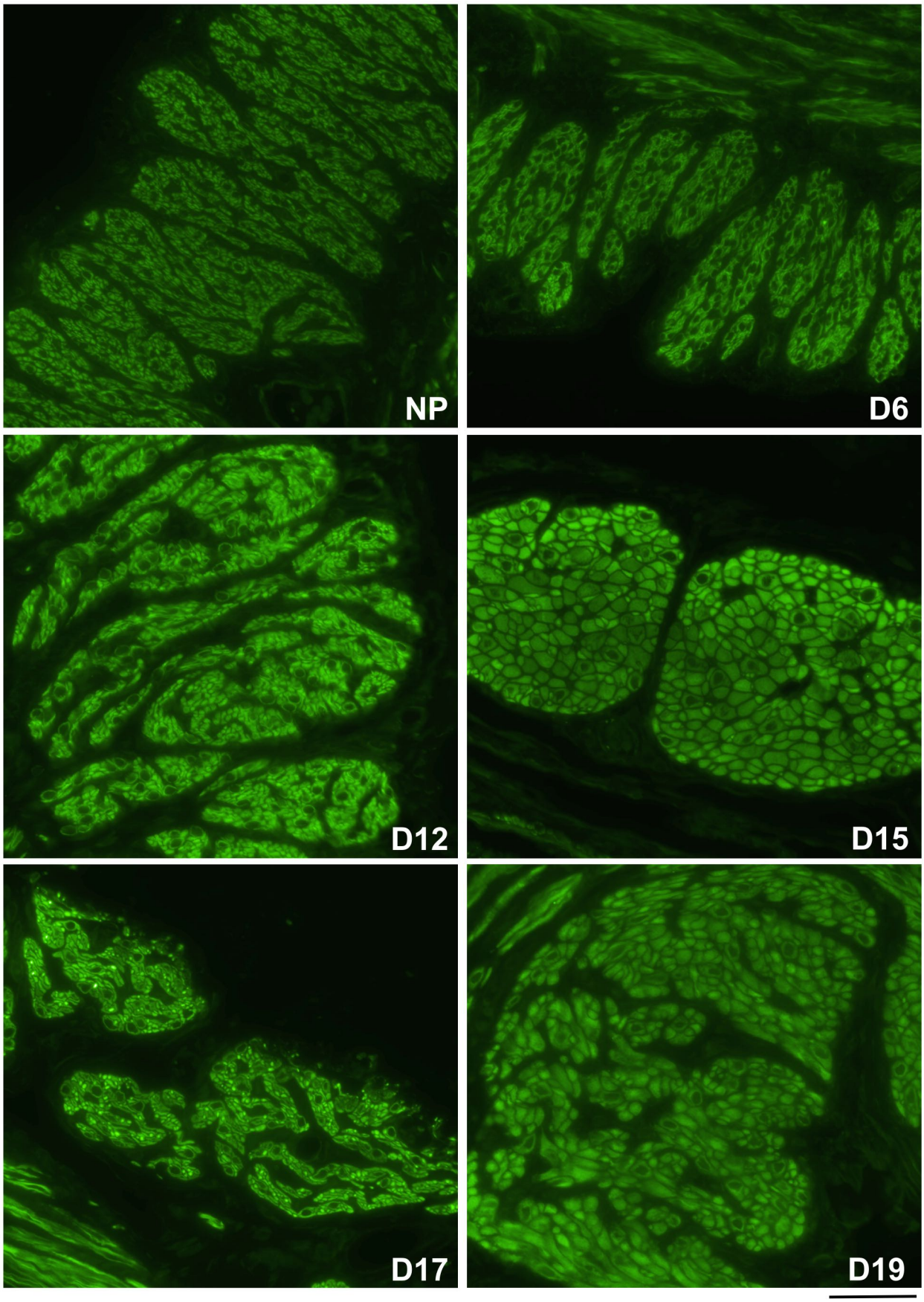
NP
D6
D12
D15
D17
D19

Figure 3.4. Immunofluorescence detection of Nox1 in longitudinal uterine smooth muscle layers from pregnant rat uterine horns at day (D) 21, D22, and D23 of gestation and from uterine horns at 1-day post-partum (PP). Representative images are shown for each timepoint. Expression was detected using a rabbit polyclonal anti-Nox1 antibody followed by an anti- rabbit FITC conjugated antibody. An increase in cytoplasmic detection was observed at D23 and PP. Immunostaining at PP was observed to be concentrated within the muscle bundles in specific myocytes. Nox1 was virtually undetectable in the interstitium relative to the smooth muscle. IgG, non-specific rabbit immunoglobulin used in place of the primary antiserum. Scale bar = 50μm.

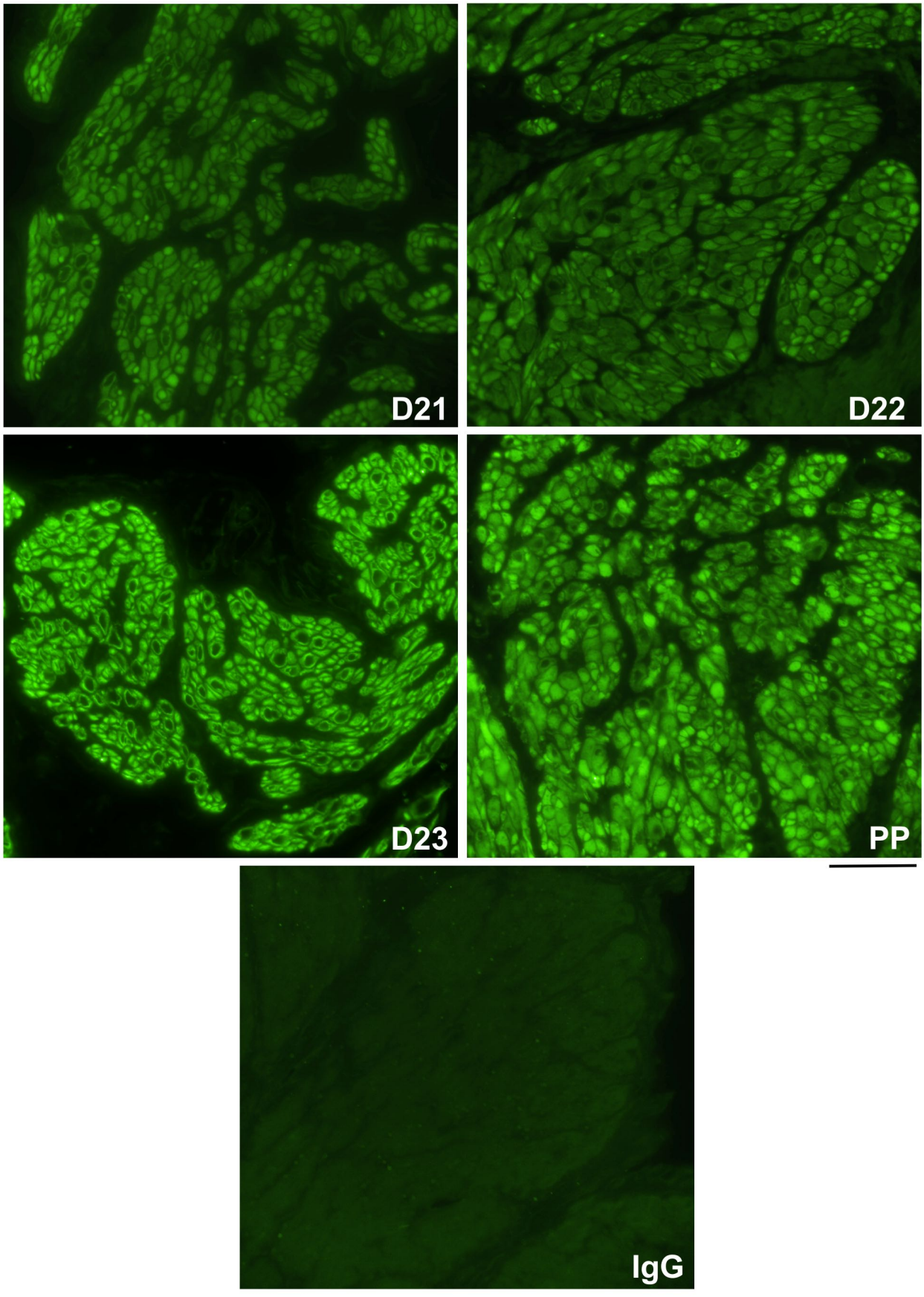
D21
D22
D23
PP
IgG

Figure 3.5. Immunofluorescence detection of Nox1 in circular uterine smooth muscle layers from non-pregnant (NP) rats and pregnant rat uterine horns at day (D) 6, D12, D15, D17 and D19 of gestation. Representative images are shown for each timepoint. Expression was detected using a rabbit polyclonal anti-Nox1 antibody followed by an anti-rabbit FITC conjugated antibody. Detection of Nox1 was observed in myocyte cytoplasm and associated with plasma membranes. Nox1 was virtually undetectable in the interstitium relative to the smooth muscle. Scale bar = 50μm.

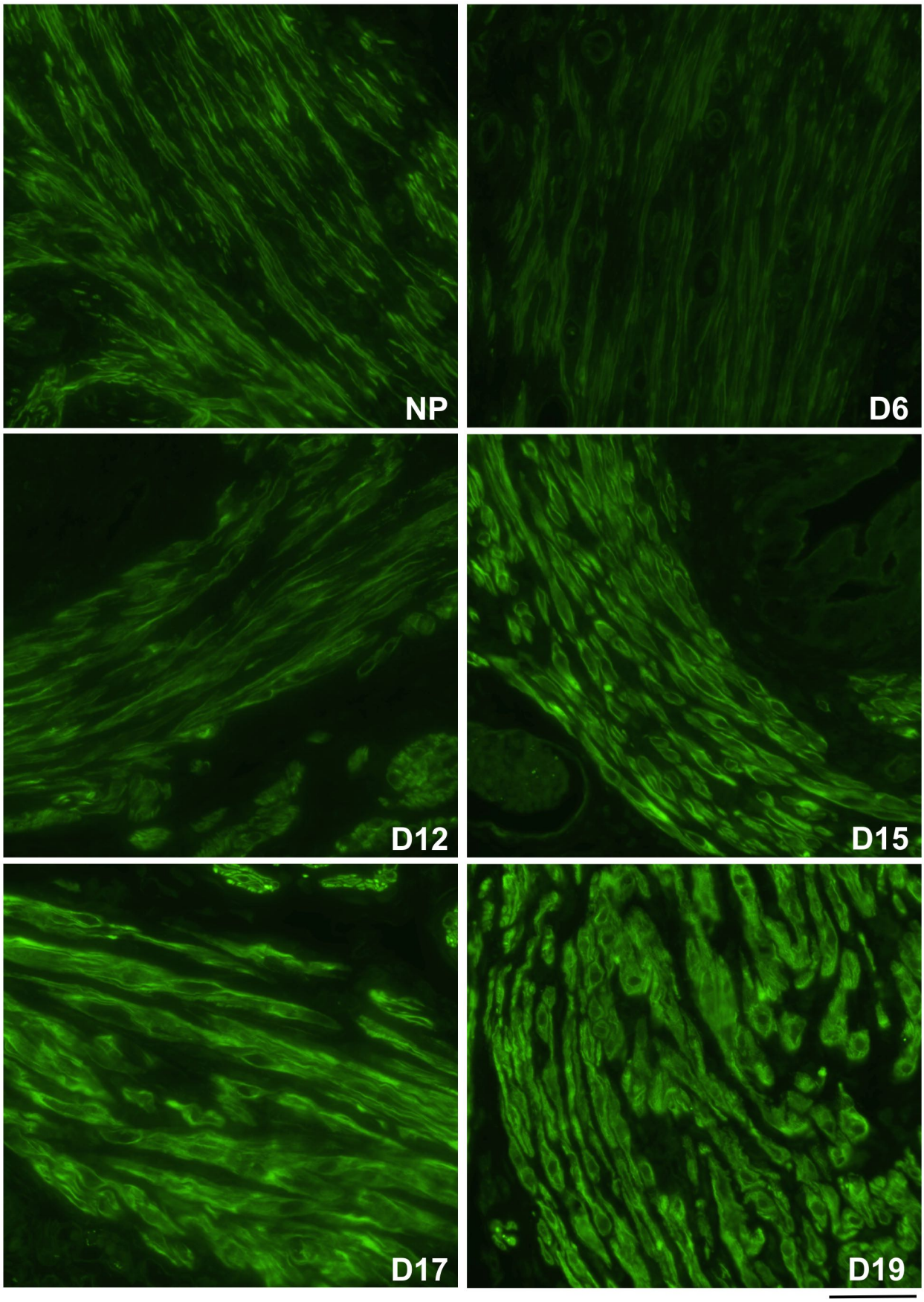
NP
D6
D12
D15
D17
D19

Figure 3.6. Immunofluorescence detection of Nox1 in circular uterine smooth muscle layers from pregnant rat uterine horns at day (D) 21, D22, and D23 of gestation and from uterine horns at 1-day post-partum (PP). Representative images are shown for each timepoint. Expression was detected using a rabbit polyclonal anti-Nox1 antibody followed by an anti- rabbit FITC conjugated antibody. An increase in cytoplasmic detection was observed at D23 and PP. Immunostaining at PP was observed to be concentrated within the muscle bundles in specific myocytes. IgG, non-specific rabbit immunoglobulin used in place of the primary antiserum. Scale bar = 50μm.

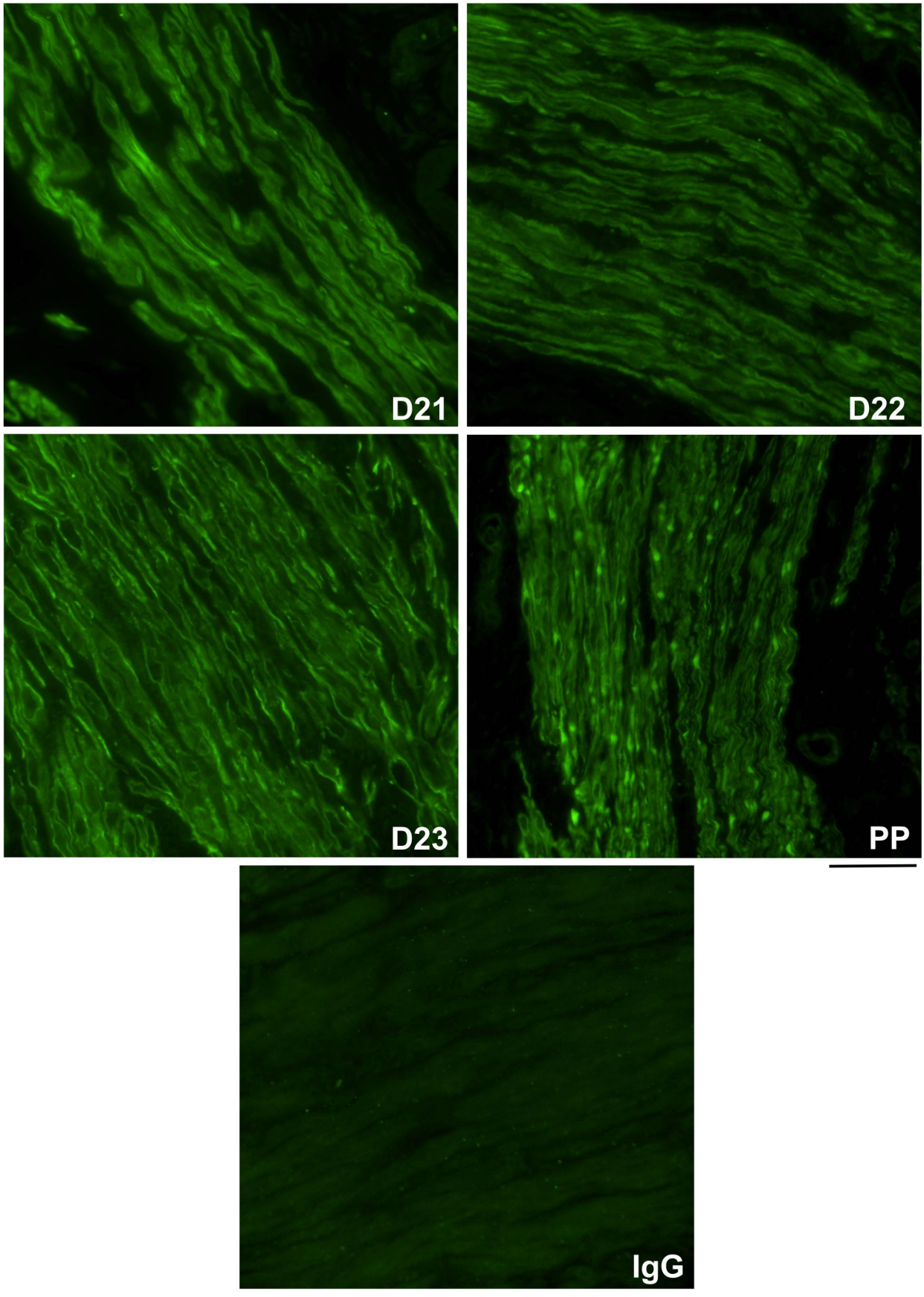
D21
D22
D23
PP
IgG

Figure 3.7. Immunofluorescence detection of Nox4 in longitudinal uterine smooth muscle layers from non-pregnant (NP) rats and pregnant rat uterine horns at day (D) 6, D12, D15, D17 and D19 of gestation. Representative images are shown for each timepoint. Expression was detected using a rabbit polyclonal anti-Nox4 antibody followed by an anti-rabbit FITC conjugated antibody. The detection of Nox4 progressively increased, with maximal detection observed during mid-gestation from D12 to D19, particularly in perinuclear regions of myocytes. Some Nox4 immunostaining was also observed in interstitial cells between muscle bundles (e.g. D17). Scale bar = 50μm.

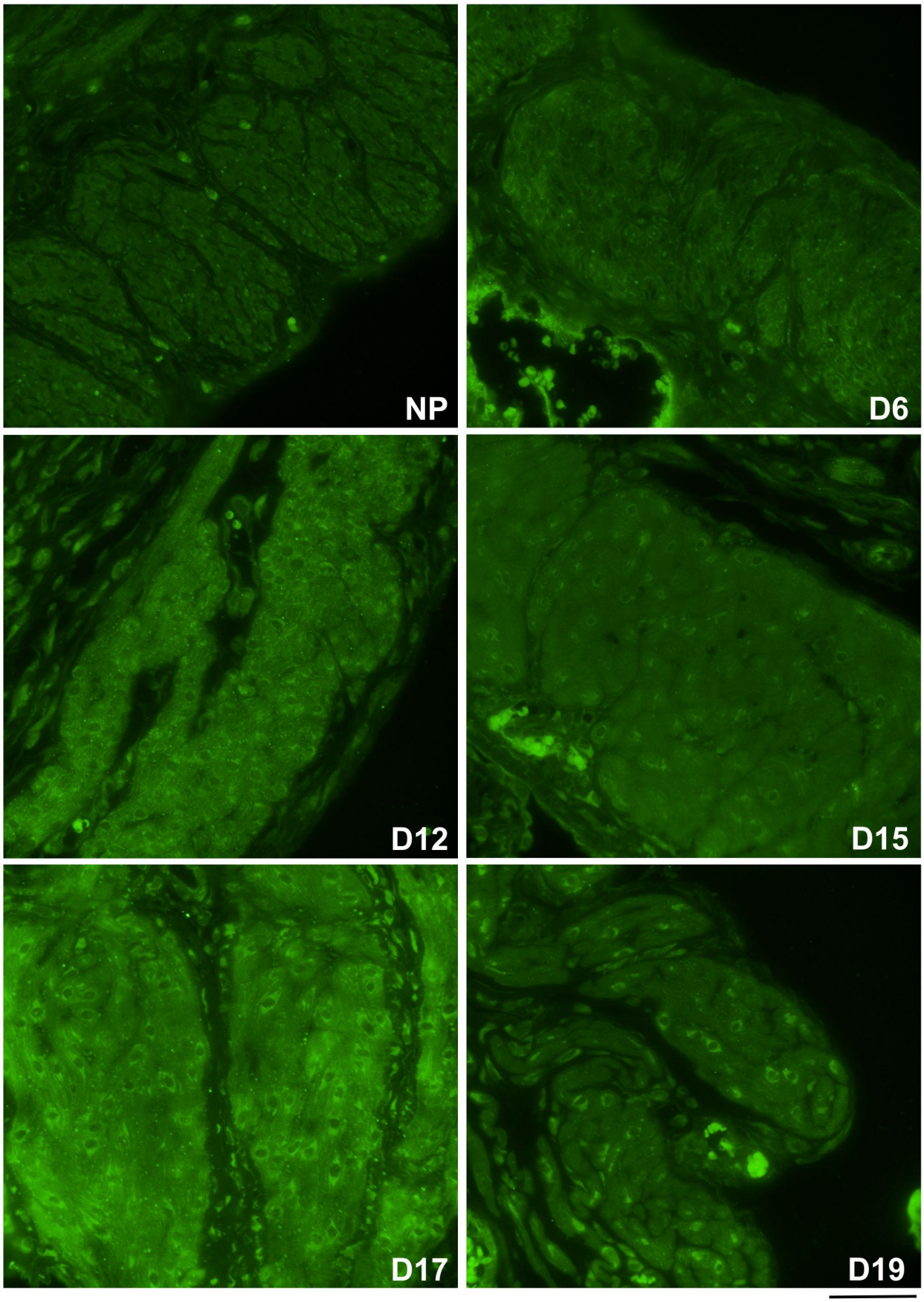
NP
D6
D12
D15
D17
D19

Figure 3.8. Immunofluorescence detection of Nox4 in longitudinal uterine smooth muscle layers from pregnant rat uterine horns at day (D) 21, D22, and D23 of gestation and 1-day post-partum (PP). Representative images are shown for each timepoint. Expression was detected using a rabbit polyclonal anti-Nox4 antibody followed by an anti-rabbit FITC conjugated antibody. The detection of Nox4 in perinuclear sites progressively subsided from D21 to PP. IgG, non-specific rabbit immunoglobulin used in place of the primary antiserum. Scale bar = 50μm.

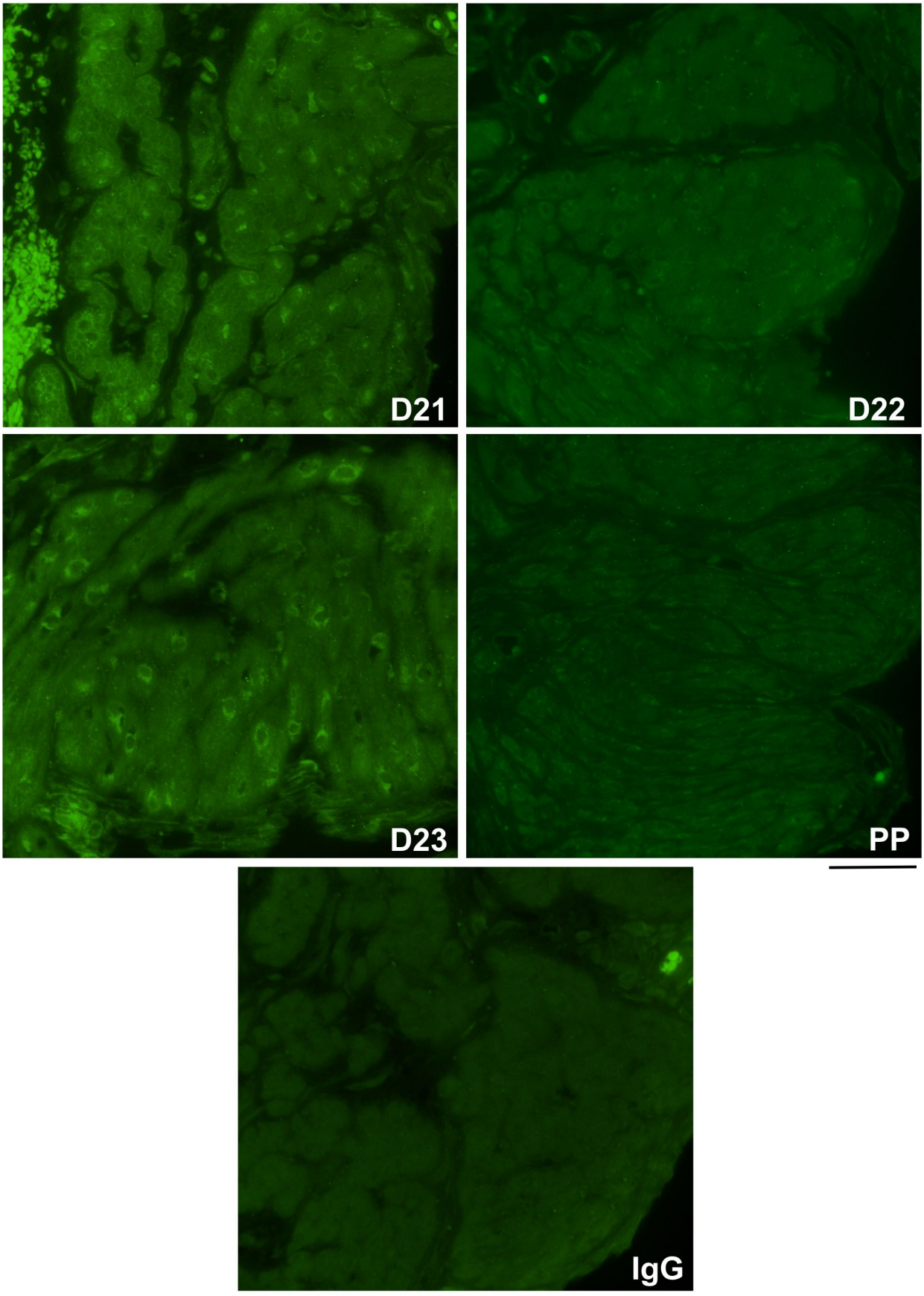
D21
D22
D23
PP
IgG

Figure 3.9. Immunofluorescence detection of Nox4 in circular uterine smooth muscle layers from non-pregnant (NP) rats and pregnant rat uterine horns at day (D) 6, D12, D15, D17 and D19 of gestation. Representative images are shown for each timepoint. Expression was detected using a rabbit polyclonal anti-Nox4 antibody followed by an anti-rabbit FITC conjugated antibody. The detection of Nox4 progressively increased, with maximal detection observed during mid-gestation from D12 to D19, particularly in perinuclear regions of myocytes. Some Nox4 immunostaining was also observed in interstitial cells between myocytes (e.g. D12). Scale bar = 50μm.

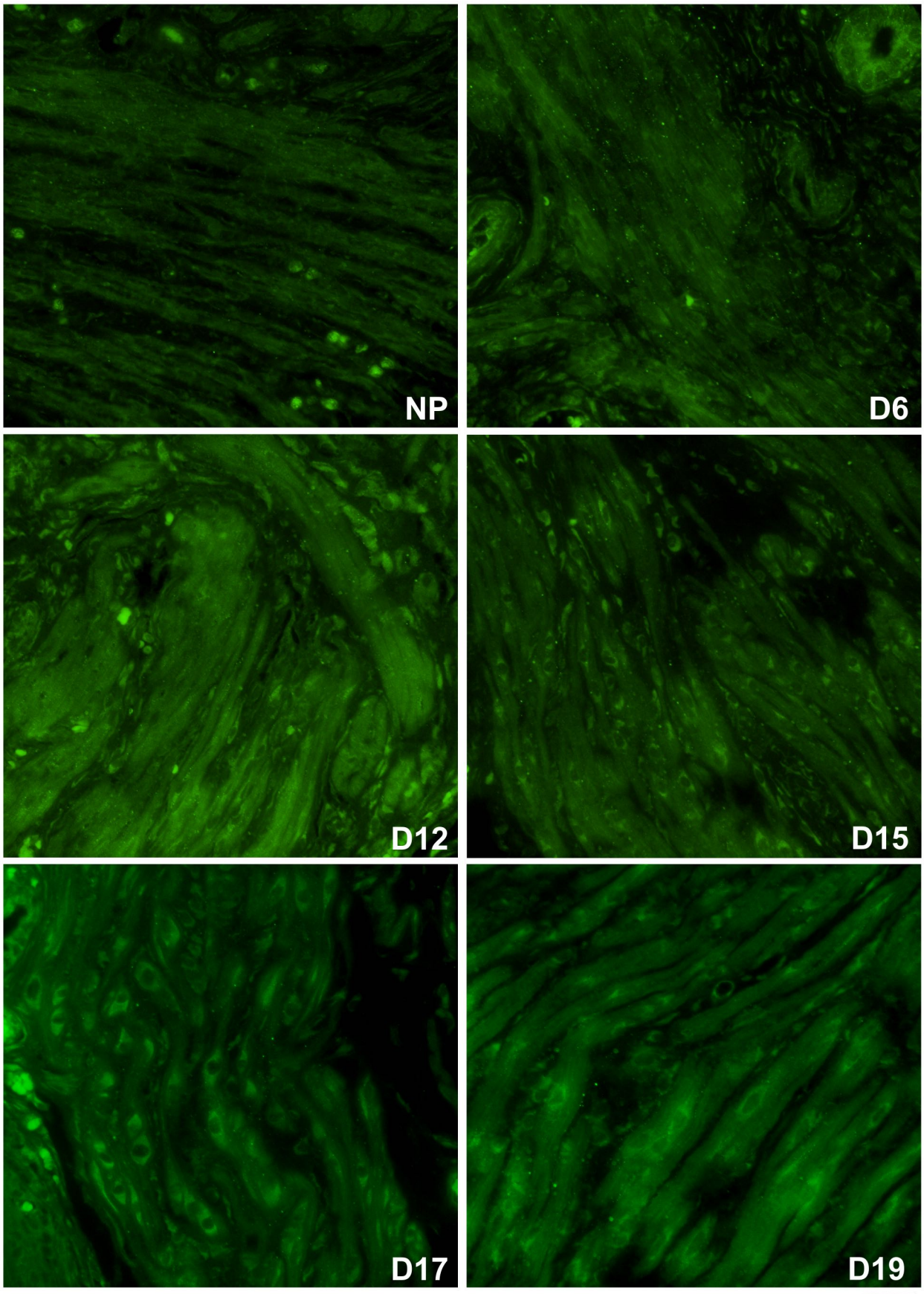
NP
D6
D12
D15
D17
D19

3.10). At times, Nox4 immunostaining was observed in some interstitial cells between muscle bundles from D12 to D21 of gestation in both muscle layers (Figures 3.7-3.10).

To better assess the spatial localization of Nox4 in the circular and longitudinal muscle layers, differential contrast enhancement was performed on images captured with a 100x oil objective. In the longitudinal and circular muscle layers, it was confirmed that Nox4 prominently accumulated in perinuclear regions within myocytes and in some instances associated with myocyte membranes (Figure 3.11, 3.12).

3.3. Expression of NoxO1, NoxA1 and p22phox Protein Subunits in Pregnant Rat Myometrium

Immunoblot analysis of NoxO1 protein expression in myometrium revealed detection of the subunit at all timepoints examined, but with very low levels at D15 followed by a significant increase during late gestation and labour (Figure 3.13). NoxO1 expression on D21, D22, D23 and PP was significantly greater than expression at NP, D6, D12 and D15 (*). Expression on D22 and D23 was significantly greater than on D17 (#) while NoxO1 levels on D21, D22 and D23 were significantly elevated compared to levels at D19 (@). Lastly, NoxO1 expression on D22 was significantly greater than expression on D21, D23 and PP (^) while expression on D17 was significantly higher than at D15 (**).

NoxA1 protein expression in myometrium was also detectable at all timepoints examined, but with higher expression during early gestation (Figure 3.14). Expression of NoxA1 was significantly higher on D12 compared to NP, D6, D21, D23 and PP (*). In contrast, immunoblot analysis of p22phox demonstrated robust detection in NP myometrium and early gestational timepoints with markedly decreasing levels of expression as gestation proceeded (Figure 3.15). Expression at NP was significantly higher compared to expression on D21 to D23 (*). Expression on D6 was significantly greater compared to expression on D19 to PP (**) while expression on D12 was significantly higher compared to expression on D17 to PP (***). Lastly, expression on D15 was significantly higher compared to expression on D23 (#).

Figure 3.10. Immunofluorescence detection of Nox4 in circular uterine smooth muscle layers from pregnant rat uterine horns at day (D) 21, D22, and D23 of gestation and 1-day post-partum (PP). Representative images are shown for each timepoint. Expression was detected using a rabbit polyclonal anti-Nox4 antibody followed by an anti-rabbit FITC conjugated antibody. The detection of Nox4, particularly in perinuclear regions, progressively subsided from D21 to PP. IgG, non-specific rabbit immunoglobulin used in place of the primary antiserum. Scale bar = 50μm.

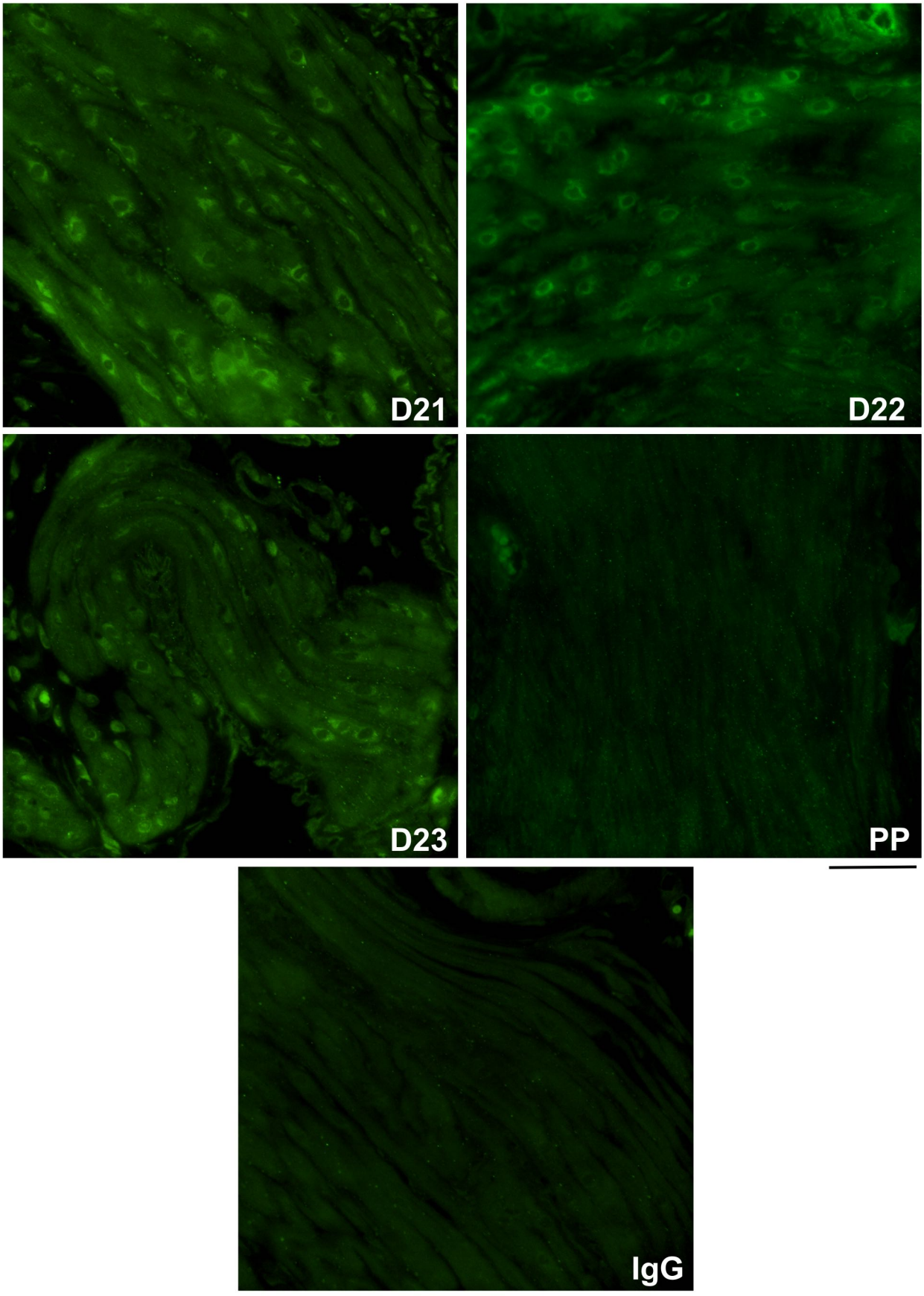
D21
D22
D23
PP
IgG

Figure 3.11. Assessment of Nox4 immunostaining in longitudinal muscle of rat myometrium during pregnancy by differential contrast enhancement. Select tissue sections of interest were chosen and a z-series of optical images (7 images; each 0.25 μm thick) collected with a 100X oil objective. Images were then processed post acquisition with the CellSens Differential Contrast Enhancement plugin. Images of Nox4 immunostaining in longitudinal uterine smooth muscle layers from pregnant rats at day (D) 6, D12, D15, D17, D19 and D21 of gestation were analyzed. Representative images are shown for each timepoint. Note the specific perinuclear localization. Scale bar = 25μm.

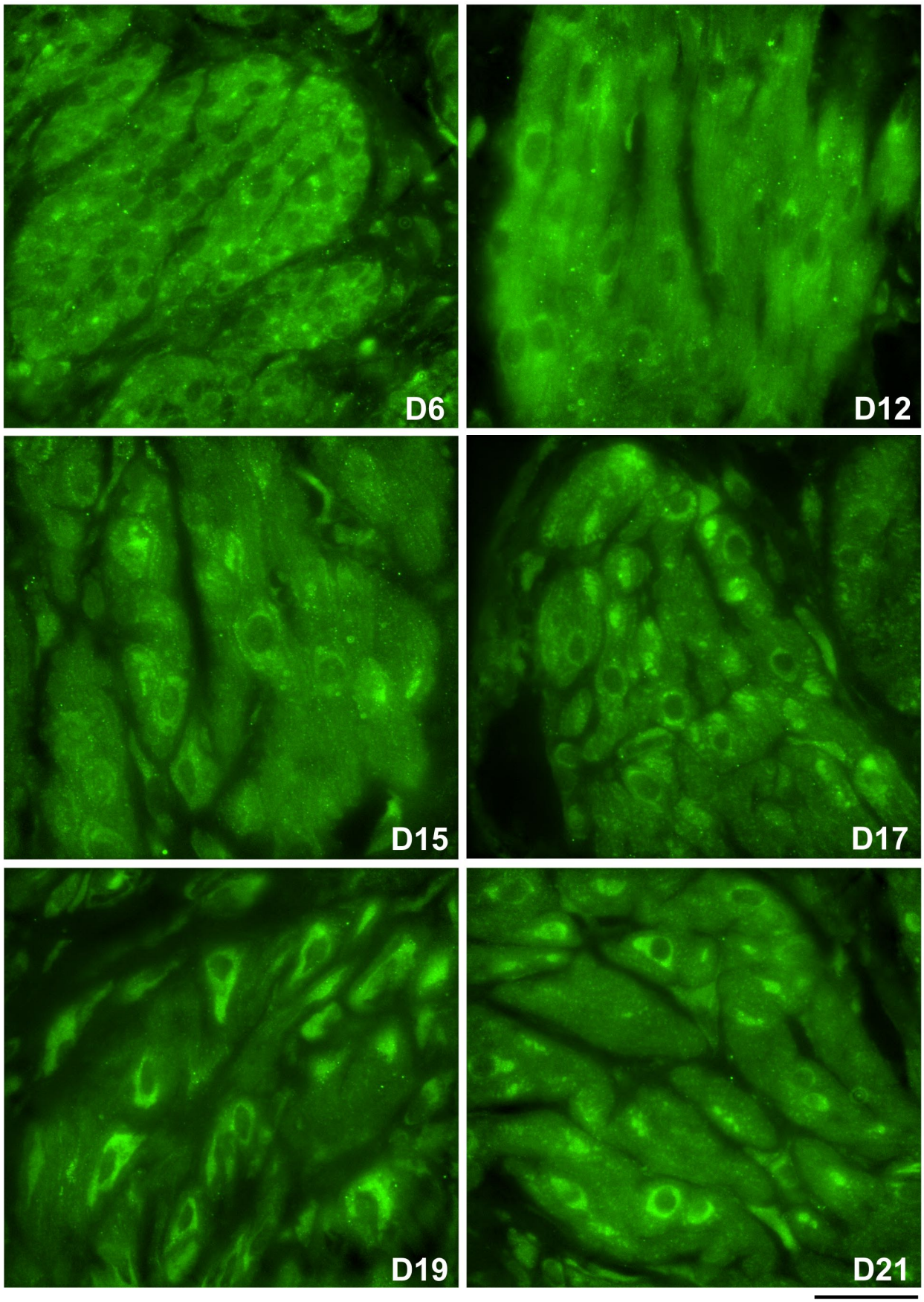
D6
D12
D15
D17
D19
D21

Figure 3.12. Assessment of Nox4 immunostaining in circular muscle of rat myometrium during pregnancy by differential contrast enhancement. Select tissue sections of interest were chosen and a z-series of optical images (7 images; each 0.25 μm thick) collected with a 100X oil objective. Images were then processed post acquisition with the CellSens Differential Contrast Enhancement plugin. Images of Nox4 immunostaining in circular uterine smooth muscle layers from pregnant rats on day (D) 6, D12, D15, D17, D19 and D21 of gestation were analyzed. Representative images are shown for each timepoint. Note the specific perinuclear localization. Scale bar = 25μm.

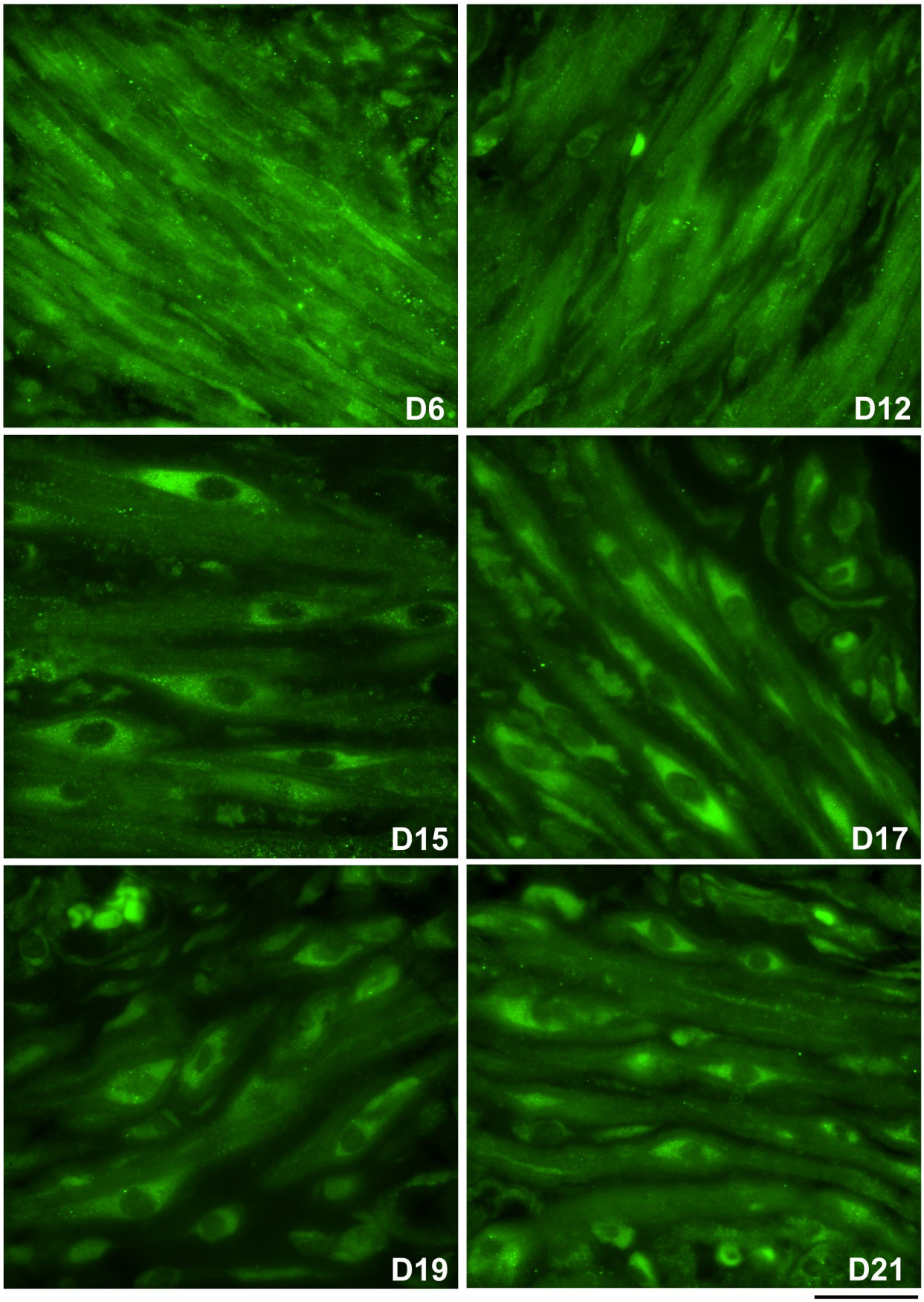
D6
D12
D15
D17
D19
D21

Figure 3.13. Immunoblot analysis of NoxO1 expression in rat myometrium throughout gestation. Representative immunoblots are shown above the densitometric analysis. Expression levels were determined in non-pregnant rat tissue (NP) and in tissue from day (D) 6, D12, D15, D17, D19, D21, D22, D23 (active labour) of pregnancy as well as 1-day post-partum (PP). *Expression on D21, D22, D23 and PP was significantly greater than expression at NP, D6, D12 and D15. **Expression on D17 was significantly higher than D15. #Expression on D22 and D23 was significantly higher than D17. @Expression on D21, D22 and D23 were significantly higher than D19. ^Expression on D22 was significantly higher than D21, D23 and PP. Values were considered significantly different when $P<0.05$. Glyceraldehyde 3-Phosphate Dehydrogenase (GAPDH) protein expression was used as a normalization control for densitometric analysis. Densitometric data are from 4 independent experiments (n=4 per timepoint).

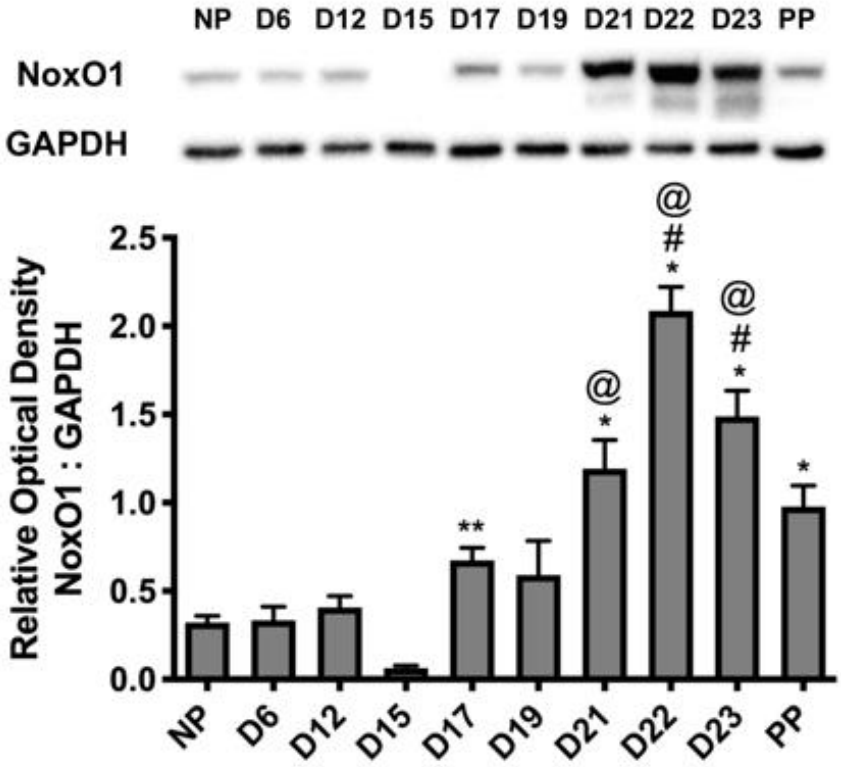
NP D6 D12 D15 D17 D19 D21 D22 D23 PP
NoxO1
GAPDH
Relative Optical Density
NoxO1 : GAPDH
2.5
2.0
1.5
1.0
0.5
0.0
**
@
*
@
#
*
@
#
*
*
NP
D6
D12
D15
D17
D19
D21
D22
D23
PP

Figure 3.14. Immunoblot analysis of NoxA1 expression in rat myometrium throughout gestation. Representative immunoblots are shown above the densitometric analysis. Expression levels were determined in non-pregnant rat tissue (NP) and in tissue from day (D) 6, D12, D15, D17, D19, D21, D22, D23 (active labour) of pregnancy as well as 1-day post-partum (PP). *Expression on D12 was significantly higher than NP, D6, D21, D23 and PP ($P<0.05$). Glyceraldehyde 3-Phosphate Dehydrogenase (GAPDH) protein expression was used as a normalization control for densitometric analysis. Densitometric data are from 4 independent experiments (n=4 per timepoint).

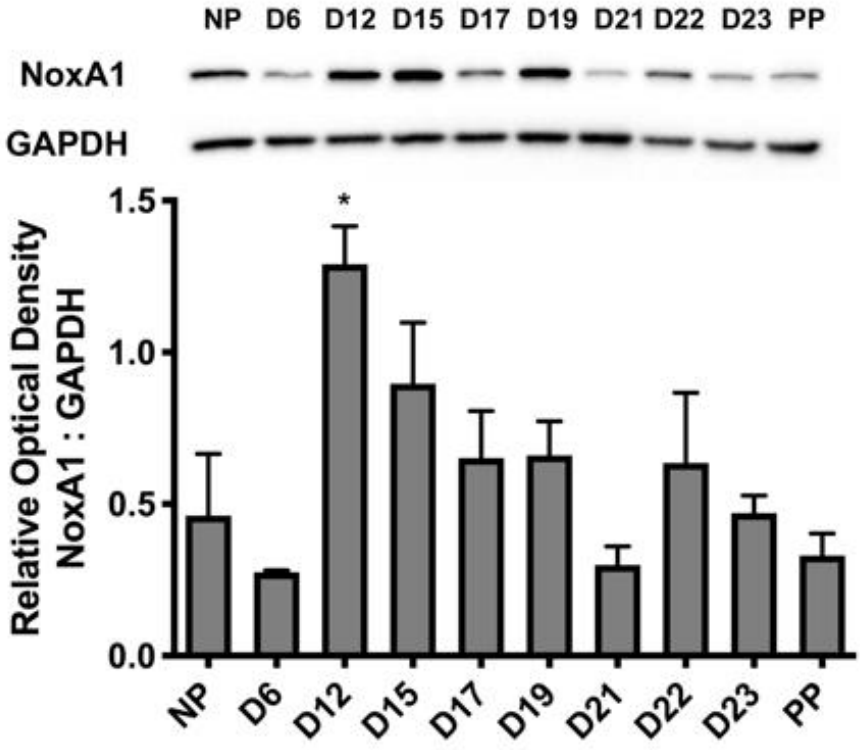
NP D6 D12 D15 D17 D19 D21 D22 D23 PP
NoxA1
GAPDH
Relative Optical Density
NoxA1 : GAPDH
1.5
1.0
0.5
0.0
*
NP D6 D12 D15 D17 D19 D21 D22 D23 PP

Figure 3.15. Immunoblot analysis of p22phox expression in rat myometrium throughout gestation. Representative immunoblots are shown above the densitometric analysis. Expression levels were determined in non-pregnant tissue (NP) and in tissue from day (D) 6, D12, D15, D17, D19, D21, D22, D23 (active labour) of pregnancy as well as 1-day post-partum (PP). *Expression at NP was significantly higher than D21, D22 and D23. **Expression on D6 was significantly higher than D19, D21, D22, D23 and PP. ***Expression at D12 was significantly higher than D17, D19, D21, D22, D23 and PP. #Expression on D15 was significantly higher than D23. Values were considered significantly different when $P<0.05$. Glyceraldehyde 3-Phosphate Dehydrogenase (GAPDH) protein expression was used as a normalization control for densitometric analysis. Densitometric data are from 4 independent experiments (n=4 per timepoint).

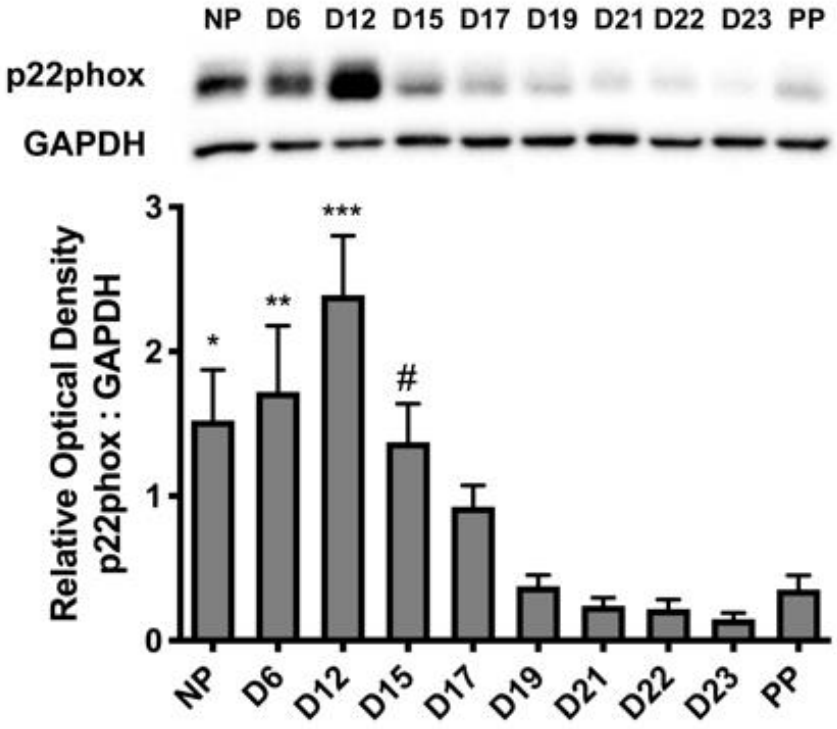
NP D6 D12 D15 D17 D19 D21 D22 D23 PP
p22phox
GAPDH
Relative Optical Density
p22phox : GAPDH
3
2
1
0
*
**
***
#
NP
D6
D12
D15
D17
D19
D21
D22
D23
PP

3.4. Spatial localization of NoxO1 in Pregnant Rat Myometrium

The spatial localization of NoxO1 in rat myometrium was assessed throughout gestation by immunofluorescence analysis. There was little detection of NoxO1 in NP myometrium and at D6 of gestation in both muscle layers. In the longitudinal muscle layer, NoxO1 localization was particularly prominent from D15 to PP with detection in the myocyte cytoplasm and associated with plasma membranes (Figures 3.16, 3.17). In the circular muscle layer, NoxO1 expression was detectable in perinuclear and membrane-associated regions of myometrial cells from D15 to D23 of gestation (Figures 3.18, 3.19).

3.5. Co-localization of Nox1 and NoxA1 in Pregnant Rat Myometrium

With Nox1 and NoxA1 protein expression as well as spatial localization individually assessed, the availability of appropriate antisera facilitated examination of how Nox1 may interact with required NoxA1. To assess any potential association of Nox1 with NoxA1 in situ, the spatial co-immunofluorescence localization of both proteins in rat myometrium was assessed. Nox1 localization was detected as described in *Section 3.2*.

In NP and D6 samples of both muscle layers, there was very low detection of NoxA1 immunostaining relative to later gestational timepoints, especially in the circular muscle layer (Figure 3.20, 3.25). Thereafter, NoxA1 immunostaining was more detectable in both muscle layers as pregnancy progressed (Figures 3.21-3.24 and 3.26-3.29). NoxA1 immunostaining was detectable throughout the entire myocyte including the cytoplasm and in association with membranes. In some timepoints, there appeared to be clear perinuclear accumulation of NoxA1 (Figures 3.21, 3.27) but no detection within the nucleus itself. Relative to smooth muscle layers, NoxA1 in the surrounding interstitium was virtually undetectable. Non-specific background immunofluorescence was assessed using mouse or rabbit IgG in place of primary antisera (Fig 3.30). Overall, co-localization of Nox1 and NoxA1 was observed throughout gestation, but from D17 onwards Nox1 immunostaining was frequently more detectable as concentrated foci in cytoplasmic regions compared to NoxA1 (Figures 3.20-3.29).

Figure 3.16. Immunofluorescence detection of NoxO1 in longitudinal uterine smooth muscle layers from non-pregnant (NP) rats and pregnant rat uterine horns at day (D) 6, D12, D15, D17 and D19 of gestation. Representative images are shown for each timepoint. Expression was detected using a rabbit polyclonal anti-NoxO1 antibody followed by an anti-rabbit FITC conjugated antibody. Cytoplasmic detection of NoxO1 progressively increased from NP to D19 of gestation. Scale bar = 50μm.

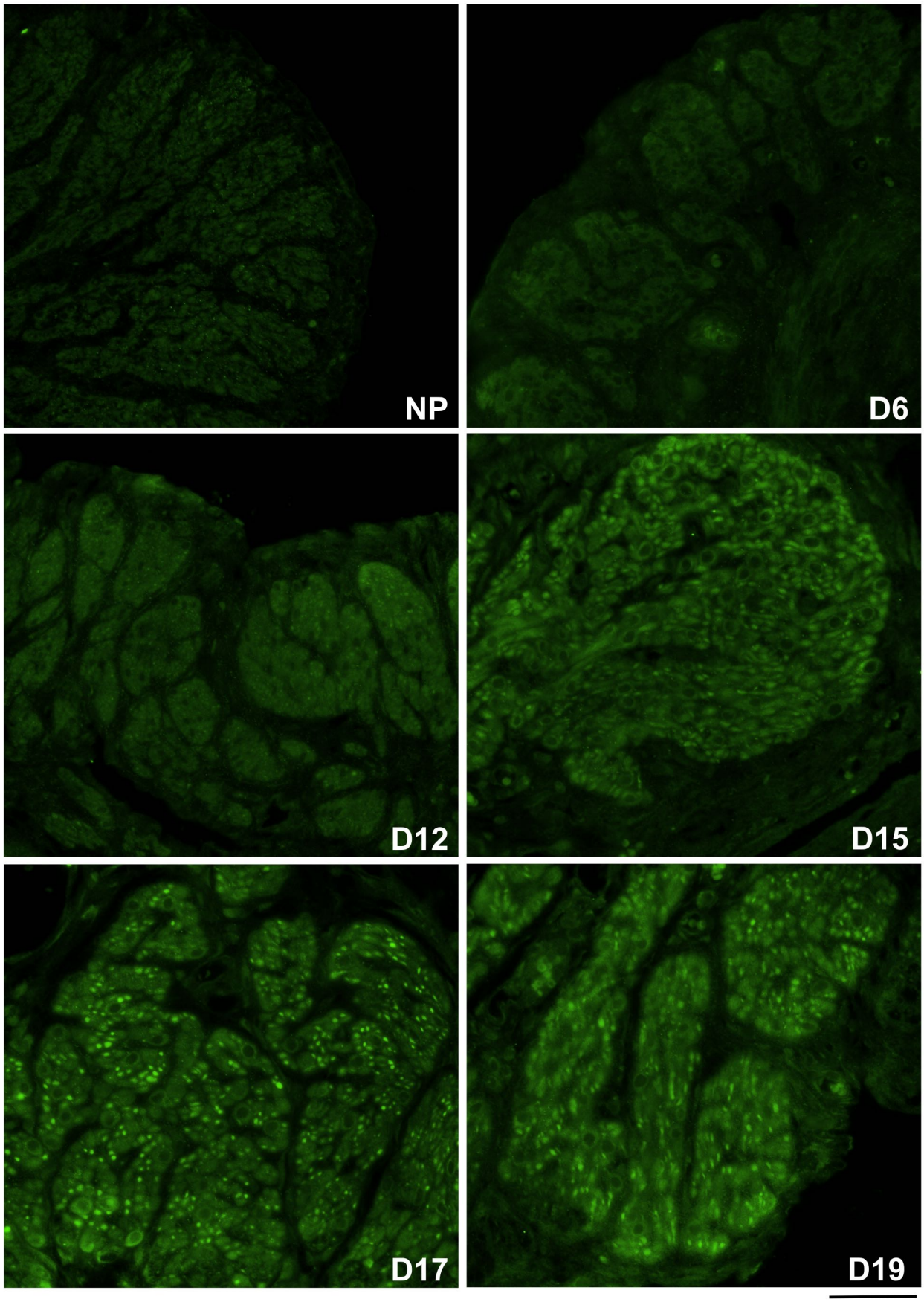
NP
D6
D12
D15
D17
D19

Figure 3.17. Immunofluorescence detection of NoxO1 in longitudinal uterine smooth muscle layers from pregnant rat uterine horns at day (D) 21, D22, and D23 of gestation and 1-day post-partum (PP). Representative images are shown for each timepoint. Expression was detected using a rabbit polyclonal anti-NoxO1 antibody followed by an anti-rabbit FITC conjugated antibody. NoxO1 immunostaining was observed in the myocyte cytoplasm and associated with plasma membranes. IgG, non-specific rabbit immunoglobulin used in place of the primary antiserum. Scale bar = 50μm.

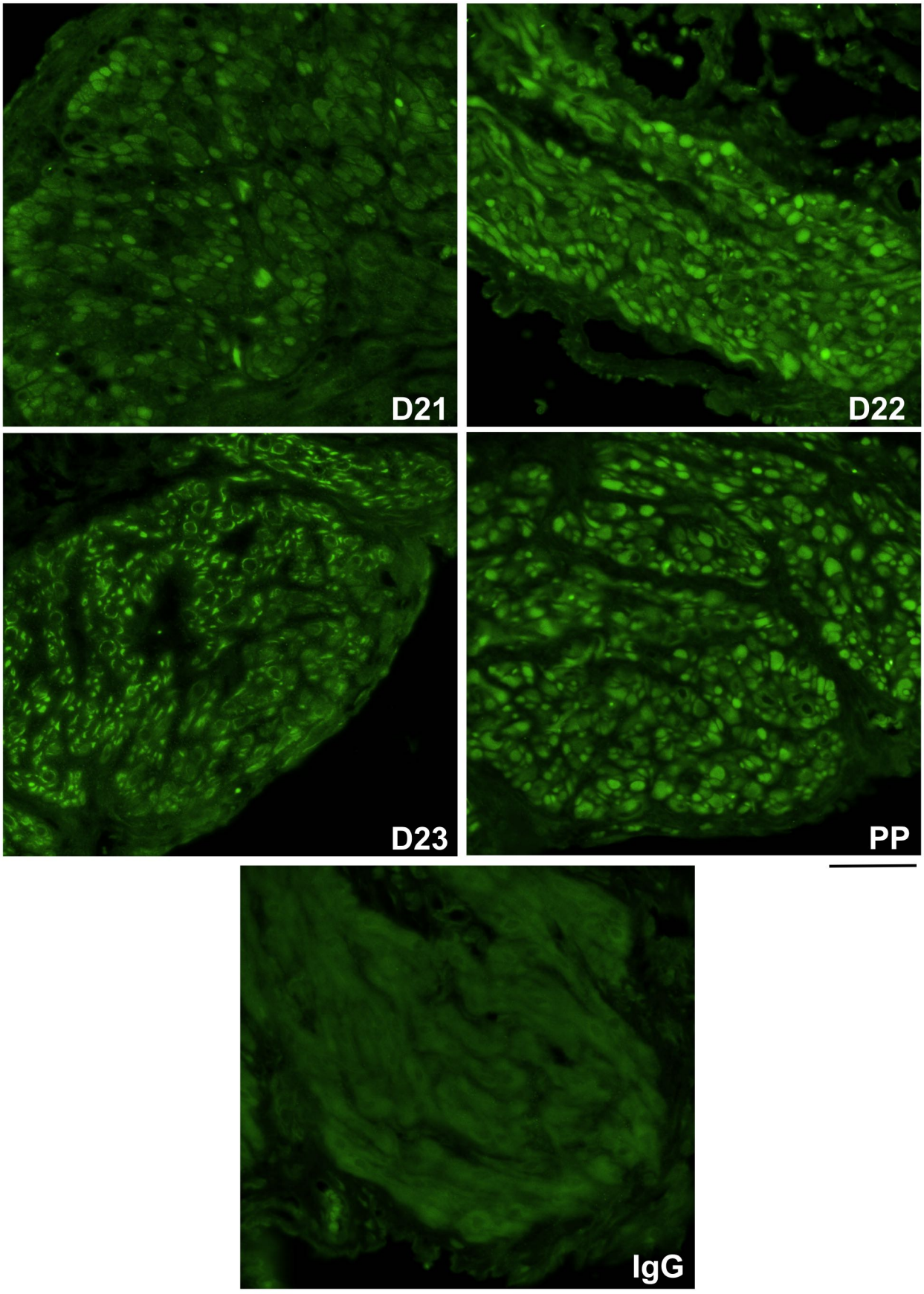
D21
D22
D23
PP
IgG

Figure 3.18. Immunofluorescence detection of NoxO1 in circular uterine smooth muscle layers from non-pregnant (NP) rats and pregnant rat uterine horns at day (D) 6, D12, D15, D17 and D19 of gestation. Representative images are shown. Expression was detected using a rabbit polyclonal anti-NoxO1 antibody followed by an anti-rabbit FITC conjugated antibody. Cytoplasmic and membrane-associated detection of NoxO1 progressively increased from NP to D19 of gestation. Scale bar = 50μm.

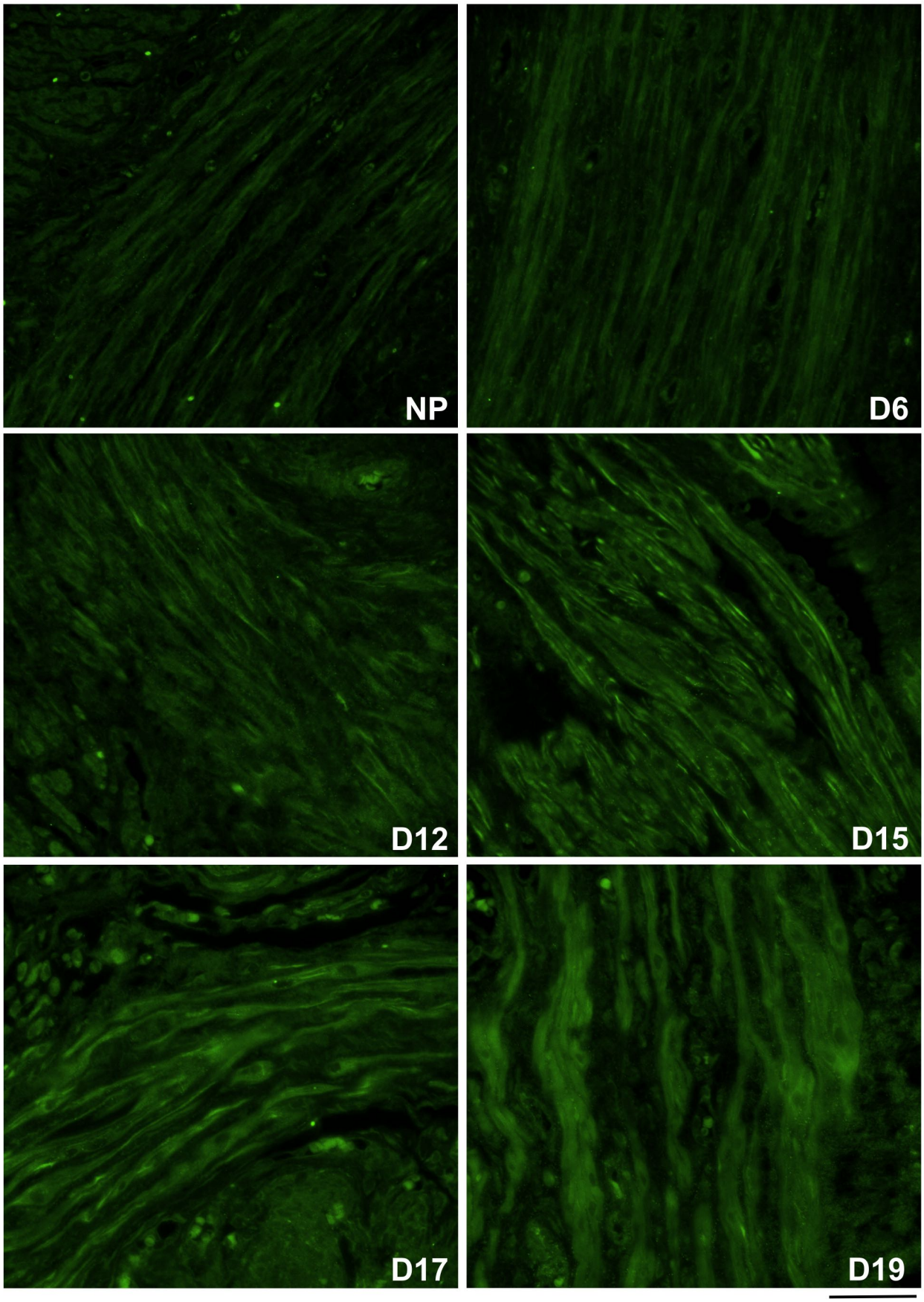
NP
D6
D12
D15
D17
D19

Figure 3.19. Immunofluorescence detection of NoxO1 in circular uterine smooth muscle layers from pregnant rat uterine horns at day (D) 21, D22, and D23 of gestation and 1-day post-partum (PP). Representative images are shown for each timepoint. Expression was detected using a rabbit polyclonal anti-NoxO1 antibody followed by an anti-rabbit FITC conjugated antibody. NoxO1 immunostaining was observed surrounding the nucleus and in membrane-associated regions of myocytes. IgG, non-specific rabbit immunoglobulin used in place of the primary antiserum. Scale bar = 50μm.

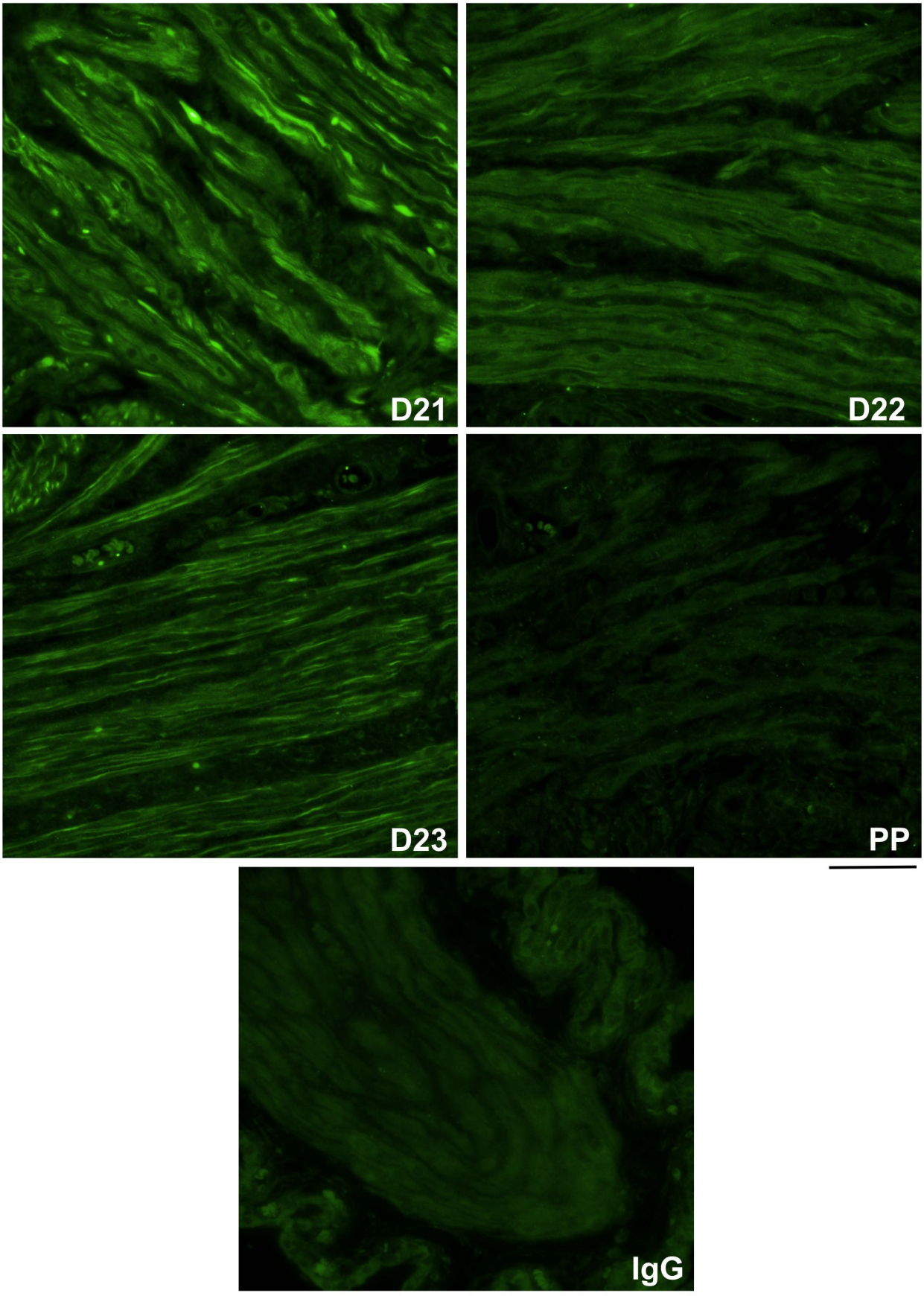
D21
D22
D23
PP
IgG

Figure 3.20. Co-immunofluorescence detection of Nox1 and NoxA1 in longitudinal uterine smooth muscle layers of non-pregnant (NP) and pregnant rats at day (D) 6 of gestation. Representative images are shown for each timepoint. Expression was detected using a rabbit polyclonal anti-Nox1 antibody followed by an anti-rabbit FITC conjugated antibody and a mouse monoclonal anti-NoxA1 antibody followed by an anti-mouse RRX conjugated antibody. Nox1 immunostaining was observed in the myocyte cytoplasm. Low detection of NoxA1 was also observed in myocyte cytoplasm. Some co-localization of Nox1 and NoxA1 was apparent (yellow) at both timepoints. Scale bar = 50μm.

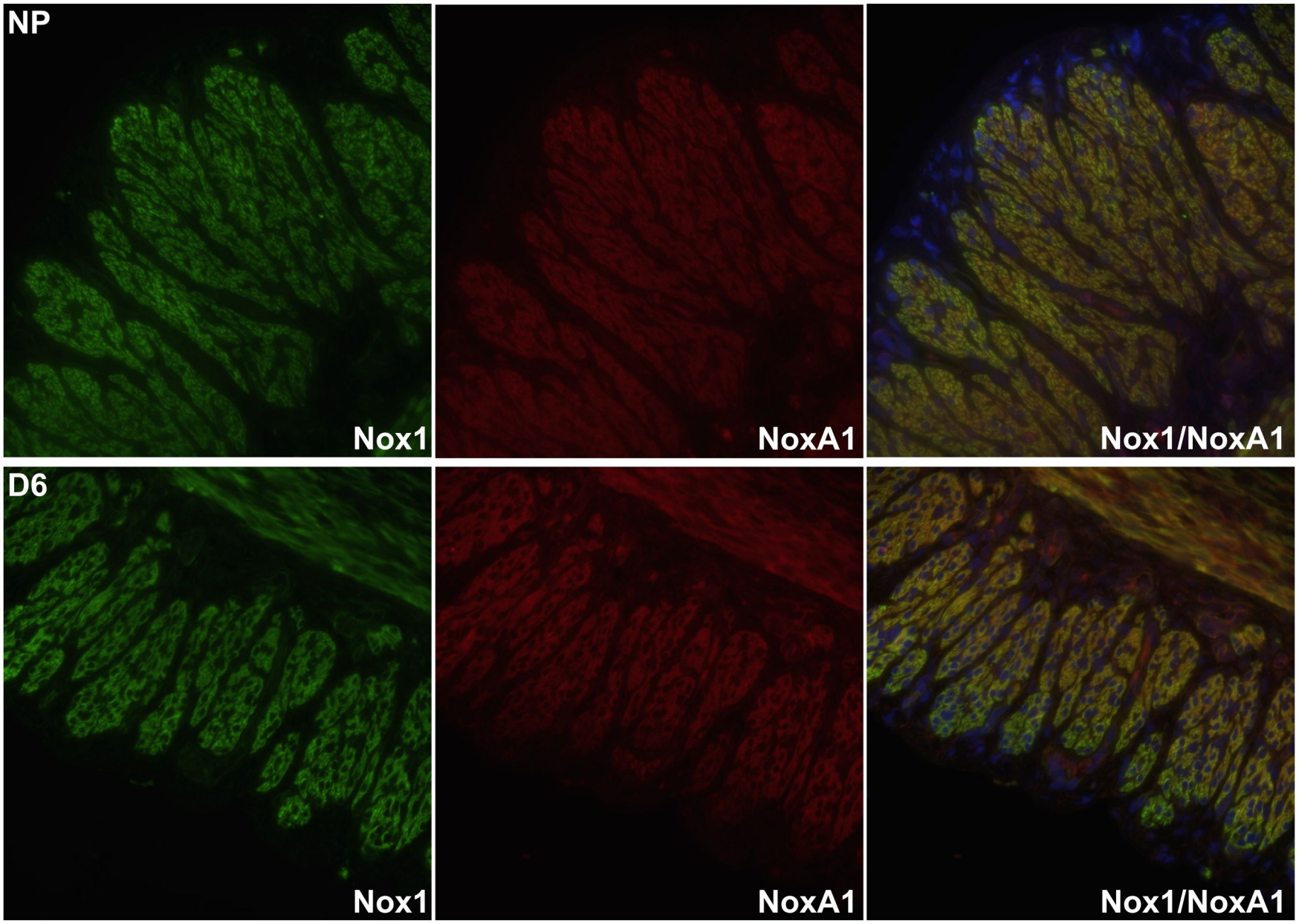
NP
Nox1
NoxA1
Nox1/NoxA1
D6
Nox1
NoxA1
Nox1/NoxA1

Figure 3.21. Co-immunofluorescence detection of Nox1 and NoxA1 in longitudinal uterine smooth muscle layers from pregnant rats at day (D) 12 and D15 of gestation. Representative images are shown for each timepoint. Expression was detected using a rabbit polyclonal anti-Nox1 antibody followed by an anti-rabbit FITC conjugated antibody and a mouse monoclonal anti-NoxA1 antibody followed by an anti-mouse RRX conjugated antibody. Nox1 and NoxA1 immunostaining was observed throughout the entire myocyte, including the cytoplasm with some perinuclear accumulation. Co-localization of Nox1 and NoxA1 (yellow) in uterine myocytes was apparent at both timepoints. Scale bar = 50μm.

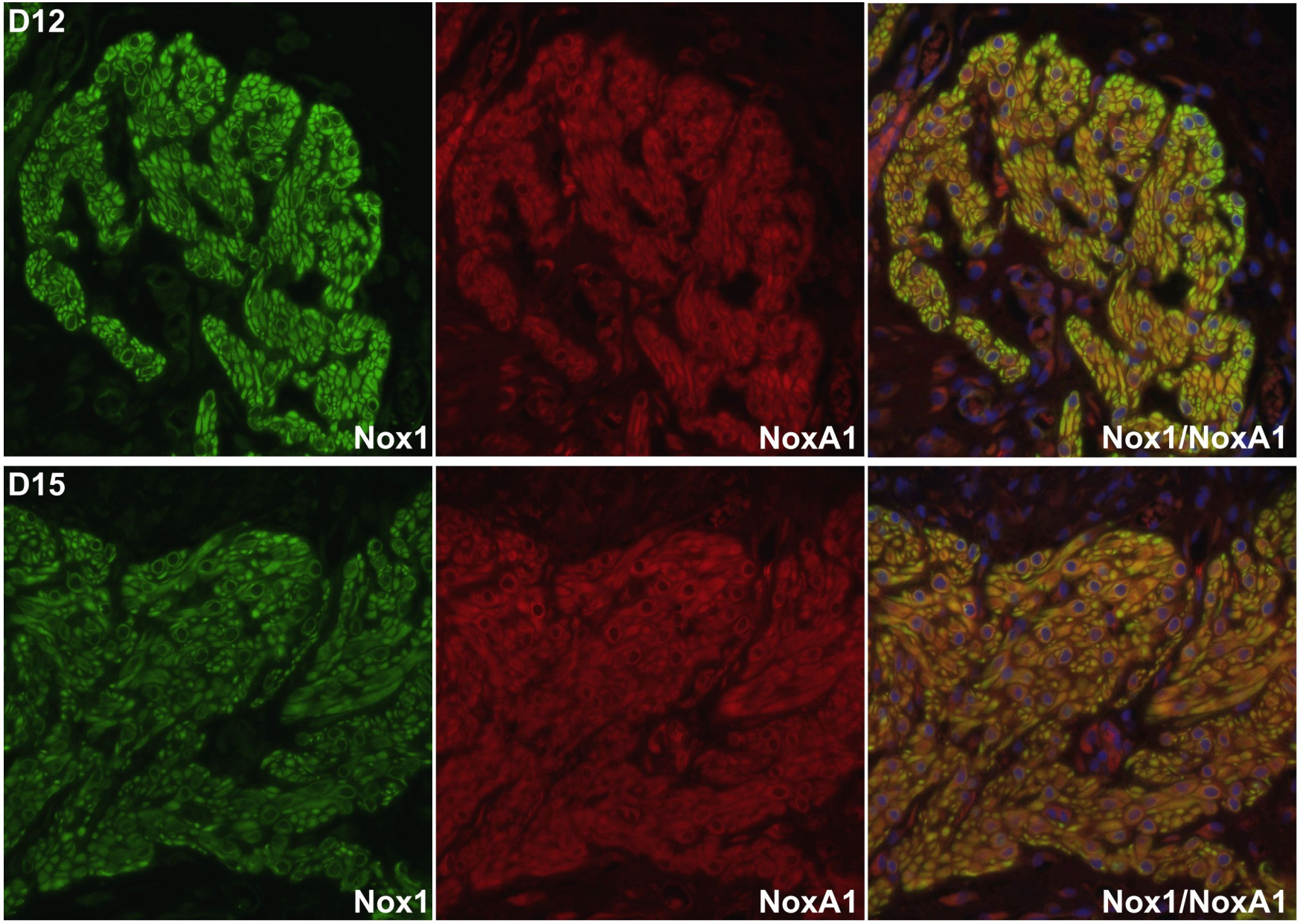
D12
Nox1
NoxA1
Nox1/NoxA1
D15
Nox1
NoxA1
Nox1/NoxA1

Figure 3.22. Co-immunofluorescence detection of Nox1 and NoxA1 in longitudinal uterine smooth muscle layers from pregnant rats at day (D) 17 and D19 of gestation. Representative images are shown for each timepoint. Expression was detected using a rabbit polyclonal anti-Nox1 antibody followed by an anti-rabbit FITC conjugated antibody and a mouse monoclonal anti-NoxA1 antibody followed by an anti-mouse RRX conjugated antibody. Nox1 and NoxA1 immunostaining was observed throughout the entire myocyte, but Nox1 was also noted in concentrated cytoplasmic foci that were not observed for NoxA1 immunolocalization. Co-localization of Nox1 and NoxA1 in uterine myocytes (yellow) was apparent at both timepoints. Scale bar = 50μm.

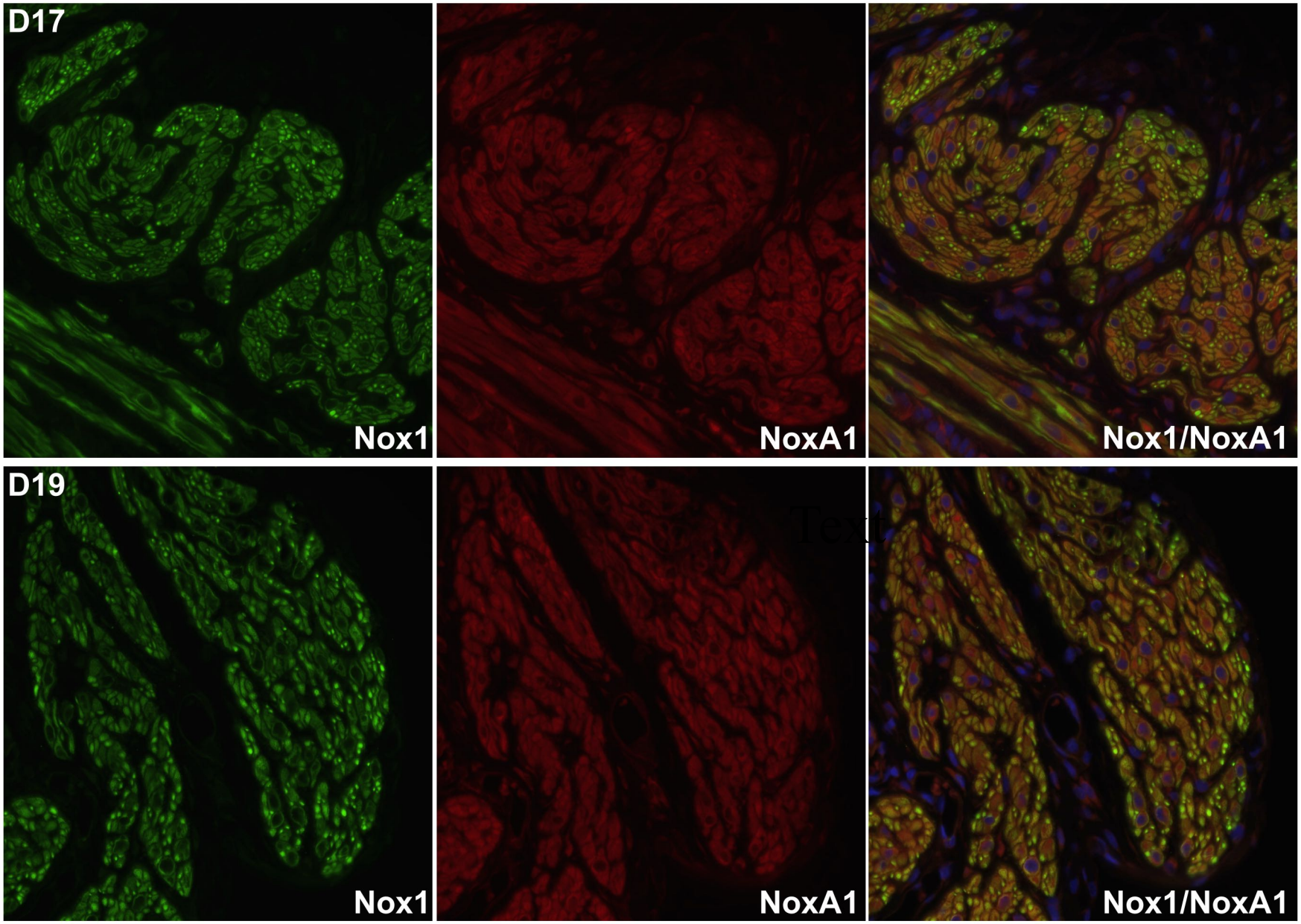
D17
Nox1
NoxA1
Nox1/NoxA1
D19
Nox1
NoxA1
Nox1/NoxA1

Figure 3.23. Co-immunofluorescence detection of Nox1 and NoxA1 in longitudinal uterine smooth muscle layers from pregnant rats at day (D) 21 and D22 of gestation. Representative images are shown for each timepoint. Expression was detected using a rabbit polyclonal anti-Nox1 antibody followed by an anti-rabbit FITC conjugated antibody and a mouse monoclonal anti-NoxA1 antibody followed by an anti-mouse RRX conjugated antibody. Nox1 and NoxA1 immunostaining was observed throughout the entire myocyte, but Nox1 immunostaining became highly detectable in some myocytes relative to others, unlike NoxA1. Co-localization of Nox1 and NoxA1 in uterine myocytes (yellow) was apparent at both timepoints. Scale bar = 50μm.

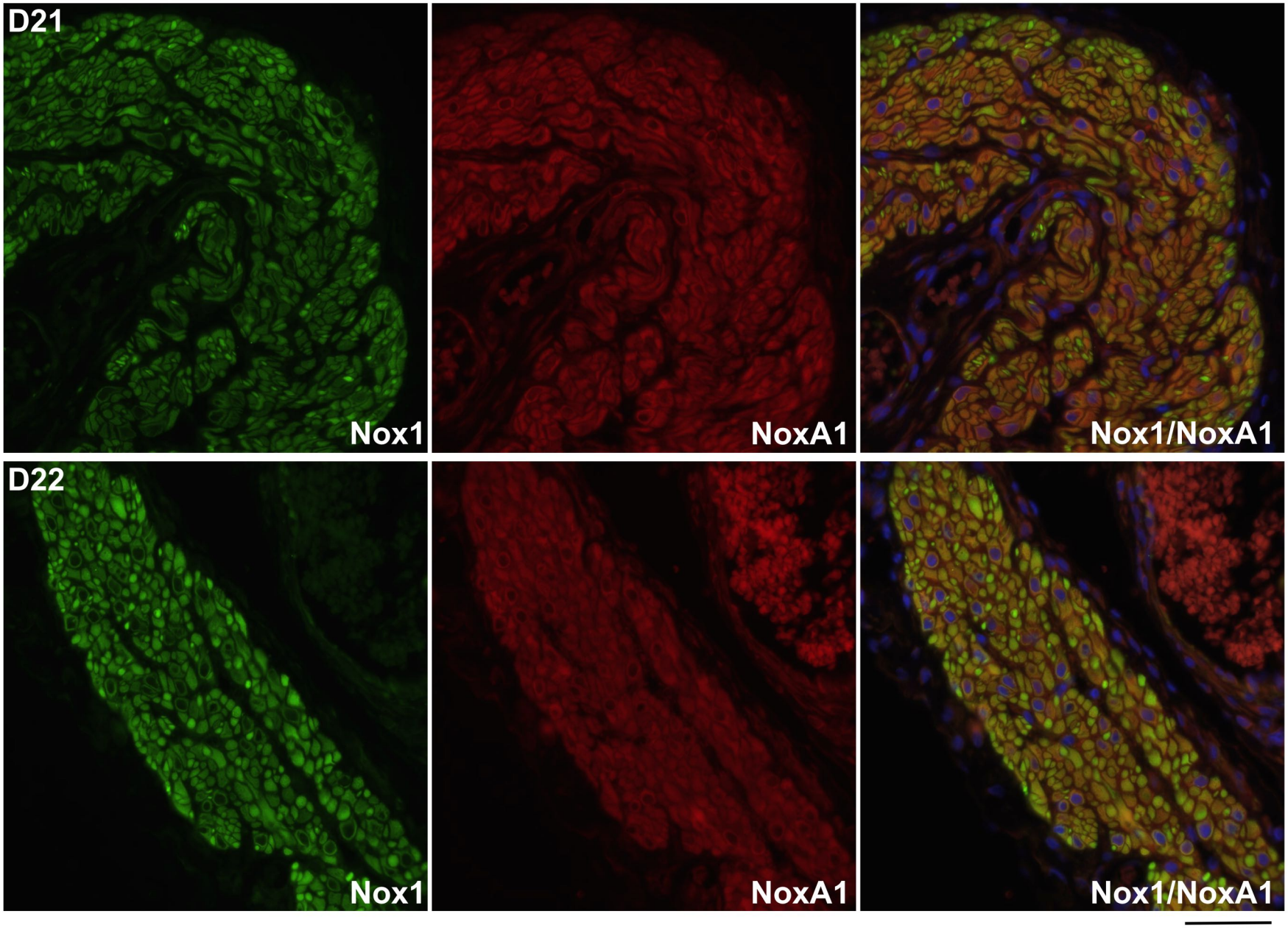
D21
Nox1
NoxA1
Nox1/NoxA1
D22
Nox1
NoxA1
Nox1/NoxA1

Figure 3.24. Co-immunofluorescence detection of Nox1 and NoxA1 in longitudinal uterine smooth muscle layers of pregnant rats at day (D) 23 of gestation and 1-day post-partum (PP). Representative images are shown for each timepoint. Expression was detected using a rabbit polyclonal anti-Nox1 antibody followed by an anti-rabbit FITC conjugated antibody and a mouse monoclonal anti-NoxA1 antibody followed by an anti-mouse RRX conjugated antibody. Nox1 and NoxA1 immunostaining was observed throughout the entire myocyte, but Nox1 became associated with membranes to a greater extent than NoxA1 at D23 and cytoplasmic foci of myocytes at PP relative to NoxA1. However, co-localization of Nox1 and NoxA1 (yellow) in uterine myocytes was apparent at both timepoints. Scale bar = 50μm.

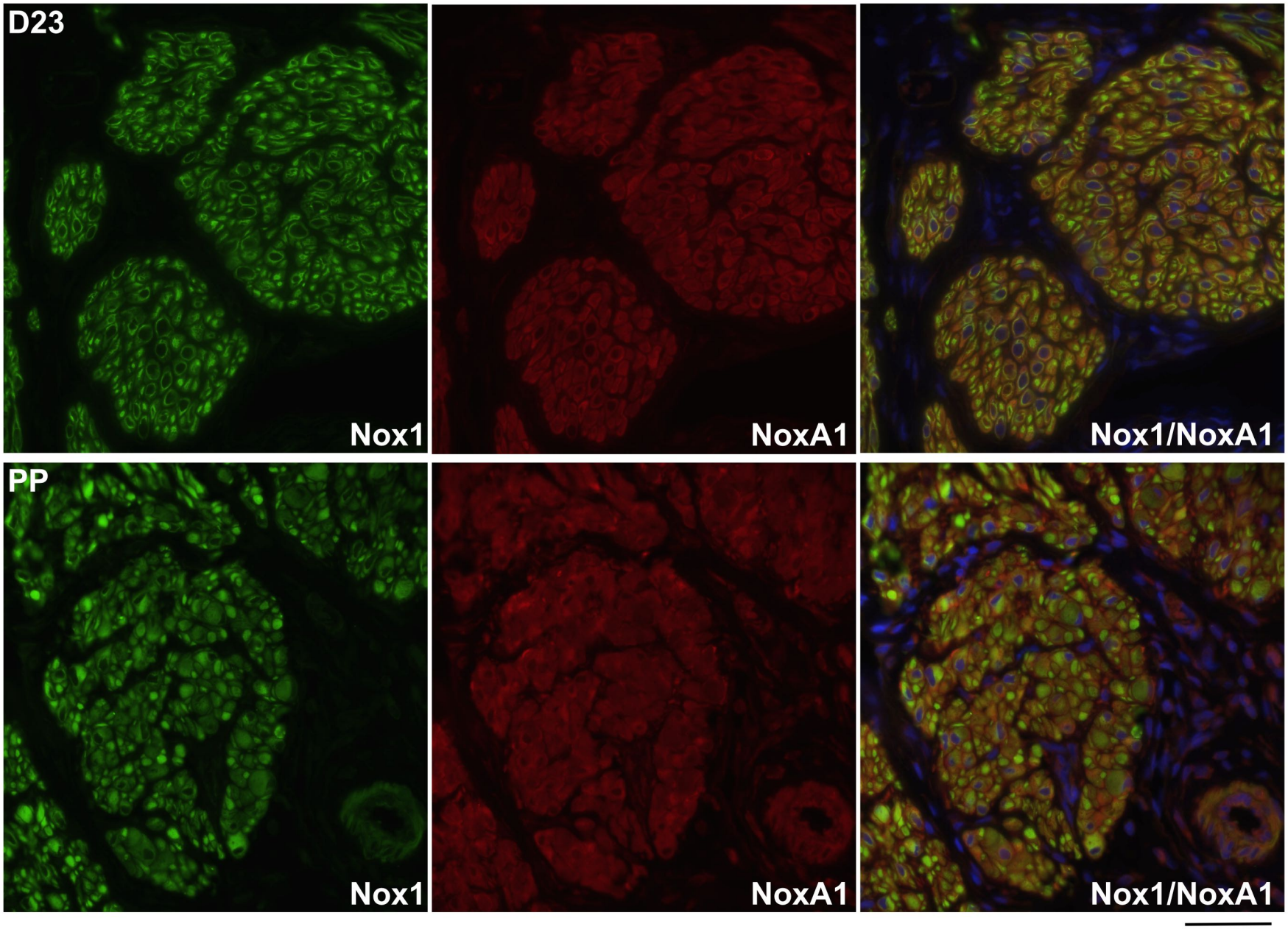
D23
Nox1
NoxA1
Nox1/NoxA1
PP
Nox1
NoxA1
Nox1/NoxA1

Figure 3.25. Co-immunofluorescence detection of Nox1 and NoxA1 in circular uterine smooth muscle layers of non-pregnant (NP) and pregnant rats at day (D) 6 of gestation. Representative images are shown for each timepoint. Expression was detected using a rabbit polyclonal anti-Nox1 antibody followed by an anti-rabbit FITC conjugated antibody and a mouse monoclonal anti-NoxA1 antibody followed by an anti-mouse RRX conjugated antibody. NoxA1 was virtually undetectable in NP tissue, while Nox1 and NoxA1 immunostaining was observed throughout myocytes at D6. Co-localization of Nox1 and NoxA1 in uterine myocytes (yellow) was apparent at D6. Scale bar = 50μm.

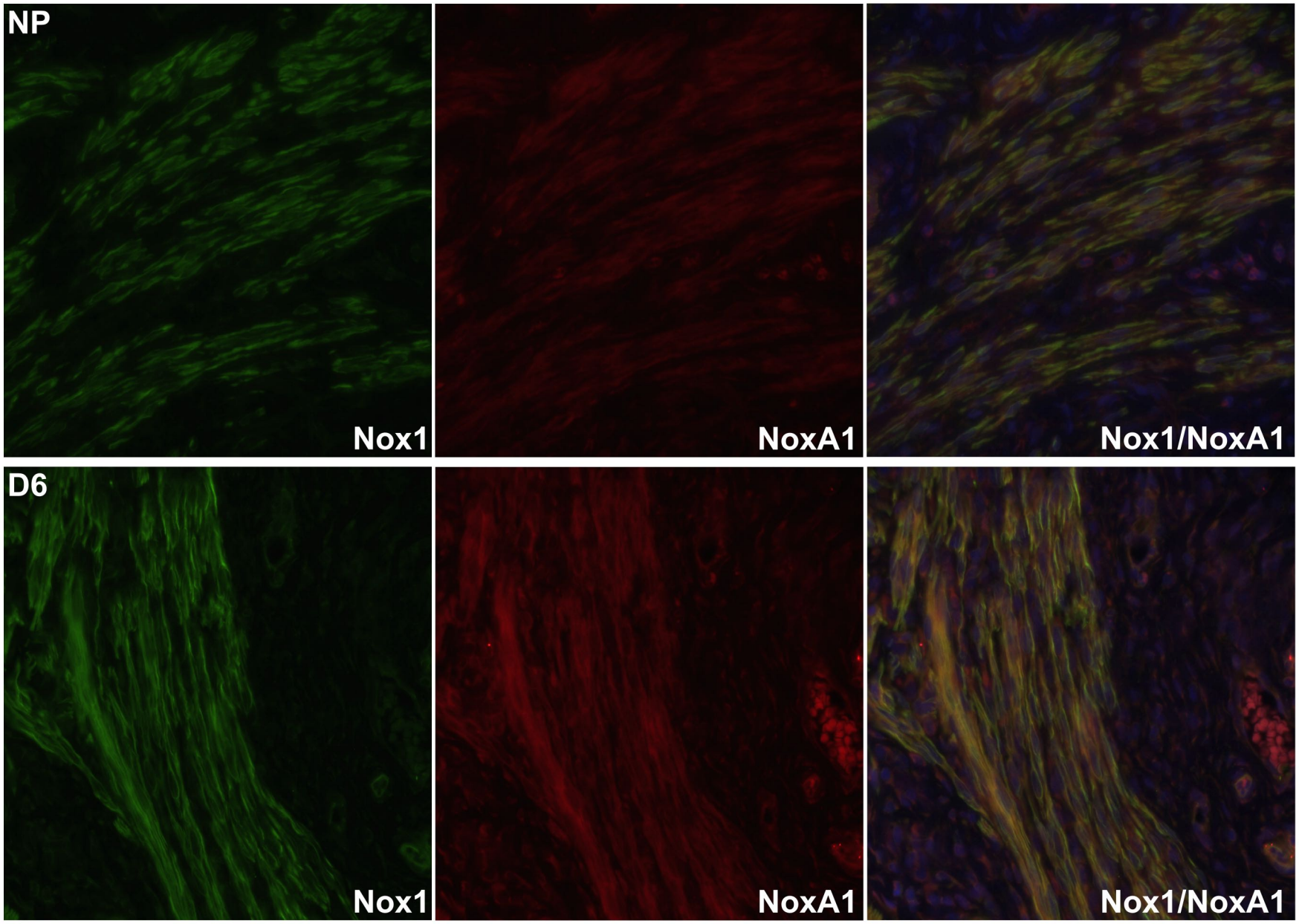
NP
Nox1
NoxA1
Nox1/NoxA1
D6
Nox1
NoxA1
Nox1/NoxA1

Figure 3.26. Immunofluorescence detection of Nox1 and NoxA1 in circular uterine smooth muscle layers from pregnant rats at day (D) 12 and D15 of gestation. Representative images are shown for each timepoint. Expression was detected using a rabbit polyclonal anti-Nox1 antibody followed by an anti-rabbit FITC conjugated antibody and a mouse monoclonal anti-NoxA1 antibody followed by an anti-mouse RRX conjugated antibody. Nox1 and NoxA1 immunostaining was observed throughout the entire myocyte. Co-localization of Nox1 and NoxA1 in uterine myocytes (yellow) was apparent at both timepoints. Scale bar = 50μm.

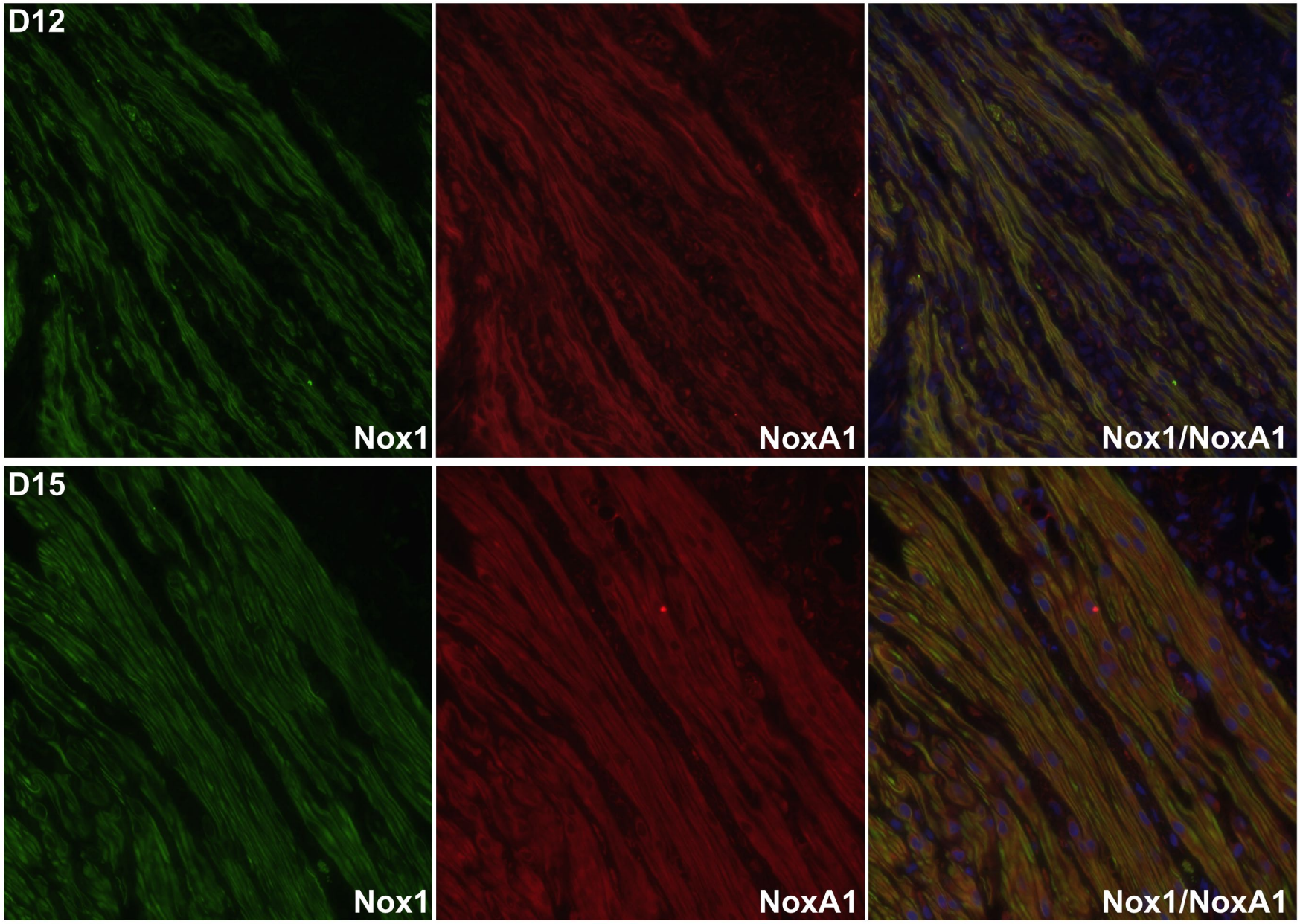
D12
Nox1
NoxA1
Nox1/NoxA1
D15
Nox1
NoxA1
Nox1/NoxA1

Figure 3.27. Immunofluorescence detection of Nox1 and NoxA1 in circular uterine smooth muscle layers from pregnant rats at day (D) 17 and D19 of gestation. Representative images are shown for each timepoint. Expression was detected using a rabbit polyclonal anti-Nox1 antibody followed by an anti-rabbit FITC conjugated antibody and a mouse monoclonal anti-NoxA1 antibody followed by an anti-mouse RRX conjugated antibody. Nox1 and NoxA1 immunostaining was observed throughout myocytes, with some perinuclear accumulation of both proteins and membrane-associated localization of Nox1. Some co-localization of Nox1 and NoxA1 in uterine myocytes (yellow) was apparent at both timepoints. Scale bar = 50μm.

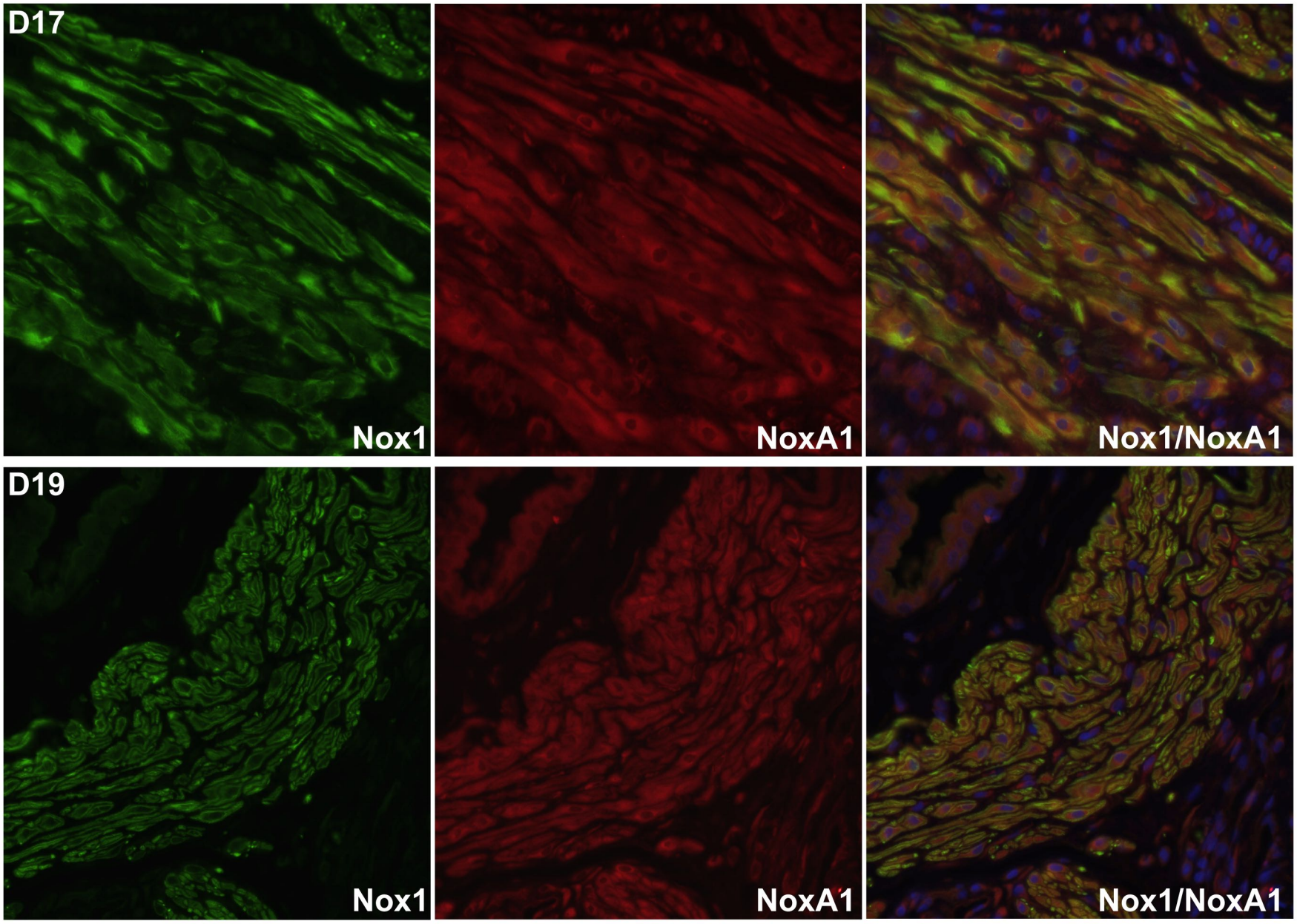
D17
Nox1
NoxA1
Nox1/NoxA1
D19
Nox1
NoxA1
Nox1/NoxA1

Figure 3.28. Immunofluorescence detection of Nox1 and NoxA1 in circular uterine smooth muscle layers from pregnant rats at day (D) 21 and D22 of gestation. Representative images are shown for each timepoint. Expression was detected using a rabbit polyclonal anti-Nox1 antibody followed by an anti-rabbit FITC conjugated antibody and a mouse monoclonal anti-NoxA1 antibody followed by an anti-mouse RRX conjugated antibody. Nox1 and NoxA1 immunostaining was observed throughout myocytes, but Nox1 immunostaining was also uniquely associated with membranes compared to NoxA1. Co-localization of Nox1 and NoxA1 in uterine myocytes (yellow) was apparent at both timepoints. Scale bar = 50μm.

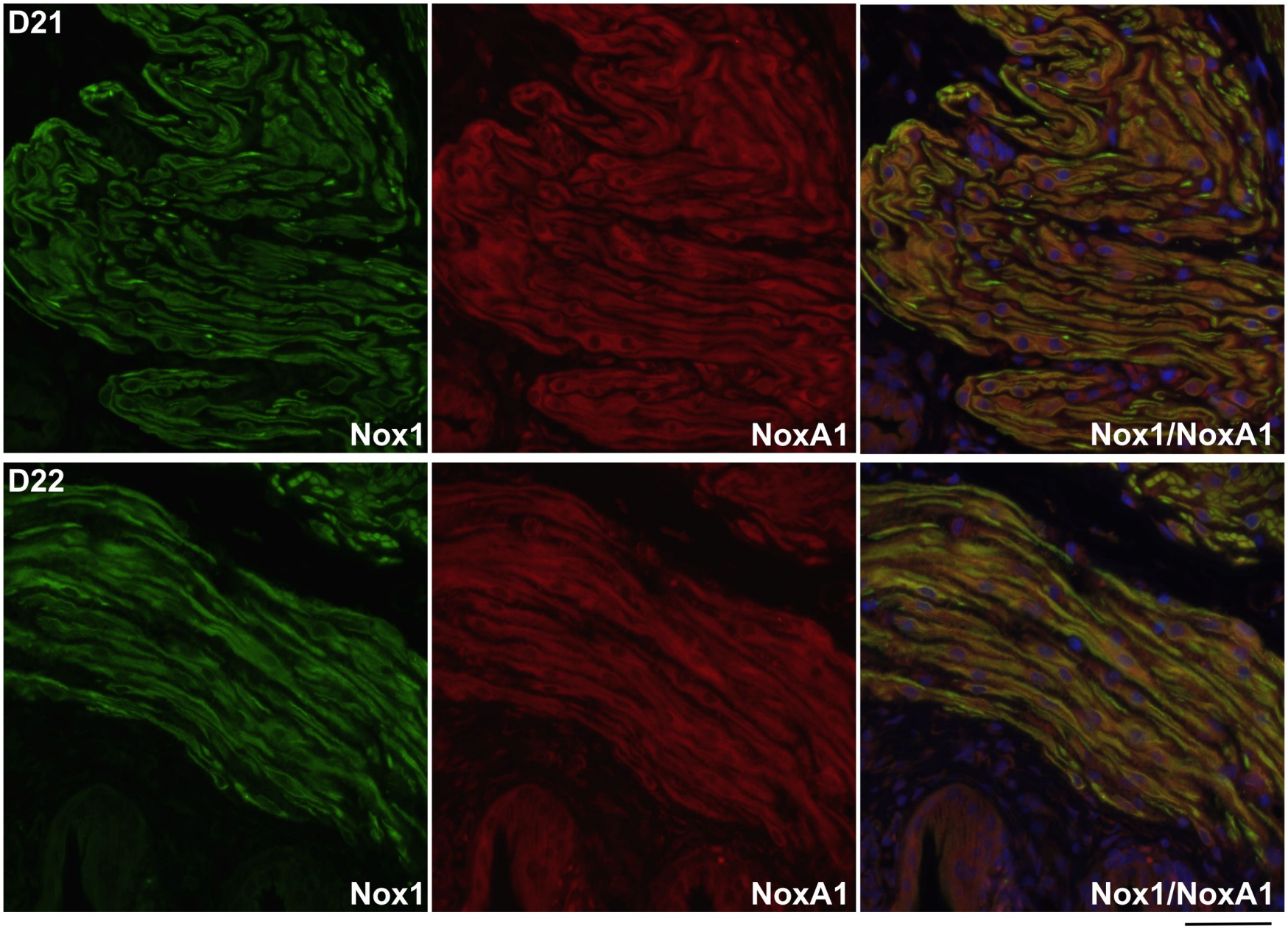
D21
Nox1
NoxA1
Nox1/NoxA1
D22
Nox1
NoxA1
Nox1/NoxA1

Figure 3.29. Immunofluorescence detection of Nox1 and NoxA1 in longitudinal uterine smooth muscle layers of pregnant rats at day (D) 23 of gestation and 1-day post-partum (PP). Representative images are shown for each timepoint. Expression was detected using a rabbit polyclonal anti-Nox1 antibody followed by an anti-rabbit FITC conjugated antibody and a mouse monoclonal anti-NoxA1 antibody followed by an anti-mouse RRX conjugated antibody. Nox1 and NoxA1 immunostaining was observed throughout myocytes, but Nox1 was especially associated with myocyte membranes compared to NoxA1 at D23, and cytoplasmic foci within myocytes at PP compared to NoxA1. Co-localization of Nox1 and NoxA1 in uterine myocytes was apparent at both timepoints. Scale bar = 50μm.

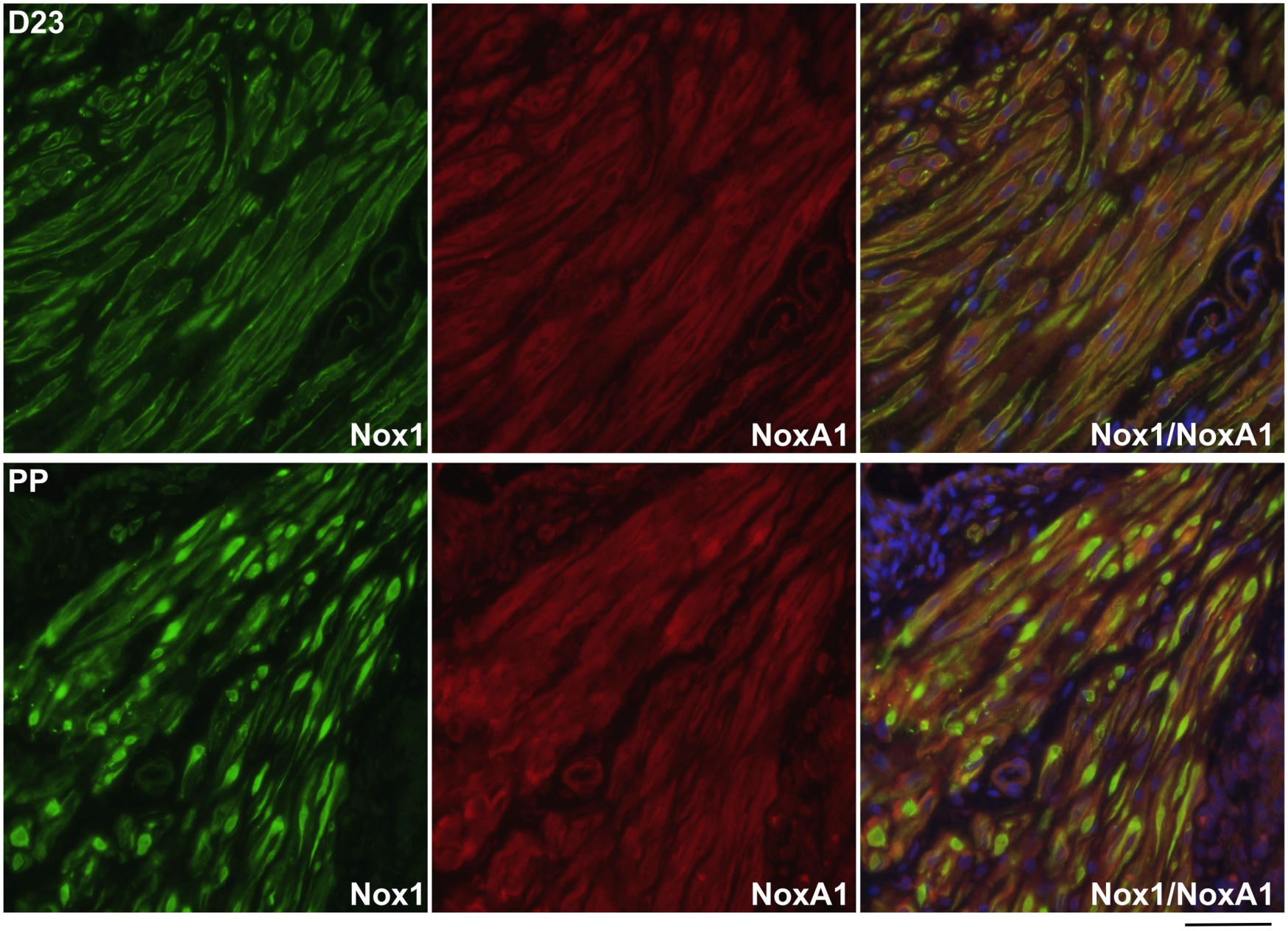
D23
Nox1
NoxA1
Nox1/NoxA1
PP
Nox1
NoxA1
Nox1/NoxA1

Figure 3.30. Confirmation of antiserum specificity in situ with non-specific rabbit and mouse immunoglobulins used in place of primary antisera. Representative images of longitudinal (LM) and circular (CM) uterine smooth muscle layers from pregnant rats are shown. Scale bar = 50μm.

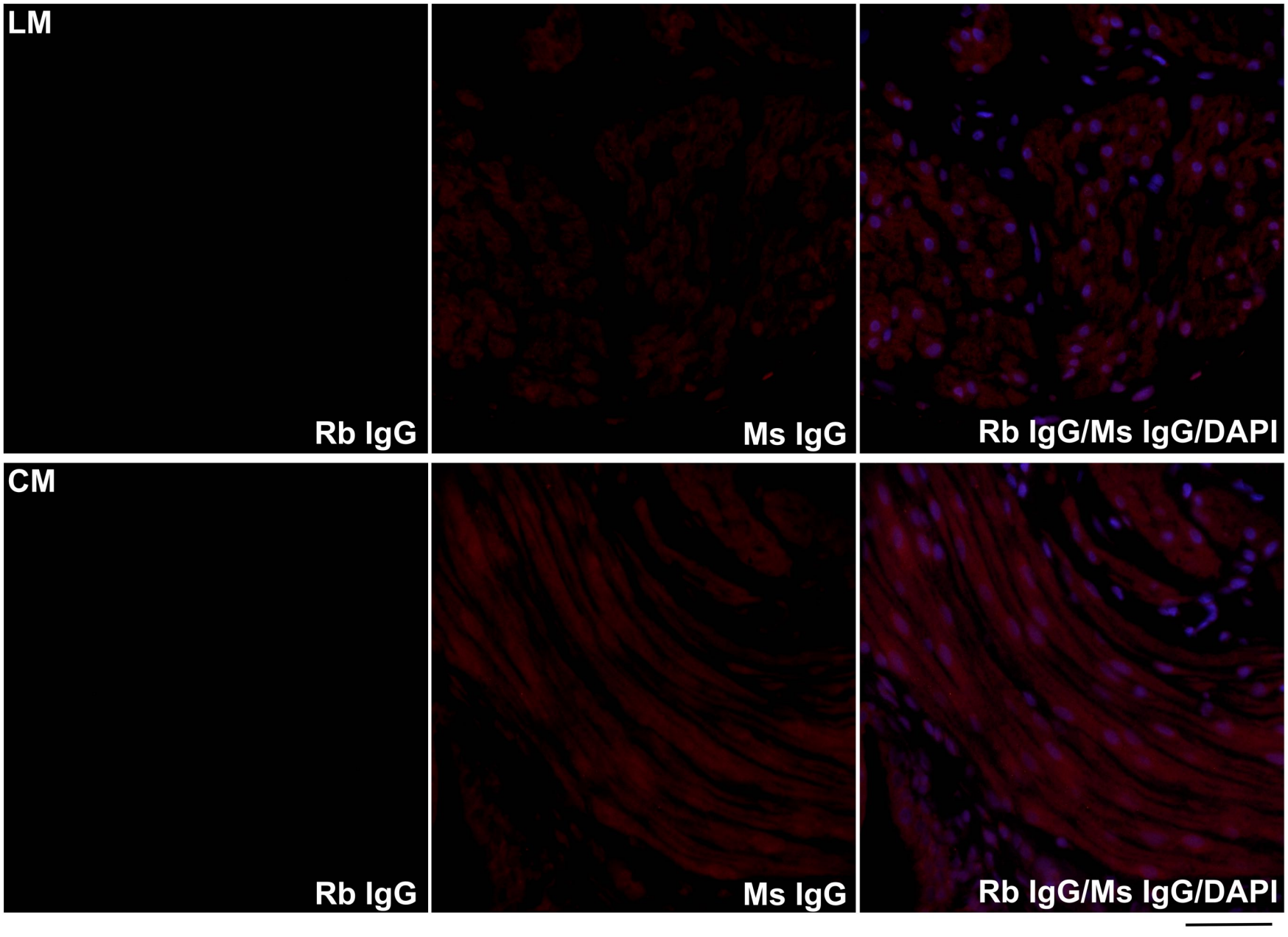
LM
Rb IgG
Ms IgG
Rb IgG/Ms IgG/DAPI
CM
Rb IgG
Ms IgG
Rb IgG/Ms IgG/DAPI

3.6. Spatiotemporal expression of Nox1 and NoxO1 in Unilaterally Pregnant Rats

Since Nox1 and NoxO1 expression increased prior to and during labour (D22 and D23), the potential regulatory effect of uterine distension on protein expression was assessed using a unilaterally pregnant rat model. Immunoblot analysis of Nox1 and NoxO1 expression revealed no statistically significant differences in protein expression in non-gravid (NG) compared to gravid (G) uterine horns of unilaterally pregnant rats at either D19 or D23 of gestation (Figure 3.31, 3.32). The spatial localization of Nox1 in the myometrium was similar to the localization reported in *Section 3.2* but there were no marked differences in immunofluorescence detection of Nox1 between G and NG uterine horns at D19 and D23 (Figure 3.33, 3.34).

3.7. The Influence of Pro-Inflammatory Conditions on Nox Protein and Subunit Expression

Since oxidative stress and inflammation can be interdependent processes, the potential role of inflammation on regulation of Nox1, Nox4 and NoxO1 protein expression was determined in two models of myometrial cell inflammation. For LPS experiments, hTERT-HM cells were incubated with either 100ng/mL LPS or PBS vehicle control for 0.5h, 1h, 3h and 6h. For IL-1β experiments, hTERT-HM cells were incubated with either 1ng/mL IL-1β or HSA vehicle control for 0.5h, 1h, 3h and 6h. Immunoblot analyses of cell lysates collected during these time course experiments were then conducted. Treatment of cells with LPS or IL-1β and generation of pro-inflammatory conditions had no statistically significant effects on Nox1, Nox4 or NoxO1 protein expression with one exception (Figures 3.35-3.37, 3.39, 3.40). Expression of Nox1 was significantly elevated after 0.5h (**) and 1h (*) incubation of hTERT-HM cells with IL-1β when compared to cells incubated with the vehicle control (Figure 3.38).

Figure 3.31. Immunoblot analysis of Nox1 expression in myometrium from non-gravid (NG) and gravid (G) uterine horns of unilaterally pregnant rats. Representative immunoblots are shown above the densitometric analysis at A) D19 and B) D23 of gestation. No significant differences in expression were observed ($P>0.05$). Glyceraldehyde 3-Phosphate Dehydrogenase (GAPDH) protein expression was used as a normalization control for densitometric analysis. Densitometric data are from 4 independent experiments.

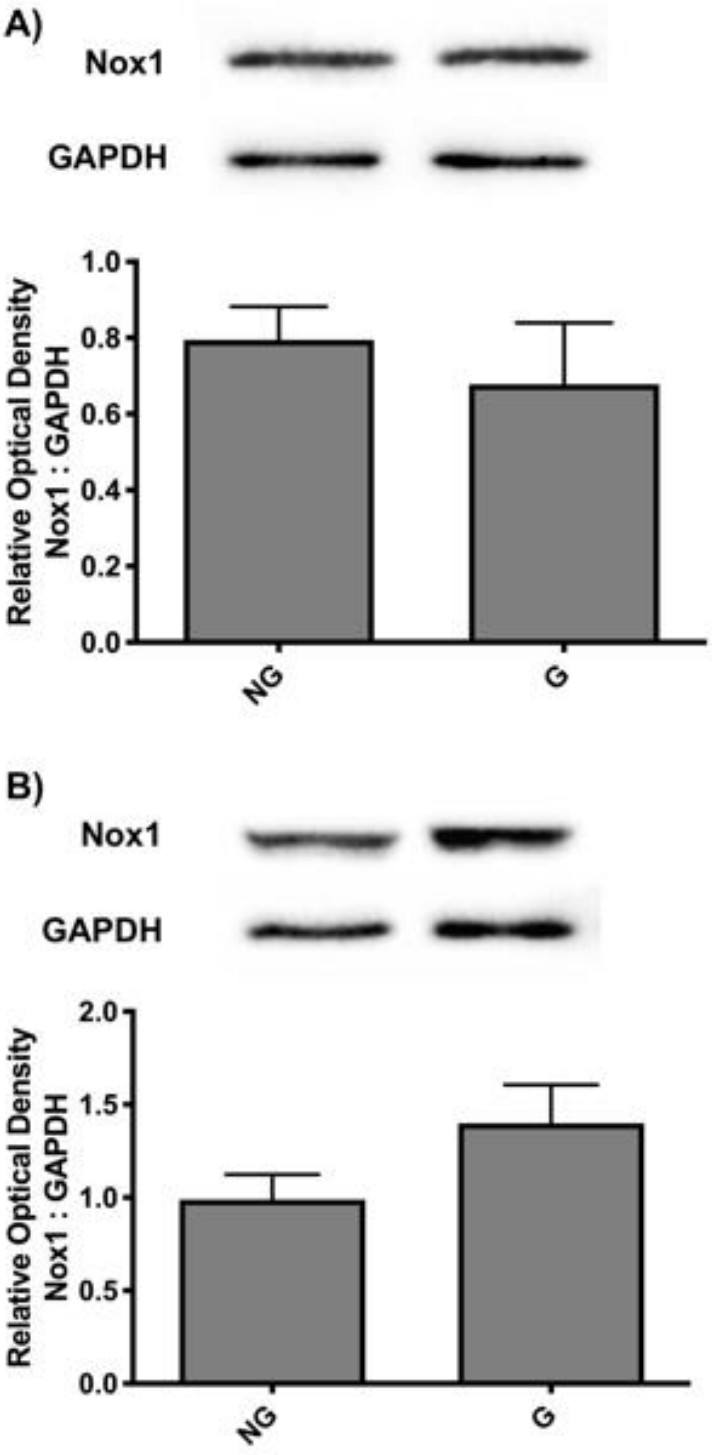
A)
Nox1
GAPDH
Relative Optical Density
Nox1 : GAPDH
1.0
0.8
0.6
0.4
0.2
0.0
NG
G
B)
Nox1
GAPDH
Relative Optical Density
Nox1 : GAPDH
2.0
1.5
1.0
0.5
0.0
NG
G

Figure 3.32. Immunoblot analysis of NoxO1 expression in myometrium from non-gravid (NG) and gravid (G) uterine horns of unilaterally pregnant rats. Representative immunoblots are shown above the densitometric analysis at A) D19 and B) D23 of gestation. No significant differences in expression were observed ($P>0.05$). Glyceraldehyde 3-Phosphate Dehydrogenase (GAPDH) protein expression was used as a normalization control for densitometric analysis. Densitometric data are from 4 independent experiments.

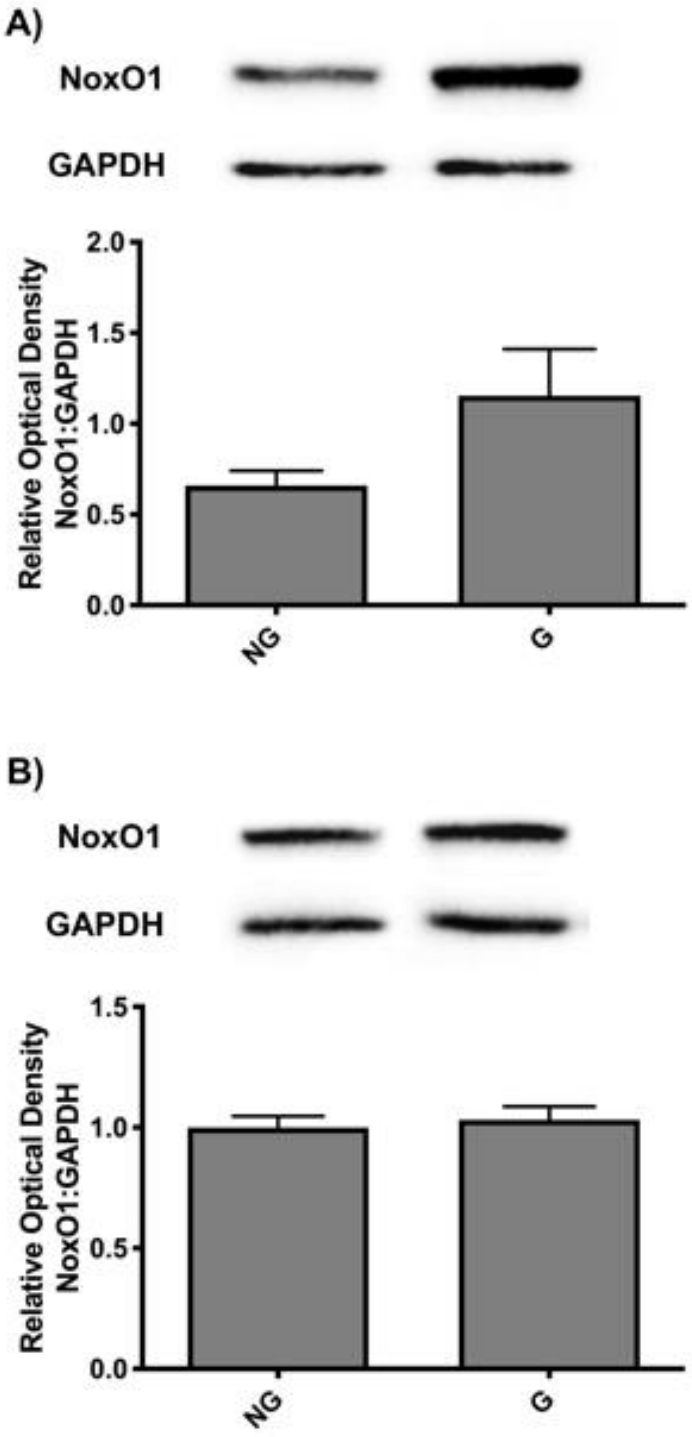
A)
NoxO1
GAPDH
Relative Optical Density
NoxO1:GAPDH
2.0
1.5
1.0
0.5
0.0
NG
G
B)
NoxO1
GAPDH
Relative Optical Density
NoxO1:GAPDH
1.5
1.0
0.5
0.0
NG
G

Figure 3.33. Immunofluorescence detection of Nox1 in smooth muscle layers from non-gravid (NG) and gravid (G) uterine horns of unilaterally pregnant rats at D19 of gestation. Representative images of longitudinal (LM) and circular (CM) uterine muscle are shown. Expression was detected using a rabbit polyclonal anti-Nox1 antibody followed by an anti-rabbit FITC conjugated antibody. The spatial detection of Nox1 did not appear to be influenced by gravidity in either muscle layer. IgG, non-specific rabbit immunoglobulin used in place of the primary antiserum. Scale bar = 50μm.

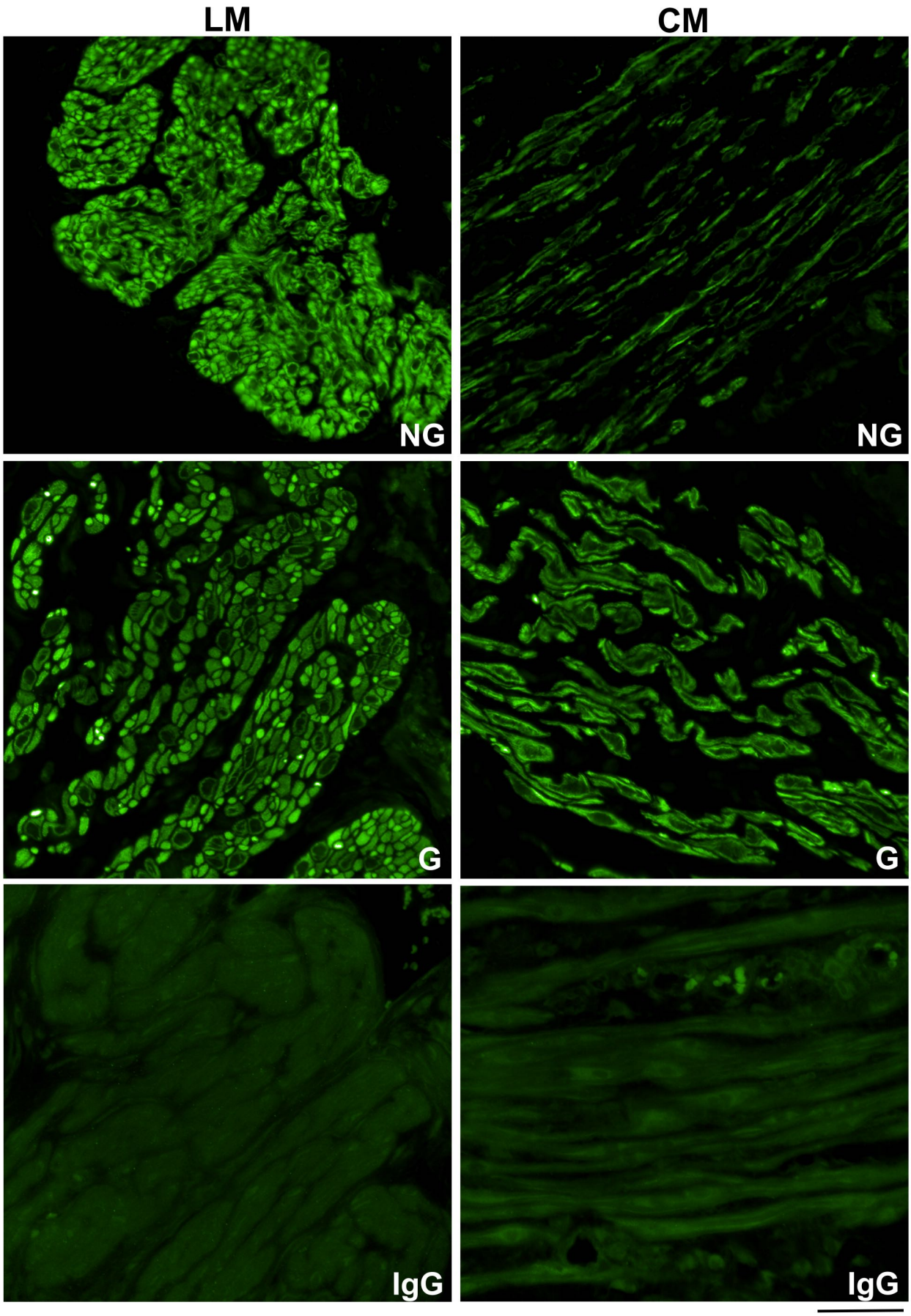
LM
CM
NG
NG
G
G
IgG
IgG

Figure 3.34. Immunofluorescence detection of Nox1 in smooth muscle layers from non-gravid (NG) and gravid (G) uterine horns of unilaterally pregnant rats at D23 of gestation. Representative images of longitudinal (LM) and circular (CM) uterine muscle are shown. Expression was detected using a rabbit polyclonal anti-Nox1 antibody followed by an anti-rabbit FITC conjugated antibody. The spatial detection of Nox1 did not appear to be influenced by gravidity in either muscle layer. IgG, non-specific rabbit immunoglobulin used in place of the primary antiserum. Scale bar = 50μm.

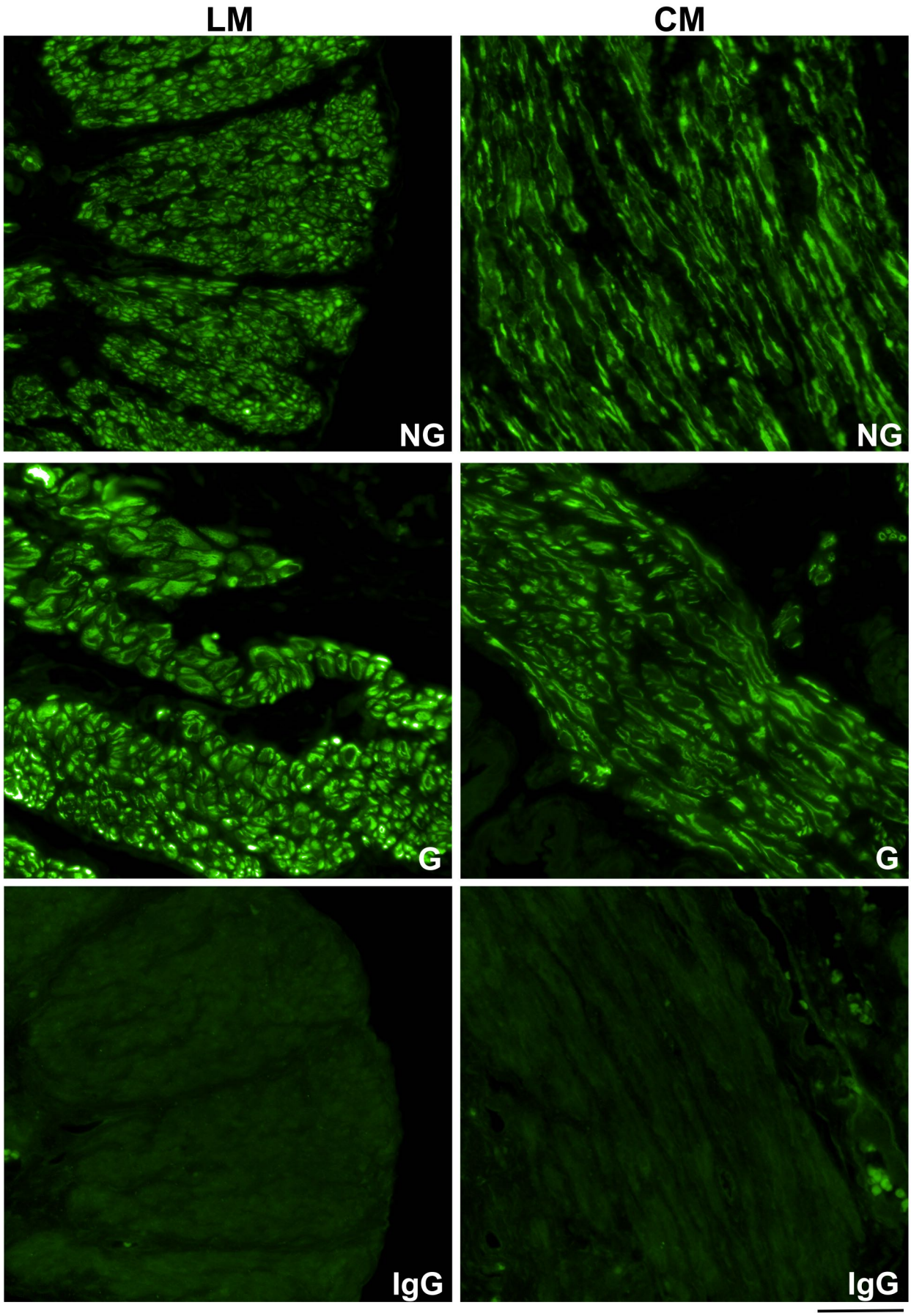
LM
CM
NG
NG
G
G
IgG
IgG

Figure 3.35. Assessment of the effect of pro-inflammatory conditions on Nox1 protein expression in hTERT-HM myometrial cells. hTERT-HM cells were incubated with either 0 (vehicle) or 100ng/ml of lipopolysaccharide (LPS) for 0.5, 1, 3 or 6 h. Cell lysates were collected for subsequent SDS-PAGE and immunoblot analysis. Nox1 protein expression was not significantly altered by LPS treatment compared to vehicle incubated cells ($P>0.05$). Representative immunoblots are shown and the densitometric analysis represents data from three independent experiments. Glyceraldehyde 3-Phosphate Dehydrogenase (GAPDH) expression was used as a normalization control.

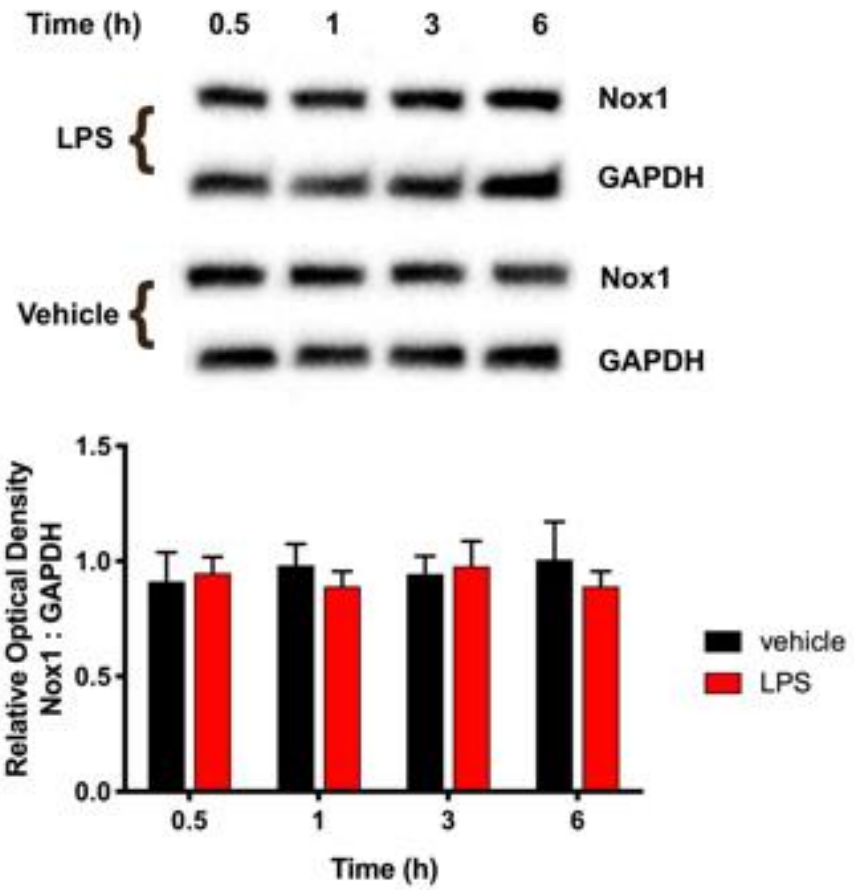
Time (h)
0.5
1
3
6
LPS
Nox1
GAPDH
Vehicle
Nox1
GAPDH
Relative Optical Density
Nox1 : GAPDH
1.5
1.0
0.5
0.0
0.5
1
3
6
Time (h)
vehicle
LPS

Figure 3.36. Assessment of the effect of pro-inflammatory conditions on Nox4 protein expression in hTERT-HM myometrial cells. hTERT-HM cells were incubated with either 0 (vehicle) or 100ng/ml of lipopolysaccharide (LPS) for 0.5, 1, 3 or 6 h. Cell lysates were collected for subsequent SDS-PAGE and immunoblot analysis. Nox4 protein expression was not significantly altered by LPS treatment compared to vehicle incubated cells ($P>0.05$). Representative immunoblots are shown and the densitometric analysis represents data from three independent experiments. Glyceraldehyde 3-Phosphate Dehydrogenase (GAPDH) expression was used as a normalization control.

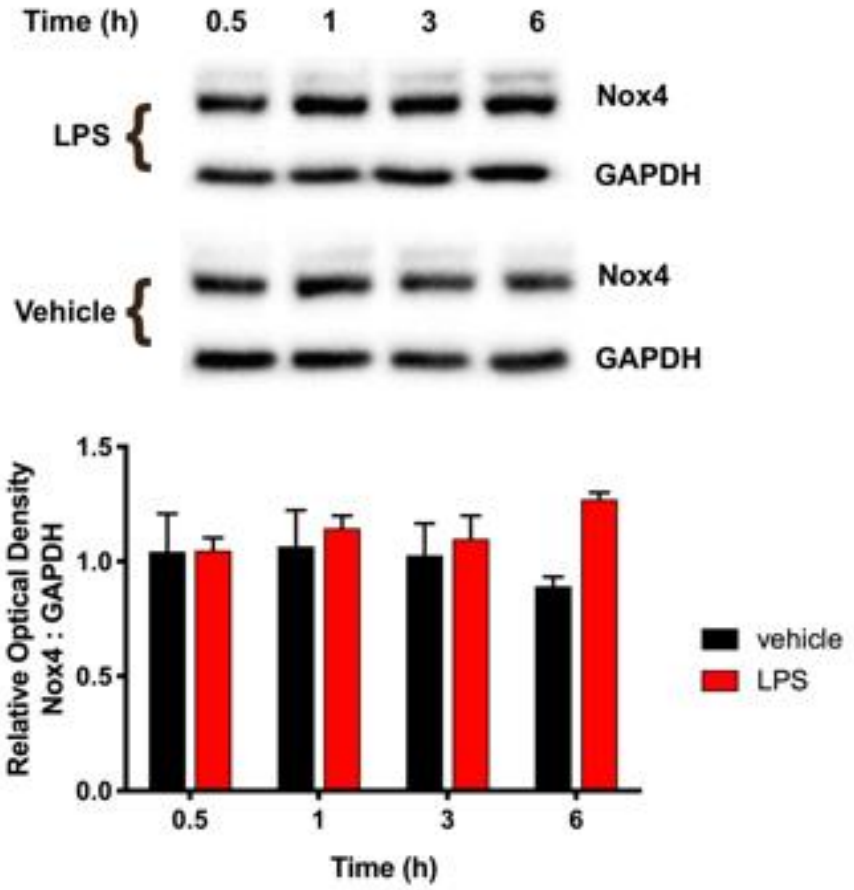
Time (h)
0.5
1
3
6
LPS
Nox4
GAPDH
Vehicle
Nox4
GAPDH
Relative Optical Density
Nox4 : GAPDH
1.5
1.0
0.5
0.0
0.5
1
3
6
Time (h)
vehicle
LPS

Figure 3.37. Assessment of the effect of pro-inflammatory conditions on NoxO1 protein expression in hTERT-HM myometrial cells. hTERT-HM cells were incubated with either 0 (vehicle) or 100ng/ml of lipopolysaccharide (LPS) for 0.5, 1, 3 or 6 h. Cell lysates were collected for subsequent SDS-PAGE and immunoblot analysis. NoxO1 protein expression was not significantly altered by LPS treatment compared to vehicle incubated cells (P>0.05). Representative immunoblots are shown and the densitometric analysis represents data from three independent experiments. Glyceraldehyde 3-Phosphate Dehydrogenase (GAPDH) expression was used as a normalization control.

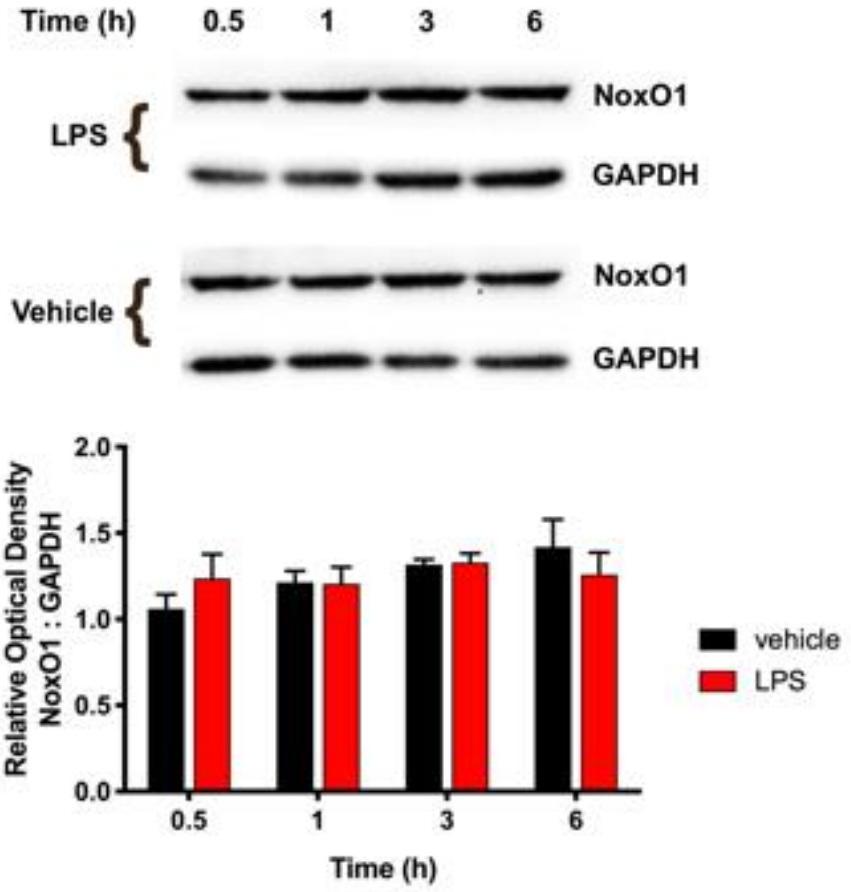
Time (h)
0.5
1
3
6
LPS
NoxO1
GAPDH
Vehicle
NoxO1
GAPDH
Relative Optical Density
NoxO1 : GAPDH
2.0
1.5
1.0
0.5
0.0
0.5
1
3
6
Time (h)
vehicle
LPS

Figure 3.38. Assessment of the effect of IL-1β-induced pro-inflammatory conditions on Nox1 protein expression in hTERT-HM myometrial cells. hTERT-HM cells were incubated with either 0 (vehicle) or 1 ng/ml of interleukin-1β (IL-1β) for 0.5, 1, 3 or 6 h. Cell lysates were collected for subsequent SDS-PAGE and immunoblot analysis. Representative immunoblots are shown and the densitometric analysis represents data from three independent experiments. **Nox1 expression after 0.5 h incubation with IL-1β was significantly increased compared to expression in cells incubated with vehicle. *Nox1 expression after 1 h incubation with cytokine was also significantly increased compared to expression in vehicle incubated cells ($P<0.05$). Glyceraldehyde 3-Phosphate Dehydrogenase (GAPDH) expression was used as a normalization control.

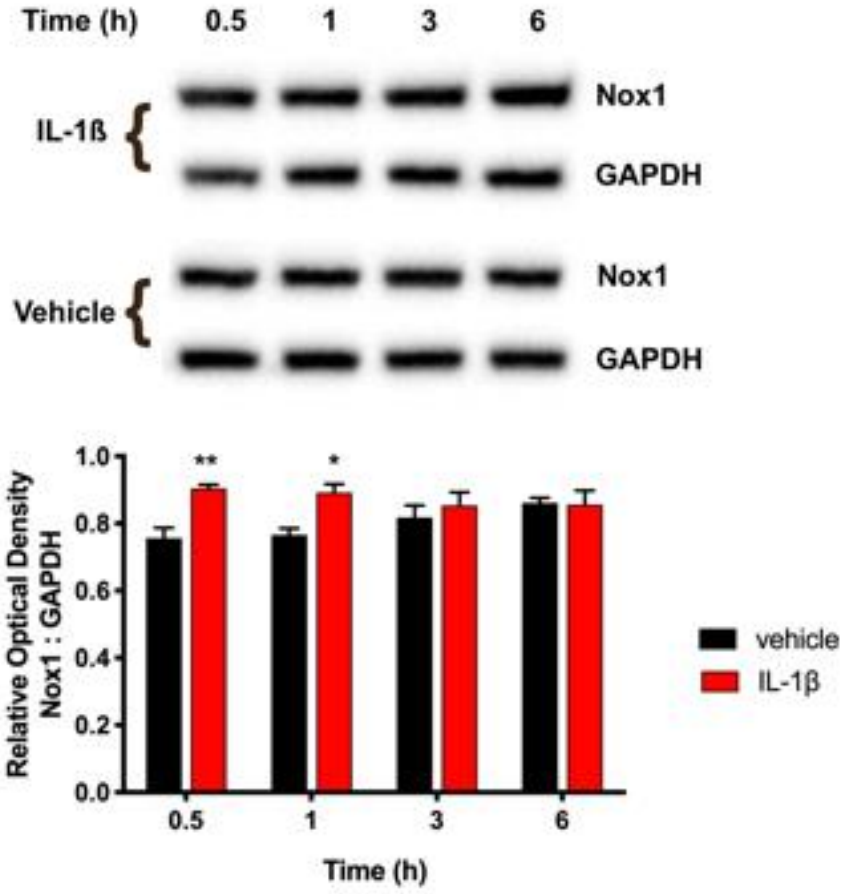
Time (h)
0.5
1
3
6
IL-1ß
Nox1
GAPDH
Vehicle
Nox1
GAPDH
Relative Optical Density
Nox1 : GAPDH
1.0
0.8
0.6
0.4
0.2
0.0
**
*
0.5
1
3
6
Time (h)
vehicle
IL-1β

Figure 3.39. Assessment of the effect of IL-1β-induced pro-inflammatory conditions on Nox4 protein expression in hTERT-HM myometrial cells. hTERT-HM cells were incubated with either 0 (vehicle) or 1 ng/ml of interleukin 1β (IL-1β) for 0.5, 1, 3 or 6 h. Cell lysates were collected for subsequent SDS-PAGE and immunoblot analysis. Nox4 protein expression was not significantly altered by IL-1β treatment compared to vehicle incubated cells (P>0.05). Representative immunoblots are shown and the densitometric analysis represents data from three independent experiments. Glyceraldehyde 3-Phosphate Dehydrogenase (GAPDH) expression was used as a normalization control.

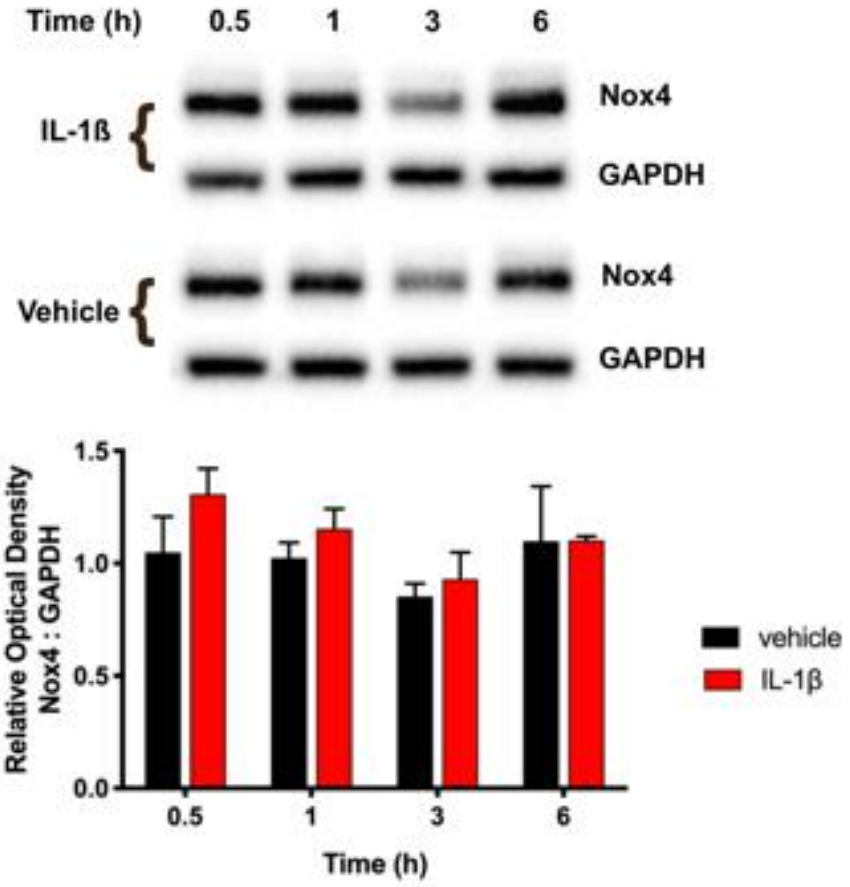
Time (h)
0.5
1
3
6
IL-1ß
Nox4
GAPDH
Vehicle
Nox4
GAPDH
Relative Optical Density
Nox4 : GAPDH
1.5
1.0
0.5
0.0
0.5
1
3
6
Time (h)
vehicle
IL-1β

Figure 3.40. Assessment of the effect of IL-1β-induced pro-inflammatory conditions on NoxO1 protein expression in hTERT-HM myometrial cells. hTERT-HM cells were incubated with either 0 (vehicle) or 1 ng/ml of interleukin 1β (IL-1β) for 0.5, 1, 3 or 6 h. Cell lysates were collected for subsequent SDS-PAGE and immunoblot analysis. NoxO1 protein expression was not significantly altered by IL-1β treatment compared to vehicle incubated cells (P>0.05). Representative immunoblots are shown and the densitometric analysis represents data from three independent experiments. Glyceraldehyde 3-Phosphate Dehydrogenase (GAPDH) expression was used as a normalization control.

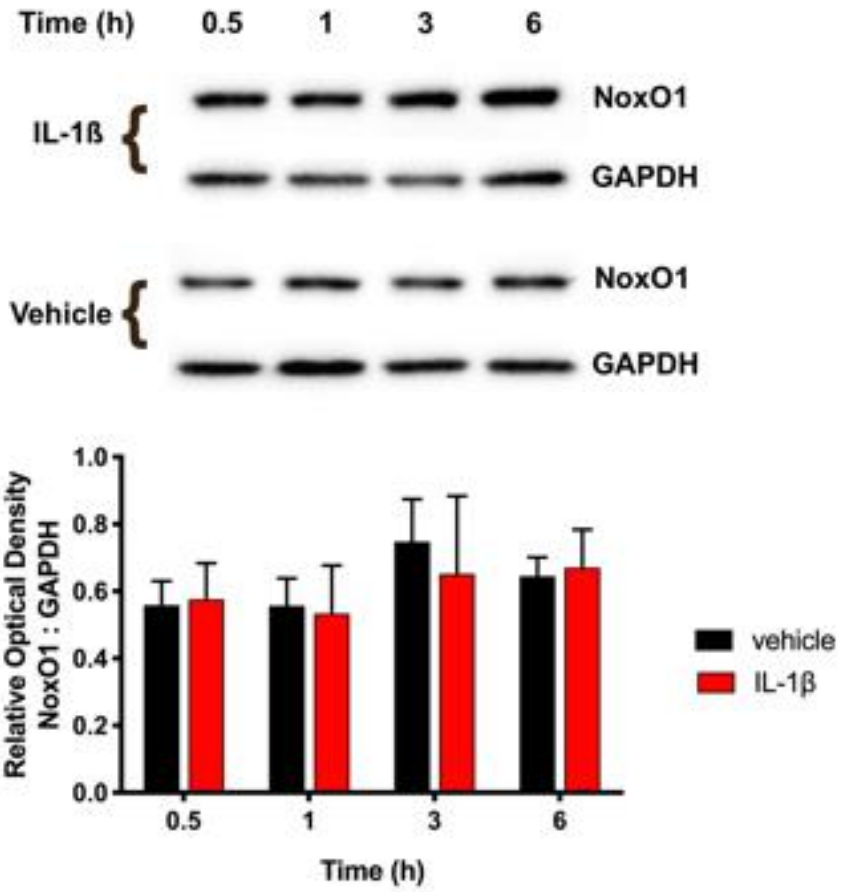
Time (h)
0.5
1
3
6
IL-1ß
NoxO1
GAPDH
Vehicle
NoxO1
GAPDH
Relative Optical Density
NoxO1 : GAPDH
1.0
0.8
0.6
0.4
0.2
0.0
0.5
1
3
6
Time (h)
vehicle
IL-1β

4. Discussion

Throughout gestation the uterus must transform from a quiescent tissue into a powerful contractile muscle capable of coordinated labour contractions. Similarly, the immune system must also transform to firstly, accept the implanting blastocyst and secondly, to allow mother and infant to become one symbiotic being. NADPH oxidases have been identified as important producers of ROS in a variety of cell types including the endothelium, epithelium, neurons, and tissues such as smooth muscle or regions of the reproductive tract (Bedard and Krause, 2007). These ROS act as important second messengers during times of oxidative stress as well as during inflammation, both of which are abundant during pregnancy. It is hypothesized that Nox enzymes play a role in myometrial adaptation, hypertrophy and reorganization and may be involved in the inflammatory responses leading up to labour. Thus, the expression patterns and spatiotemporal localization of Nox1, Nox4, and their functionally essential subunits NoxO1, NoxA1 and p22phox were examined in pregnant rat myometrium.

4.1. Presence of Nox1 and Nox4 in Myometrium

In the current study, immunoblot analysis of Nox1 in rat myometrium revealed detection of the protein throughout gestation, but with increased expression during the contractile and labour phases of myometrial differentiation, coinciding with the activation/labour phase of immunological transformation. Immunostaining of Nox1 was detectable throughout gestation in both muscle layers, with an increase in detection observed at labour and PP. Detection of Nox1 was restricted to smooth muscle with an extensive cytoplasmic staining pattern and some association with plasma membranes. Others have examined Nox1 localization in VSMC and also observed localization at the plasma membrane as well as in vesicle-like structures near the membrane (Hanna et al. 2004; Hilenski et al. 2004). The cytoplasmic staining pattern observed in this study is likely a result of protein translation and subsequent insertion into organelles, such as ER and Golgi, prior to delivery to the membrane; however, we cannot rule out functional significance of Nox1 within these organelles.

This study is the first to characterize, in detail, the detection of Nox1 protein expression in pregnant rat myometrium throughout gestation. Cui et al (2010) reported diffuse expression of Nox1 protein in myometrial smooth muscle cells by immunohistochemical analysis of tissue biopsies obtained from term pregnant women; however, Fletcher et al. (2014) did not detect

Nox1 mRNA by real time qPCR in myometrial cells obtained from non-pregnant women undergoing hysterectomy and following immortalization with telomerase reverse transcriptase. In the latter report, no positive controls were used to ensure validity of the chosen qPCR primers which may explain the lack of Nox1 detection. To our current knowledge, Nox1 levels have never been examined by immunoblot analysis throughout gestation in human myometrium.

Recent reviews by Callera et al. (2007) and Ushio-Fukai (2009) have highlighted the importance of caveolae as redox signaling centers. These structures facilitate the concentration of multiple signaling molecules as a "preassembled signaling complex" at the plasma membrane allowing for rapid and efficient activation of downstream targets (Okamoto et al. 1998). Vilhardt and van Deurs (2004) found that the assembly and subsequent ROS production by Nox proteins is dependent upon interactions within caveolae. Markers for these structures, caveolin-1, -2 and -3 are abundantly expressed in both non-pregnant as well as pregnant rodent uterine tissue, with levels increasing as gestation progresses (Turi et al. 2001; Riley at al. 2005). Co-localization of Nox1 with caveolin has been observed in human VSMC by immunofluorescence analysis (Hilenski et al. 2004). It is believed that these signaling complexes participate in smooth muscle hypertrophy via Ang II stimulation (Ushio-Fukai, 2009). Upon Ang II stimulation of VSMC, the small GTPase Rac is translocated to caveolae where activation and upregulation of Nox1 occur, resulting in upregulated ROS production and EGFR transactivation (Lassegue et al. 2001; Zuo et al. 2004). Phosphorylated EGFR then localize to FA where they interact with Nox4, p22phox and paxillin to form large signaling platforms at the membrane (Ushio-Fukai, 2009).

It is also believed that caveolae regulate priming of uterine tissue for term contractions by compartmentalizing contraction filament-associated proteins such as rho-associated kinase (ROK) α and β (Riley et al. 2005). Similar to the expression pattern of Nox1, levels of ROKα and ROKβ were elevated in mice during late gestation (D19) as compared to NP levels (Riley et al. 2005). These kinases are important intermediates of the contractile pathway that becomes activated near term (Oh et al. 2003). This evidence, together with the results of this study, suggest Nox1 may mediate redox signaling through caveolae, specifically during late gestation as the myometrium prepares for contractile activation prior to labour.

Nox4 levels were constitutively detected throughout gestation but expressed to a greater extent during the proliferative and synthetic phases of myometrial transformation, coinciding with the initiation and tolerance phases of immunological transformation. Nox4 was highly

detectable in perinuclear regions and exhibited some association with myocyte plasma membranes. Nox4 has previously been identified to co-localize with ER marker PTP1B in transfected epithelial cells and with calreticulin in endothelial cells, likely accounting for the perinuclear staining seen in this study (Van Buul et al. 2005; Martyn et al. 2006). Nox4 has also been shown to co-localize with vinculin, a marker of FA at the plasma membrane, which could explain the plasma membrane staining that was observed in this thesis (Hilenski et al. 2004).

Similar to examination of Nox1, this study is the first to characterize in detail the detection of Nox4 protein expression in the rat myometrium throughout gestation. Nox4 had only previously been identified by immunoblot analysis in human myometrial tissue and uterine leiomyoma or fibroid tissue collected from non-pregnant women undergoing hysterectomy (Fletcher et al. 2014). In contrast, the detection of Nox4 in situ by immunohistochemistry has previously been confirmed in leiomyoma tissue, but not in human myometrial tissue (Fletcher at al. 2014). Interestingly, exposure of myometrial cell cultures, derived from non-pregnant myometrial tissue, to hypoxic conditions of 2% O_2 for 24h significantly increased mRNA levels of Nox4, but protein levels were not examined with this treatment regimen (Fletcher et al. 2014). It is well known that hypoxia leads to increased ROS production; thus, it is not surprising that there would be a concurrent increase in ROS-producers such as Nox proteins. Shynlova et al. (2010) found that during the transition phase from a proliferative to a synthetic phenotype, the fetus(es) takes on an ellipsoid shape resulting in localized regions of hypoxia due to increased stretch. In my study, Nox4 expression in pregnant rat myometrium was elevated during this transition phase suggesting growing fetuses cause localized hypoxia resulting in increased Nox4 expression and a subsequent increase in ROS production.

Nox isoform expression has also been examined in the immortalized human leiomyoma cell line, ULTR. Uterine leiomyomas are benign tumors derived from smooth muscle cells of the myometrium that grow under the influence of sex hormones such as estrogen and progesterone (Sabry and Al-Hendy, 2012). Nox1, Nox4 and Nox5 mRNA were abundantly expressed in ULTR cells as determined by reverse transcriptase (RT) PCR (Cui et al. 2010). However, in a study conducted by Fletcher et al. (2014), only mRNA for Nox2 and Nox4 were detectable by real time qPCR in leiomyomas. This discrepancy in Nox expression may be due to the use of non-validated qPCR primers and lack of positive controls to verify qPCR viability. Spatial localization of Nox1, Nox4 and Nox5 in ULTR cells was also examined by Cui et al. (2010) via

cell fractionation. Data revealed Nox1 localization to the membrane fraction, Nox4 to the cytosolic fraction and Nox5 in both the membrane and cytosolic fractions. Exposing ULTR cells to 100nM of Ang II stimulated Nox5 expression and redistribution but had no effect on Nox1 or Nox4 expression (Cui et al. 2010). Overall, expression of Nox isoforms may mediate Ang II-induced cellular hypertrophy and ROS production *in vivo*, as seen by Higashi et al. (2003), but not *in vitro*. Fletcher et al. (2014) has hypothesized that alterations to Nox expression profiles may lead to dysregulated cellular hypertrophy and promote the growth of fibroids. Levels of Nox4 mRNA were elevated in leiomyoma tissue, as compared to normal myometrium, promoting a prooxidant state (Fletcher et al. 2014). Under hypoxic conditions, estrogen signaling pathways can become atypically activated (Zhou et al. 2011). This not only leads to continuous fibroid differentiation but also protects the fibroid cells from apoptosis (Zhou et al. 2011). Hypoxic conditions are also known to promote the generation of superoxide by Nox enzymes, further promoting a prooxidant state where fibroid cells can thrive (Griendling et al. 2000).

4.2. Presence of Nox subunits in Myometrium

The novel characterization of NoxO1, NoxA1 and p22phox subunit expression in the rat myometrium throughout gestation was also conducted in this study. Knowing that Nox1 requires all three of these subunits for activation and ROS production, it was hypothesized that they would follow a similar expression pattern to that of Nox1 (Banfi et al. 2003). Unexpectedly, the only subunit that had a similar protein expression pattern to Nox1 was NoxO1. This subunit had very low protein levels during early gestation with levels increasing towards the end of the synthetic phase and into the contractile phase, peaking on D22. NoxA1 expression peaked during the proliferative phase, on D12, before decreasing slightly for the remainder of gestation. Lastly, p22phox expression was highly detectable in both NP tissue and during early gestation before diminishing to very low levels for the remainder of pregnancy. Fletcher et al. (2014) was able to detect NoxO1, NoxA1 and p22phox mRNA expression in human myometrial cell cultures derived from myometrium of non-pregnant women using real-time qPCR. Interestingly, these results were not consistent with those reported by Cui et al. (2010) where mRNA for NoxO1 and NoxA1 were not detected in human uterine tissue. Instead, RT-PCR revealed abundant expression of only p22phox in human uterine tissue (Cui et al. 2010). These discrepancies in subunit expression may be attributed to the commercially sourced RNA that was used for RT-

PCR in the latter study as the exact makeup of the uterine tissue samples used for RNA isolation was unknown and may have been from non-pregnant or pregnant women as well as from endometrium, myometrium or a combination of both tissues; thus, the true sample identity cannot be verified.

Experiments conducted by Takeya et al. (2003) found that Nox1 can interchangeably bind with NoxO1 or the homologue p47phox. Similarly, NoxA1 and the homologue p67phox have the same functionality but reportedly different tissue-specific expression profiles (Chabrashvili et al. 2002). Fletcher et al. (2014) was able to detect mRNA for NoxA1, NoxO1, p67phox and p47phox in myometrial tissue collected from non-pregnant women. Additionally, detectable levels of p47phox and p67phox mRNA were found in human uterine tissue but only mRNA for p67phox was detectable in ULTR cells (Cui et al. 2010). Future experiments should aim to characterize the expression of these two homologues throughout rat gestation to examine their potential role in Nox1 activation. Such information may hint at precise temporal Nox1-subunit associations during pregnancy with functional-specific consequences.

The functionality of Nox4 depends upon the presence and availability of its subunit, p22phox (Kawahara et al. 2005; Martyn et al. 2006). In this thesis, the expression of p22phox in rat myometrium was high during early gestation, peaking at D12, and diminishing thereafter. Nox4 was constitutively expressed in non-pregnant tissue and during early gestation before decreasing following D15. Although this study only examined protein levels and not enzymatic activity, it is likely that Nox4 is only most enzymatically active in non-pregnant tissue and during early gestation when p22phox expression is high, as in the absence of its subunit Nox4 functionality is diminished (Kawahara et al. 2005). Future experiments should examine enzymatic activity of Nox4 and Nox1 in myometrial tissue lysates. Additional studies examining any activating post-translational modifications of NoxO1, NoxA1 and p22phox may uncover functional significance of these subunits throughout gestation (Brandes et al. 2014).

The lack of published findings on Nox protein expression and discrepancies reported in the literature regarding Nox isoform expression can perhaps be attributed to the limited availability of commercial antisera for these proteins (Diebold et al. 2019). The work presented in this thesis is a more detailed examination that builds on the previous work done by Cui et al. (2010) and Fletcher et al. (2014) and confirms the expression of these enzymes and their subunits in mammalian myometrium; however, their exact function within these tissues remains unclear.

A future study utilizing Nox isoform specific or subunit-specific siRNA targeting within the immortalized human myometrial cell line hTERT-HM could reveal specific functions for these proteins.

4.3. Influence of Inflammation and Uterine Distension on Nox Expression

Utilizing hTERT-HM cells, protein levels of Nox1, Nox4 and NoxO1 were examined after stimulation of pro-inflammatory conditions using either 100ng/ml LPS or 1ng/ml IL-1β. In all immunoblot experiments conducted, there were no significant differences in Nox4 and NoxO1 protein expression after induction of inflammatory conditions with LPS or IL-1β. Nox1 was the only protein that had significantly elevated levels after 0.5h and 1h incubation with IL-1β but not LPS. However, the relative expression increases over vehicle controls at the two timepoints were small and thus may not be physiologically relevant. Nevertheless, the results could indicate that a pro-inflammatory response caused by IL-1β leads to an increase in Nox1 expression as seen by Aguado et al. (2016) in IL-1β treated rat aortic smooth muscle cells. Importantly, the induction of inflammatory conditions in the hTERT-HM cells by LPS or IL-1β was verified by significantly increased production of granulocyte-macrophage colony-stimulating factor, interferon- γ, IL-6, IL-8 and MCP-1 by the cells upon cytokine or LPS incubation (Hahn, 2018; Bailey, 2020).

It is well established that pregnancy is not a time of maternal immune weakness but rather of maternal immune modulation (Mor et al. 2011). Much like the transformation seen throughout gestation in myometrial phenotype, the immune system also transforms. Of particular interest is the pro-inflammatory response that occurs during late gestation, prior to labour. This response is characterized by infiltration of the myometrium by macrophages and neutrophils, upon infiltration, these immune cells secrete cytokines (Thomson et al. 1999; Young et al. 2002; Osman et al. 2003). In most mammals, this response is triggered by a drop in circulating progesterone levels, also allowing increased expression of cytokines such as TNF-α, IL-1β, IL-6, IL-12 and MCP-1 by the myometrium (Shynlova et al. 2008; Shynlova et al. 2013a). In humans, increased expression of cytokines occurs despite progesterone levels remaining high (Tornblom et al. 2005). Thus, in this thesis, the observed increase in Nox1 expression in the rat myometrium during late pregnancy and labour could be the result of increased cytokine production within the tissue. Exposure to cytokines TNF-α and IL-1β has been shown to directly stimulate ROS

generation, both by mitochondria and Nox enzymes, in other cell types such as human retinal pigment epithelial cells (Yang et al. 2007). Interestingly, the use of a Nox inhibitor prevented ROS induction by IL-1β but not by TNF-α in human retinal epithelial cells (Yang et al. 2007). Hadi et al. (2015) reported high amounts of ROS production in preterm labouring myometrial tissue as compared to non-labouring controls with 90% of ROS generation occurring in the invading macrophages. Recent work has revealed a complex relationship between TNF-α, ROS and their roles in inflammation as well as in inflammatory diseases (Blaser et al. 2016). In the early stages of inflammation, TNF-α stimulation leads to ROS production and downstream activation of nuclear factor-κB, a well-established marker of the immune response (Morgan and Liu 2011). On the other hand, chronic or prolonged ROS generation and accumulation often leads to pathophysiology (Blaser et al. 2016).

With all of the available information linking ROS to inflammation and inflammatory diseases, the results of this set of experiments were puzzling. It was hypothesized that induction of inflammatory conditions using IL-1β or LPS would cause a significant increase in Nox1, Nox4 and NoxO1 protein levels, but that was not the case. Because only protein levels were examined, enzymatic activity remains unknown and the role of these proteins in contributing to myometrial inflammation cannot yet be ruled out. Future studies should focus on assessing the enzymatic activity of these Nox proteins during a stimulated pro-inflammatory response in hTERT-HM cells as well as assessing whether or not ROS are produced by hTERT-HM cells upon pro-inflammatory stimulation *in vitro*. Inflammatory conditions may also stimulate post-translational modifications of Nox proteins rendering them undetectable with the antisera used in this study. Additionally, the incubation period utilized for IL-1β and LPS to generate pro-inflammatory responses was a rather acute period of time (0.5h to 6h of incubation). Longer incubation periods may be necessary to allow increased Nox protein or subunit translation to be detected via immunoblot analysis. These types of cellular experiments may also not accurately replicate the inflammatory response that occurs *in vivo* unless pro-inflammatory conditions are extended at least 24h. While *in vitro* experiments provide valuable insight in many circumstances, it is key to remember that these cellular models are also lacking elements that are normally present *in vivo*. This point was recently illustrated by Wendremaire et al. (2020) who found that LPS-induced myometrial contractions could only be stimulated in human myometrial cells cultured on collagen-lattices that were co-cultured with peripheral blood mononuclear cell-

derived macrophages. Thus, *in vitro* models may not accurately replicate the conditions seen *in vivo* and may explain, in part, why there was only a small response in Nox1 expression and no response observed in Nox4 and NoxO1 protein levels following pro-inflammatory stimulation in this thesis. Importantly, Wendremaire et al. (2020) demonstrated that Nox inhibition using apocynin in LPS/macrophage-induced myometrial co-cultures inhibited contractions and differentiation, highlighting a potential role for Nox proteins in myometrial events such as labour.

Pregnancy is, without a doubt, a time of vast growth. The uterus must expand in concert with the developing fetus(es) with fetal growth inducing uterine growth through distension stresses. The unilaterally pregnant rat model is ideal for studying the effects of uterine stretch as the non-gravid control horn remains under the same hormonal control as the gravid-stretched horn (White and MacPhee, 2011). Nox1 and NoxO1 protein levels were examined on D19 and D23 of gestation in both non-gravid and gravid horns since this period was marked by increased expression of both proteins. There were no significant differences in protein expression of Nox1 or NoxO1 in gravid compared to non-gravid uterine horns on either day examined.

Future experiments should examine the enzymatic activation of these enzymes under unilateral stretch which could offer more insight as to the exact function of these enzymes. This could be accomplished *in vitro* if hTERT-HM cells could be cultivated in modified culture dishes and cyclically stretched (e.g https://www.flexcellint.com) to then assess ROS production with cell permeable ROS sensitive dyes in the absence or presence of Nox inhibitors. Additionally, uterine stretch does not only occur during later gestation but throughout pregnancy. Perhaps examination of Nox protein expression during mid-gestation would reveal significant trends in protein levels.

4.4. Potential Roles of Nox Signaling in Myometrial Transformation during Pregnancy

Significant uterine growth occurs during the proliferative phase of myometrial transformation when levels of growth factors IGF-I, IGFBP-1 and anti-apoptotic factor Bcl-2 are high (Shynlova et al. 2006). Expression of Nox4 and p22phox followed a similar pattern of expression with higher expression early in gestation as compared to PP. Handayaningsih et al. (2011) reported an increase in ROS production by skeletal muscle myocytes after treatment with IGF-I and enhanced IGF-I-induced phosphorylation of the IGF-I receptor after treatment with

H_2O_2. In a Nox4 knockdown cell model, IGF-I-induced phosphorylation of IGF-I receptor was reduced, indicating the involvement of Nox4 in IGF-I signaling *in vitro* (Handayaningsih et al. 2011). Future studies should further examine the role of Nox4 in IGF-I-induced hypertrophy in myometrial cells and examine this relationship *in vivo*. The proliferative phase coincides with the initiation phase of immunological transformation when expression of cytokines such as IL-6, IL-8 and TNF-α are high (Fest et al. 2007). These cytokines not only attract immune cells to the implantation site but may also play a role in Nox4 expression. Moe et al. (2006) reported increased expression of Nox4 protein and increased superoxide production in aortic smooth muscle cells and embryonic kidney cells following TNF-α stimulation, suggesting that Nox4 produced ROS may play a role in the redox signaling that occurs during proinflammatory responses. Future studies examining the potential role of Nox4 in uterine inflammation should consider using TNF-α stimulation as well as exploring the use of a chronic inflammation model as the acute model used in this study yielded minimal results.

As the myometrium transitions from the proliferative to the synthetic phase, the myocytes switch from hyperplastic to hypertrophic growth. During this transition phase, the uterus is exposed to increased levels of oxidative stress as the growing fetuses create localized regions of hypoxia (Shynlova et al. 2010). Exposing Nox4 deficient mice to oxidative stress resulted in increased inflammation and endothelial dysfunction as compared to wildtype controls (Schroder et al. 2012). In the vascular system, H_2O_2 has been shown to elicit positive effects when present in low concentrations and it is believed that H_2O_2 released by Nox4 may mediate these effects via protein kinase-G Iα and endothelial nitric oxide synthase activation (Cai, 2005; Burgoyne et al. 2007; Schroder et al. 2012). However, alterations in Nox4 expression can result in a prooxidant state that may promote the unregulated growth of fibroid tissue as seen in myometrial leiomyomas (Fletcher et al. 2014).

Synthesis and deposition of ECM components elastin, procollagen I and II, and fibronectin by myocytes creates a scaffolding support system for the muscle as the uterus continues to expand (Shynlova et al. 2004; Shynlova et al. 2009a). Myocytes remain connected to the ECM through FAs, structures that undergo significant turnover from D15 of gestation onwards (MacPhee and Lye, 2000). Nox4 and p22phox are known to co-localize with vinculin, a commonly used marker of FAs (Hilenski et al. 2004). Work by Lyle et al. (2009) found that Nox4/p22phox localization to FAs and subsequent ROS production is mediated by Poldip2 and

in the absence of this protein FA numbers were reduced. These structures are also important in cell-cell communication and, under Ang II stimulation, form large signaling platforms with caveolae where redox signaling events promote cellular growth (Ushio-Fukai et al. 2001). Caveolae are important protein recruitment sites for Nox proteins as well as other signaling proteins and are known sites of signal transduction (Callera et al. 2007). Hilenski et al. (2004) identified co-localization of Nox1 with caveolin in VSMC and Vilhardt and van Deurs (2004) found that these interactions are essential for proper Nox assembly and enzymatic function. Interestingly, upon Ang II stimulation, Lassegue et al. (2001) reported upregulation of Nox1 mRNA in rat VSMC but Cui et al. (2010) observed no change in Nox1 localization or protein expression in human ULTR cells. Future studies are needed to further examine the potential growth promoting role of Nox1, through caveolae, and Nox4, through FAs, specifically in smooth muscle cells as tumor derived cell lines may exhibit altered growth signaling pathways.

4.5. Major Findings

Research produced by this thesis, based on two research objectives, has produced two major sets of conclusions.

Objective 1: Determine where and when NADPH oxidases are found in rat myometrium during gestation.

Major Findings:

This study was the first to methodically characterize the detection of Nox1 and Nox4 protein expression in the rat myometrium throughout gestation. Both immunoblot and immunofluorescence analysis demonstrated increased expression of Nox1 during the contractile and labour phases of myometrial differentiation, coinciding with the activation/labour phase of immunological transformation. Nox1 was detectable in situ particularly at labour and PP with an extensive cytoplasmic staining pattern and some association with plasma membranes. In contrast, increased expression of Nox4 during the proliferative and synthetic phases of myometrial differentiation was observed, coinciding with the initiation and tolerance phases of immunological transformation. Nox4 was highly detectable in situ within perinuclear regions and exhibited some association with myocyte plasma membranes. Only Nox1 appeared to be induced

by inflammation in hTERT-HM cells exposed to the pro-inflammatory stimuli LPS or IL-1□□ while uterine distension did not affect expression of Nox1 or Nox4.

Objective 2: To examine where and when Nox subunits NoxO1, NoxA1 and p22phox are expressed in the myometrium as potential regulators of Nox1 and Nox4 function.

Major Findings:

Similar to Objective 1, this study also demonstrated the novel expression of the Nox subunits in myometrium throughout pregnancy. Immunoblot analysis of NoxO1 demonstrated increased expression during the contractile, labour and involution phases of myometrial differentiation, coinciding with Nox1 expression, and the activation/labour as well as involution phases of immunological transformation. NoxO1 was detectable in situ from mid-gestation onwards with a general cytoplasmic staining pattern and some association with plasma membranes. In contrast, the expression of NoxA1 and p22phox subunits were elevated during early gestation, coinciding with Nox4 expression and corresponding to the proliferative phase of myometrial differentiation as well as the initiation phase of immunological transformation. Detection of NoxA1 in situ increased as gestation progressed with the protein being detectable in the entire myocyte and having some peri-nuclear accumulation later in gestation. NoxA1 was observed to co-localize with Nox1, creating concentrated foci in the cytoplasm. However, induction of inflammation in hTERT-HM cells, by addition of the pro-inflammatory stimuli LPS or IL-1β as well as uterine distension did not significantly alter expression of NoxO1.

Overall, the findings in this thesis suggest a possible role for Nox1, Nox4 and associated subunits in specific phases of myometrial programming and immunological adaptation (Figure 4.1). During the proliferative phase of myometrial differentiation, it is hypothesized that Nox4/p22phox, and perhaps to a lesser extent Nox1/NoxA1/p22phox, could be actively participating in redox signaling events related to myometrial proliferation. This period coincides with the initiation phase of immunological transformation where pregnancy related oxidative stress initiates an inflammatory response, triggering an influx of immune cells to the site of implantation. During late gestation and labour, it is hypothesized that Nox1 localizes within caveolae to produce ROS as a result of Nox1/NoxO1 complexing and form large signaling platforms with FAs at the plasma membrane. Such platforms could also involve Nox4/p22phox

to a lesser extent. It is at these caveolae and FAs that additional signaling molecules could localize and act to prime the uterine contractile apparatus for labour.

Figure 4.1. Proposed phase specific functions of Nox1, Nox4 and associated subunits during the myometrial and immunological transformation that occurs over pregnancy. Increased expression of Nox4/p22phox during the proliferative phase of myometrial differentiation suggests this complex could be actively participating in redox signaling events related to cellular proliferation. Nox1/NoxA1/p22phox to a lesser extent could also be involved in proliferative signaling events since Nox1 was expressed at this time and NoxA1 expression was particularly induced during this period. Coinciding with myometrial proliferation, an inflammatory response is initiated by the maternal immune system in response to pregnancy related oxidative stress. Nox produced ROS are thought to play a role in recruiting immune cells to the uterus. Later in gestation as the uterus prepares for labour, levels of Nox1/NoxO1 rise and Nox4/p22phox are also expressed but to a lesser extent. During this period Nox1 is thought to localize with caveolae, forming large signaling platforms with FAs at the plasma membrane. These platforms could promote localization of additional signaling molecules and act to prime the uterine contractile apparatus prior to labour. Nox, NADPH oxidase; ROS, reactive oxygen species.

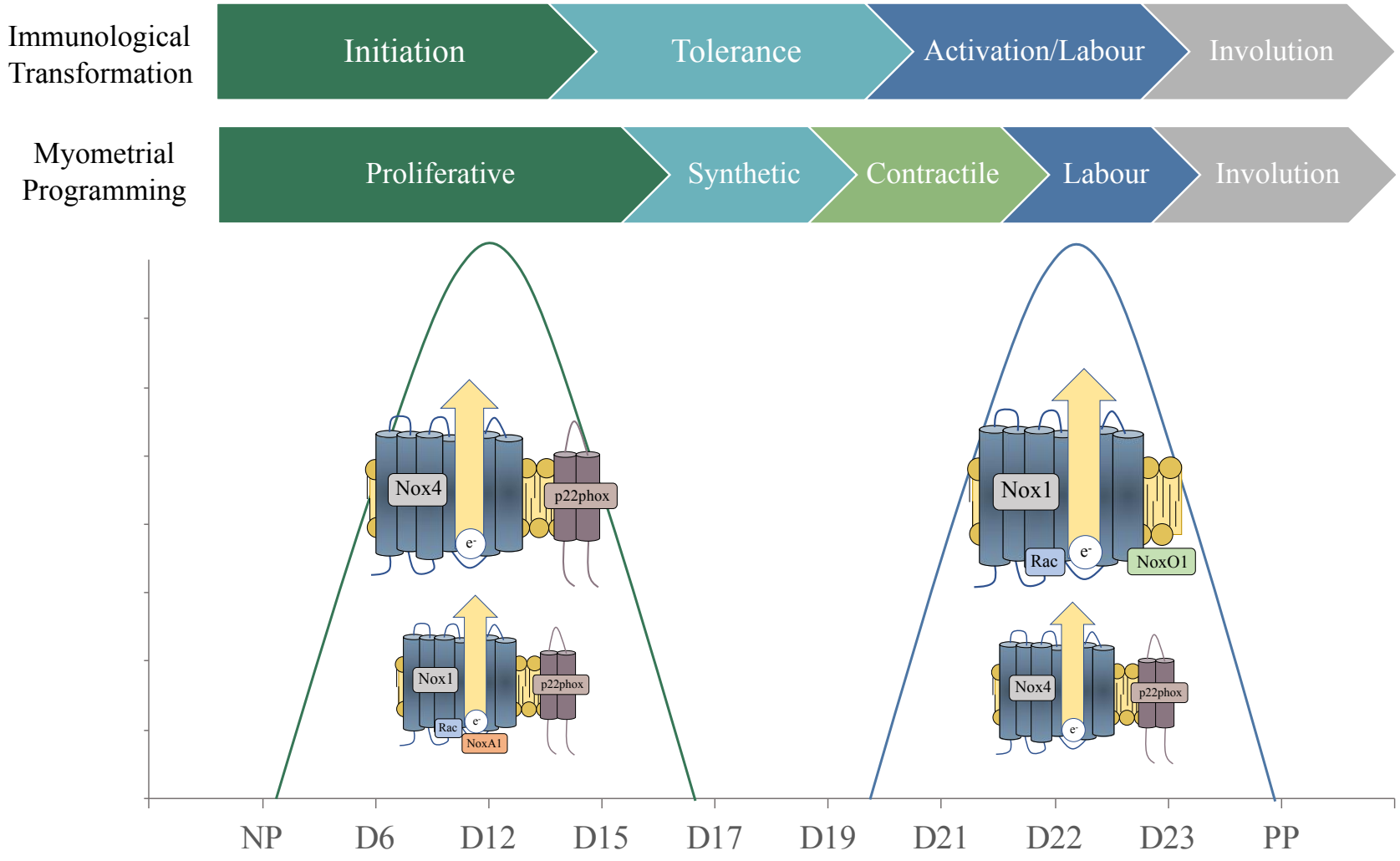
Immunological Transformation
Initiation
Tolerance
Activation/Labour
Involution
Myometrial Programming
Proliferative
Synthetic
Contractile
Labour
Involution
Nox4
p22phox
e-
Nox1
p22phox
Rac
e-
NoxA1
Nox1
Rac
e-
NoxO1
Nox4
p22phox
e-
NP
D6
D12
D15
D17
D19
D21
D22
D23
PP

Appendices

Appendix A

Permission to reproduce Figure. 1.1 as approved by Kevin Rodkin of the Canadian Institute for Health Information.

Thank you, Mikayla Waller, for your request to reproduce the following Canadian Institute for Health Information ("**CIHI**") work:

- Figure 1: "Deliveries for Rural Women as a Percentage of All Deliveries, by Health Region, Selected Provinces/Territories, 2007–2008 to 2011–2012," found on page 2 of "Hospital Births in Canada: A Focus on Women Living in Rural and Remote Areas" (the "**Work**").

Your email informed us that you wish to reproduce the Work in your Master's Thesis, for which you are a candidate at the Western College of Veterinary Medicine (the "**Purpose**").

CIHI is pleased to grant you permission to reproduce the Work for the Purpose under the following conditions:

- You will not use the Work in association with any commercial or promotional activities;
- You make no suggestion that CIHI uses, approves of, or in any way endorses you, your work, your products and/or services, any other person or entity, any other service or product, any cause, and/or any view or opinion;
- You acknowledge CIHI as the source of the Work in association with your use of the Work; and
- You may not alter, modify or otherwise change the Work such that its meaning is in any way misrepresented, concealed, or obscured.

For clarity, the permission granted to you permits you to authorize another person or entity, such as a photocopying or printing company, to make copies of the Work on your behalf.

CIHI and its licensors, if applicable, retain all rights, title and interest in the Work. For the purposes of clarity, you do not obtain ownership or any other right in the Work except as expressly provided above.

The Work is provided as-is and without warranties of any kind, including warranties of fitness for any particular purpose. You will hold CIHI harmless in respect of any losses or damages arising from your use of the Work.

This grant of permission is made under, governed by, and to be construed in accordance with the laws of the Province of Ontario and the applicable laws of Canada, without regard to principles of conflicts of laws.

Kevin

Kevin Rodkin
Program Consultant/Legal Counsel
Privacy and Legal Services
Canadian Institute for Health Information (CIHI)
495 Richmond Road, Suite 600
Ottawa, Ontario K2A 4H6
T: (613) 694-6621
F: (613) 241-8120
krodkin@cihi.ca

Appendix B

Permission to reproduce Figure. 1.6 as approved by the Copyright Clearance Center of the American Physiological Society.

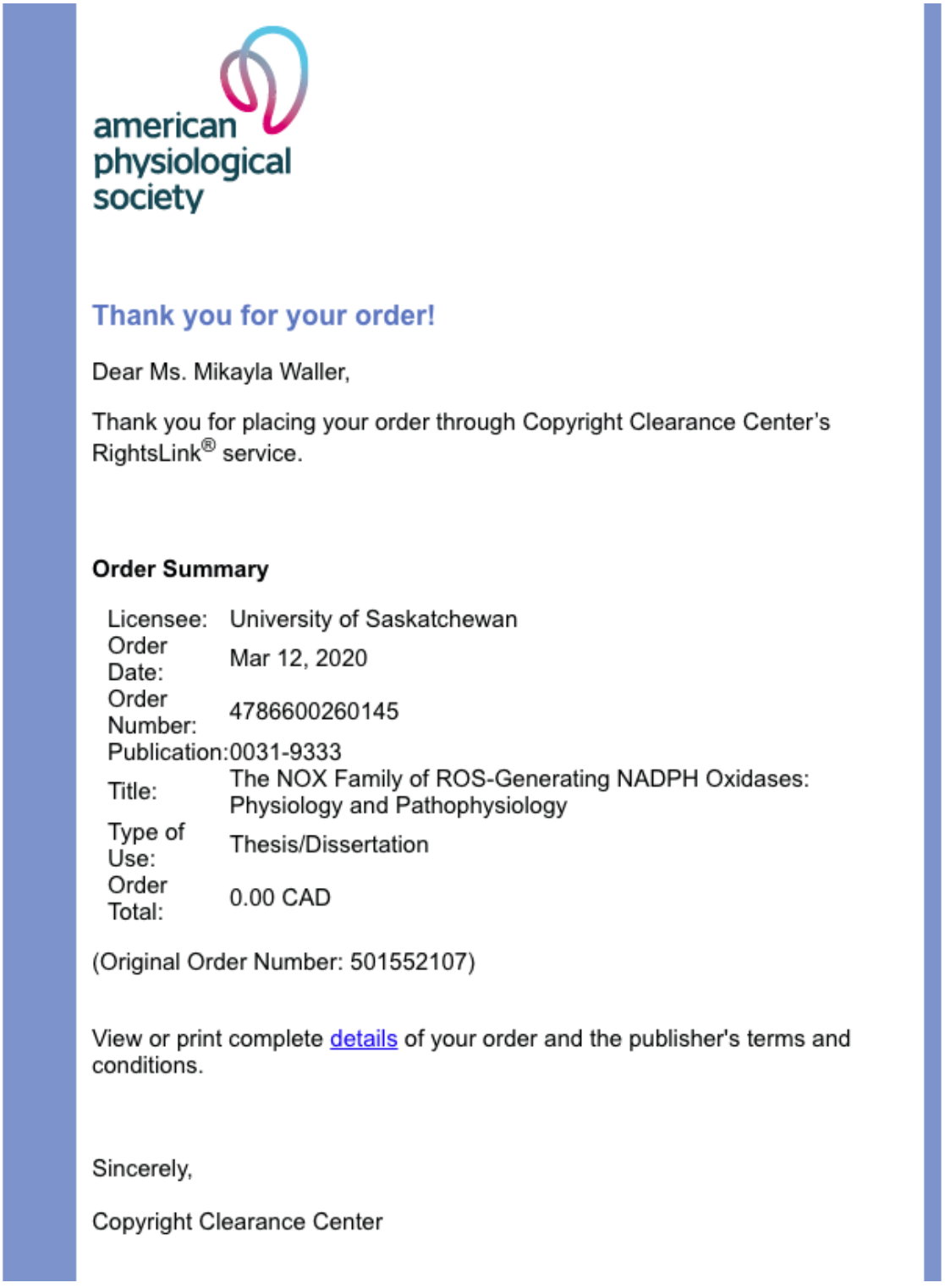

american physiological society

Thank you for your order!

Dear Ms. Mikayla Waller,

Thank you for placing your order through Copyright Clearance Center's RightsLink® service.

Order Summary

Licensee:	University of Saskatchewan
Order Date:	Mar 12, 2020
Order Number:	4786600260145
Publication:	0031-9333
Title:	The NOX Family of ROS-Generating NADPH Oxidases: Physiology and Pathophysiology
Type of Use:	Thesis/Dissertation
Order Total:	0.00 CAD

(Original Order Number: 501552107)

View or print complete details of your order and the publisher's terms and conditions.

Sincerely,

Copyright Clearance Center

Appendix C

BLAST protein alignment of *Homo sapiens* (human) and *Rattus norvegicus* (rat) Nox1 isoforms.

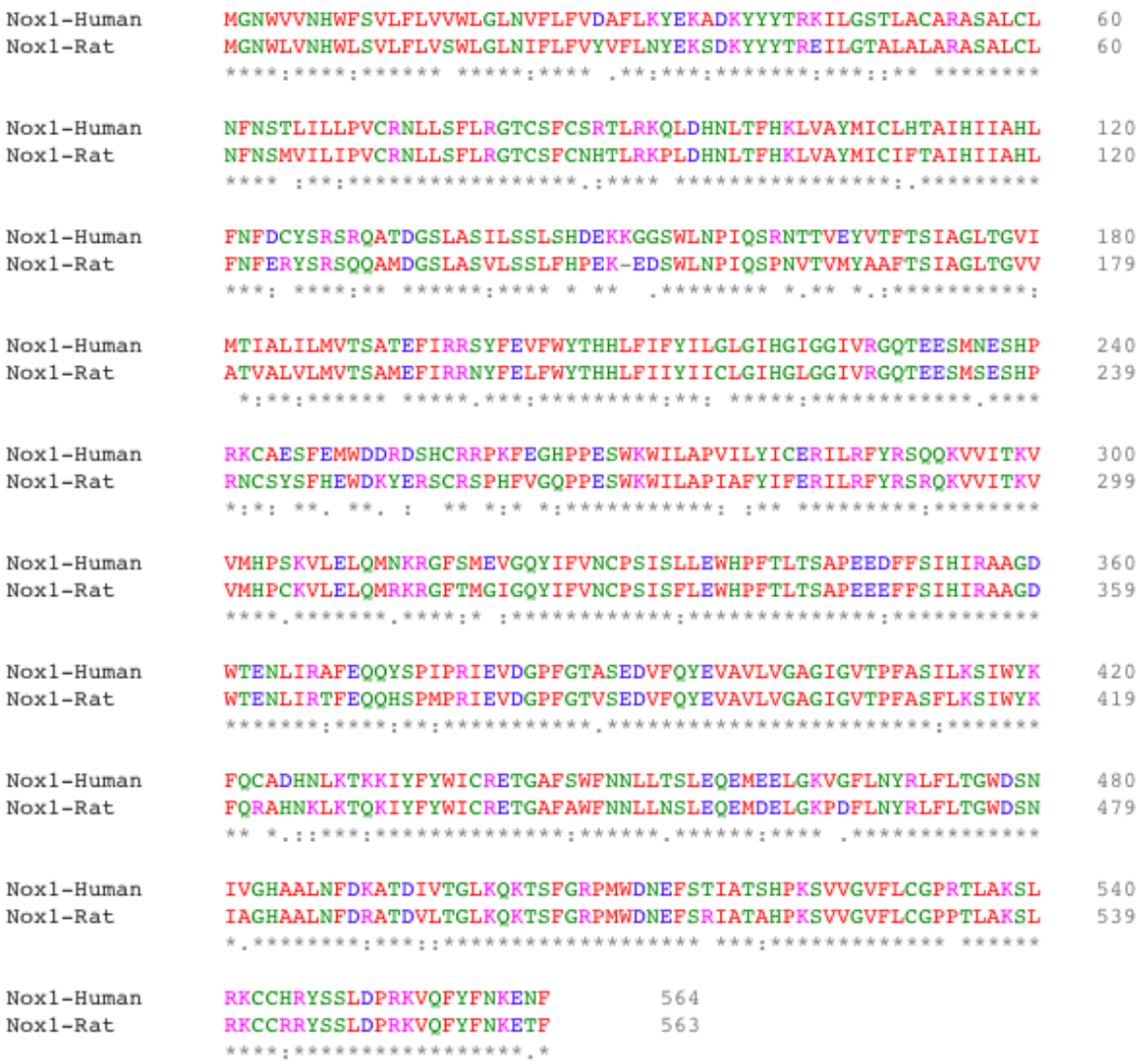

Appendix D

BLAST protein alignment of *Homo sapiens* (human) and *Rattus norvegicus* (rat) Nox4 isoforms.

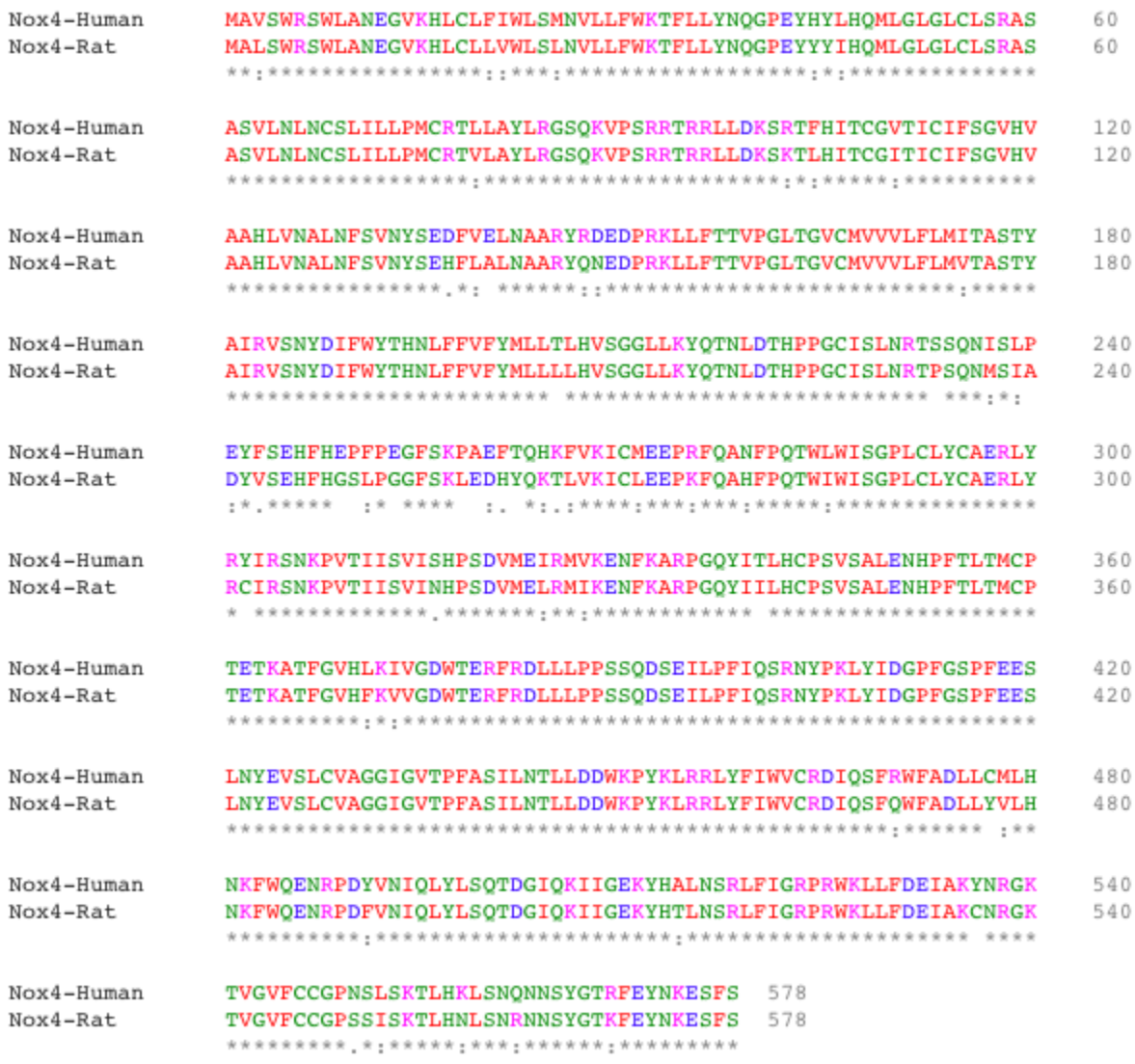

Appendix E

BLAST protein alignment of *Homo sapiens* (human) and *Rattus norvegicus* (rat) NoxO1 isoforms.

```
NoxO1-Human     MAGPRYPVSVQGAALVQIKRLQTFAFSVRWSDGSDTFVRRSWDEFRQLKKTLKETFPVEA   60
NoxO1-Rat       MASPRHPVSAHAVALVQMERLQTFAFSVCWSDNSDTFARRSWEEFRQLQKTLKKIFPVEA   60
                **.**:***.:..****::********* ***.****.****:*****:****: *****

NoxO1-Human     GLLRRSDRVLPKLLGQASLDAPLLGRVGRTSRGLARLQLLETYSRRLLATAERVARSPTI   120
NoxO1-Rat       GLLQRSERVLPKLP-----DAPLLTRRGHTGRGLLRLRLLETYVRSLLATSQHIVTSSTL   115
                ***:**:******      ***** * *:*.*** **:***** * ****:::::. * *:

NoxO1-Human     TGFFAPQPLDLEPALPPGSRVILPTPEEQPLSRAAGRLSIHSLEAQSLRCLQPFCTQDTR   180
NoxO1-Rat       NSFFAPKPLDLEPMLPPGSLVILPTPEE-PLSQPIGSLAIHSLEAQSMRCLQPFHTLDTK   174
                ..****:****** ***** ******** ***:  * *:********:****** * **:

NoxO1-Human     DRPFQAQAQESLDVLLRHPSGWWLVENEDRQTAWFPAPYLEEAAPGQGREGGPSLGSSGP   240
NoxO1-Rat       DRPFHTQAKEILDILLRHPSGWWLVENKDQQTAWFPAPYLEEIATGQGQESGMAVQGSGM   234
                ****::**:* **:**************:*:************ * ***:*.* :: .**

NoxO1-Human     QFCASRAYESSRADELSVPAGARVRVLETSDRGWWLCRYGDRAGLLPAVLLRPEGLGALL   300
NoxO1-Rat       S-------------------------------------------------------------   235
                .

NoxO1-Human     SGTGFRGGDDPAGEARGFPEPSQATAPPPTVPTRPSPGAIQSRCCTVTRRALERRPRRQG   360
NoxO1-Rat       -------------------------------------------------------------   235


NoxO1-Human     RPRGCVDSVPHPTTEQ        376
NoxO1-Rat       ----------------        235
```

Appendix F

BLAST protein alignment of *Homo sapiens* (human) and *Rattus norvegicus* (rat) NoxA1 isoforms.

```
NoxA1-Human     MASLGDLVRAWHLGAQAVDRGDWARALHLFSGVPAPPARLCFNAGCVHLLAGDPEAALRA   60
NoxA1-Rat       MSSLGDQIRDWHRGVLAVAREDWDSALCFFSDVREPLAKMYFNMGCVHLMAGDPEAALRA   60
                *:**** :* ** *. ** * **  ** :**.*  * *:: ** *****:**********

NoxA1-Human     FDQAVTKDTCMAVGFFQRGVANFQLARFQEALSDFWLALEQLRGHAAIDYTQLGLRFKLQ   120
NoxA1-Rat       FDQAVTKDTCMAVGFLQRGVANFQLQRLQEAVSDFQLALAQLRGNAAIDYTQLGLDFKLQ   120
                ***************:********* *:***:*** *** ****:********** ****

NoxA1-Human     AWEVLHNVASAQCQLGLWTEAASSLREAMSKWPEGSLNGLDSALDQVQRRGSLPPRQVPR   180
NoxA1-Rat       AWEVLYNMASVQCQAGLWTKAANTLVEAISKRPEGAQDTLEAAMDKVQKQVPLQLRQVPK   180
                *****:*:**.*** ****:**.:* **:** ***: : *::*:*:**::  *  ****:

NoxA1-Human     GEVFRPHRWHLKHLEPVDFLGKAKVVASAIPDDQGWGVRPQQPQGPGANHDARSLIMDSP   240
NoxA1-Rat       GEVFQPPRRYLKHLEPMDFLGKAKVVASVIPDDHNSDIQPQQSSQVEQAG----LQSSSP   236
                ****:* * :******:**********.****:. .::*** .          *  .**

NoxA1-Human     RAGTHQGPLDAETEVGADRCTSTAYQEQRPQVEQVGKQAPLSPGLPAMGGPGPGPCEDPA   300
NoxA1-Rat       ------------------VCKRVLS------TRGGHMSPGLWDSLLATGGPVPGPSEDSS   272
                                  *. .        ..    .  *  .* * *** ***.** :

NoxA1-Human     GAGGAGAGGSEPLVTVTVQCAFTVALRARRGADLSSLRALLGQALPHQAQLGQLSYLAPG   360
NoxA1-Rat       SAEGTATKDPESLVTVTVQCHFTVPLKVPRGTDLSSFRTLLSQALLQQTQKGQFSYKARG   332
                .* *:.: . * ******** *** *:. **:****:*:**.*** :*:* **:** * *

NoxA1-Human     EDGHWVPIPEEESLQRAWQDAAACPRGLQLQCRGAGGRPVLYQVVAQHSYSAQGPEDLGF   420
NoxA1-Rat       EDRAWVPISTEDSLQSVWRNVPVSPRGLQLQCRGAWGRPVLYQVVAQYDYRAQRPEDLDF   392
                **  ****  *:*** .*::. ..********** **********:.* ** ****.*

NoxA1-Human     RQGDTVDVLCEVDQAWLEGHCDGRIGIFPKCFVVPAGPRMSGAPGRLPRSQQGDQP       476
NoxA1-Rat       RQGDTVDVLCEVDEAWLEGHRDGRVGIFPKCFVVPAATCVEALPVPEPQ--PGEQH       446
                *************:****** ***:**********.  :.. *   *:   *:*
```

Appendix G

BLAST protein alignment of *Homo sapiens* (human) and *Rattus norvegicus* (rat) p22phox isoforms.

Appendix H

Permission to reproduce Figure. 1.9 as approved by Karen Ballen of LiebertPub.

Dear Mikayla:

Copyright permission is granted to use the requested figure in your Master's Thesis. Please give proper credit to the journal and to the publisher.

Kind regards,
Karen Ballen
Manager, Reprints/ePrints, Permissions, and Liebert Open Access
Mary Ann Liebert, Inc.
New Rochelle, NY

References

Ago T, Kitazono T, Kuroda J, Kumai Y, Kamouchi M, Ooboshi H, Wakisaka M, Kawahara T, Rokutan K, Ibayashi S, and Iida M. 2005. NAD(P)H oxidases in rat basilar arterial endothelial cells. Stroke 36:1040–1046.

Aguado A, Fischer T, Rodriguez C, Manea A, Martinez-Gonzalez J, Touyz RM, Hernanz R, Alonso MJ, Dixon DA, Briones AM, and Salaices M. 2016. HuR is required for NOX-1 but not NOX-4 regulation by inflammatory stimuli in vascular smooth muscle cells. J Hypertens 34:253-265.

Al-Matubsi HY, Eis ALW, Brodt-Eppley J, MacPhee DJ, Lye S, and Myatt L. 2001. Expression and localization of the contractile prostaglandin F receptor in regnant rat myometrium in late gestation, labour, and postpartum. Biol Repro. 64:1029-1037.

Ambasta RK, Kumar P, Griendling KK, Schmidt HH, Busse R, and Brandes RP. 2004. Direct interaction of the novel Nox proteins with p22phox is required for the formation of a functionally active NADPH oxidase. J Biol Chem 279:45935–45941.

Ambasta RK, Schreiber JG, Janiszewski M, Busse R, and Brandes RP. 2006. Noxa1 is a central component of the smooth muscle NADPH oxidase in mice. Free Radic Biol Med 41:193–201.

Andrews WW, Goldenberg RL, Mercer B, Iams J, Meis P, Moawad A, Das A, Vandorsten JP, Caritis SN, Thurnau G, Miodovnik M, Roberts J, and McNellis D. 2000. The preterm prediction study: association of second-trimester genitourinary Chlamydia infection with subsequent spontaneous preterm birth. Am J Obstet Gynecol 183:662-668.

Arakawa N, Katsuyama M, Matsuno K, Urao N, Tabuchi Y, Okigaki M, Matsubara H, and Yabe-Nishimura C. 2006. Novel transcripts of NOX1 is regulated by alternative promoters and expressed under phenotypic modulation of vascular smooth muscle cells. Biochem J 398:303-310.

Bailey G. 2020. Assessment of Heat Shock Protein Expression in Human Myometrial Cells under Pro-Inflammatory Conditions and Presence in Extracellular Vesicles. MSc Thesis. Department of Veterinary Biomedical Sciences, University of Saskatchewan.

Banfi B, Clark RA, Steger K, and Krause KH. 2003. Two novel proteins activate superoxide generation by the NADPH oxidase NOX1. J Biol Chem 278:3510–3513.

Banfi B, Malgrange B, Knisz J, Steger K, Dubois-Dauphin M, and Krause KH. 2004. NOX3: a superoxide-generating NADPH oxidase of the inner ear. J Biol Chem 279:46065–46072.

Bedard K, and Krause KH. 2007. The NOX Family of ROS-Generating NADPH Oxidases: Physiology and Pathophysiology. Physiol Rev 87:245-313.

Bengtsson B, Chow EMH, and Marshall JM. 1984. Calcium dependency of pregnant rat myometrium: comparison of circular and longitudinal muscle. Biol Reprod 30:869-878.

Bezold KY, Karjalainen MK, Hallman M, Teramo K, and Muglia LJ. 2013. The genomics of preterm birth: from animal models to human studies. Genome Med 5:34.

Blaser H, Dostert C, Mak TW, and Brenner D. 2016. TNF and ROS crosstalk in Inflammation. Trends in Cell Biol 26:249-261.

Block K, and Gorin Y. 2012. Aiding and abetting roles of NOX oxidases in cellular transformation. Nat Rev Cancer 12:627-637.

Boroditsky RS, Reyes FI, Winter JS, and Faiman C. 1978. Maternal serum estrogen and progesterone concentrations preceding normal labour. Obstet Gynecol 51:686-691.

Brandes RP, Weissmann N, and Schroder K. 2014. Nox family NADPH oxidases: Molecular mechanisms of activation. Free Radic Biol Med 76:208-226.

Brown DI, and Griendling KK. 2009. Nox proteins in signal transduction. Free Radic Biol Med 47:1239-1253.

Burgoyne JR, Madhani M, Cuello F, Charles RL, Brennan JP, Schroder E, Browning DD, and Eaton P. 2007. Cysteine Redox Sensory in PKGIα Enables Oxidant-Induced Activation. Science 317:1393-1397.

Burkin HR, Rice M, Sarathy A, Thompson S, Singer CA, and Buxton ILO. 2013. Integrin upregulation and localization to focal adhesion sites in pregnant human myometrium. Reprod Sci 20:804-812.

Cai H. 2005. Hydrogen peroxide regulation of endothelial function: Origins, mechanisms, and consequences. Cardiovasc Res 68:26-36.

Callera G, Montezano A, Yogi A, Tostes R, and Touyz R. 2007. Vascular signaling through cholesterol-rich domains: implications in hypertension. Curr Opin Nephrol Hypertens 16:90-104.

Cardenas I, Means RE, Aldo P, Koga K, Lang SM, and Booth CJ. 2010. Viral infection of the placenta leads to fetal inflammation and sensitization to bacterial products predisposing to preterm labor. J Immunol 185:1248-1257.

Chabrashvili T, Tojo A, Onozato ML, Kitiyakara C, Quinn MT, Fujita T, Welch WJ, and Wilcox CS. 2002. Expression and cellular localization of classic NADPH oxidase subunits in the spontaneously hypertensive rat kidney. Hypertension 39:269-274.

Challis JRG, Sloboda DM, Alfaidy N, Lye SJ, Gibb W, Patel FA, Whittle WL, and Newnham JP. 2002. Prostaglandins and mechanisms of preterm birth. Reproduction 124:1-17.

Cheng G, Cao Z, Xu X, Meir EG, and Lambeth JD. 2001. Homologs of gp91phox: cloning and tissue expression of Nox3, Nox4, Nox5. Gene 269:131–140.

Cheng G, and Lambeth JD. 2004. NOXO1, Regulation of Lipid Binding, Localization, and Activation of Nox1 by the Phox Homology (PX) Domain. J Biol Chem 279:4737- 4742.

Cheng G, and Lambeth JD. 2005. Alternative mRNA splice forms of NOXO1: differential tissue expression and regulation of Nox1 and Nox3. Gene 356:118–126.

Cheng G, Diebold BA, Hughes Y, and Lambeth JD. 2006. Nox1-dependent Reactive Oxygen Generation Is Regulated by Rac1. J Biol Chem 281:17718-17726.

CIHI (Canadian Institute for Health Information). 2013. Hospital Births in Canada: A Focus on Women Living in Rural and Remote Areas. Ottawa, ON.

Clempus RE, Sorescu D, Dikalova AE, Pounkova L, Jo P, Sorescu GP, Schmidt HH, Lassegue B, Griendling KK. 2007. Nox4 is required for maintenance of the differentiated vascular smooth muscle cell phenotype. Arterioscler Thromb Vasc Biol 27:42–48.

Condon J, Yin S, Mayhew B, Word RA, Wright WE, Shay JW and Rainey WE. 2002. Telomerase immortalization of human myometrial cells. Biol Reprod 67:506–514.

Cretoiu SM, Cretoiu D, Marin A, Radu BM and Popescu LM. 2013. Telocytes: ultrastructural, immunohistochemical and electrophysiological characteristics in human myometrium. Reproduction 145:357-370.

Croke JM, Pike LRG, and MacPhee DJ. 2007. The focal adhesion protein Hic-5 is highly expressed in the rat myometrium during later pregnancy and labour and co-localizes with FAK. Reprod Biol Endocrinol 5:22.

Cuevas KD, Silver DR, Brooten D, Youngblut JM, and Bobo CM. 2005. The Cost of Prematurity: Hospital Charges at Birth and Frequency of Rehospitalizations and Acute Care Visits over the First Year of Life: A Comparison by Gestational Age and Birth Weight. Am J Nurs 105:56–64.

Cui XL, Brockman D, Campos B, and Myatt L. 2006. Expression of NADPH oxidase isoform 1 (Nox1) in human placenta: involvement in preeclampsia. Placenta 27:422–431.

Cui XL, Chang B, and Myatt L. 2010. Expression and Distribution of NADPH Oxidase Isoforms in Human Myometrium—Role in Angiotensin II-induced Hypertrophy1. Biol Reprod 82:305–312.

Dallenbach-Hellweg G. 1981. The Normal Histology of the Endometrium. In: Histopathology of the Endometrium. Springer, Berlin, Heidelberg.

Day RM, and Suzuki YJ. 2006. Cell proliferation, reactive oxygen and cellular glutathione. Dose Response 3:425-442.

De Deken X, Wang D, Many MC, Costagliola S, Libert F, Vassart G, Dumont JE, and Miot F. 2000. Cloning of two human thyroid cDNAs encoding new members of the NADPH oxidase family. J Biol Chem 275:23227–23233.

Dekel N, Gnainsky Y, Granot I, and Mor G. 2010. Inflammation and implantation. Am J Reprod Immunol 63:17–21.

Diebold BA, Wilder SG, De Deken X, Meitzler JL, Doroshow JH, McCoy JW, Zhu Y, and Lambeth D. 2019. Guidelines for the Detection of NADPH Oxidases by Immunoblot and RT-qPCR. Methods Mol Biol 1982: 191-299.

Dutta EH, Behnia F, Boldogh I, Saade GR, Taylor BD, Kacerovsky M, and Menon R. 2016. Oxidative stress damage-associated molecular signaling pathways differentiate spontaneous preterm birth and preterm premature rupture of the membranes. Mol Hum Reprod 22:143-157.

Ellmark SH, Dusting GJ, Fui MN, Guzzo-Pernell N, and Drummond GR. 2005. The contribution of Nox4 to NADPH oxidase activity in mouse vascular smooth muscle. Cardiovasc Res 65:495–504.

Ferguson KK, McElrath TF, Chen YH, Loch-Caruso R, Mukherjee B, and Meeker JD. 2015. Repeated measures of urinary oxidative stress biomarkers during pregnancy and preterm birth. Am J Obstet Gynecol 212:208.e1-208.e8.

Fernandez I, Martin-Garrido A, Zhou DW, Clempus R.E, Seidel-Rogol B, Valdivia A, Lassegue B, Garcia, AJ, Griendling KK, and San Martin A. 2015. Hic-5 mediates TGFB-induced adhesion in vascular smooth muscle cells by a Nox4-dependent mechanism. Arterioscler Thromb Vasc Biol 35:1198–1206.

Fest S, Aldo PB, Abrahams VM, Visintin I, Alvero A, Chen R, Chavez SL, Romero R, and Mor G. 2007. Trophoblast–Macrophage Interactions: Regulatory Network for the Protection of Pregnancy. Am J Reprod Immunol 57:55–66.

Flaherty JP, Spruce CA, Fairfield HE, and Bergstrom DE. 2010. Generation of a Conditional Null Allele of NADPH Oxidase Activator 1 (Noxa1). Genesis 48:568-575.

Fletcher NM, Saed MG, Abuanzeh A, Abu-Soud HM, Al-Hendy A, Diamond MP, and Saed GM. 2014. Nicotinamide Adenine Dinucleotide Phosphate Oxidase is Differentially Regulated in Normal Myometrium Versus Leiomyoma. Reprod Sci 21:1145-1152.

Furmanik G, Chatrou M, Willems B, van Gorp R, Schmidt H, van Eys G, Bochaton-Pialat ML, Proudfoot D, Biessen E, Hedin U, Perisic Matic L, Mees B, Shanahan C, Reutelingsperger C, and Schurgers L. 2020. Reactive Oxygen-Forming Nox5 Links Vascular Smooth Muscle Cell Phenotypic Switching and Extracellular Vesicle-Mediated Vascular Calcification. Circ Res 127:203-329.

Gabella G. 1990. Hypertrophy of visceral smooth muscle. Anat Embryol 182:409–424.

Garfield JRE, Sims SM, Kannan MS, and Daniel EE. 1978. Possible role of gap junctions in activation of myometrium during parturition. Am J Physiol 235:168-179.

Gavazzi G, Banfi B, Deffert C, Fiette L, Schappi M, Herrmann F, and Krause KH. 2005. Decreased blood pressure in NOX1-deficient mice. FEBS Lett 580:497-504.

Geiszt M, Kopp JB, Varnai P, and Leto TL. 2000. Identification of renox, an NAD(P)H oxidase in kidney. Proc Natl Acad Sci USA 97:8010– 8014.

Gibb W, Lye SJ, and Challis JRG. 2006. Parturition. In Knobil and Neill's physiology of reproduction. Edited by Neill JD. New York: Academic Press. 2925-2974.

Goldenberg RL, Mercer BM, Meis PJ, Copper RL, Das A, and McNellis D. 1996. The preterm prediction study: fetal fibronectin testing and spontaneous preterm birth. Obstet Gynecol 87:643-648.

Goldenberg RL, and Culhane JF. 2005. Prepregnancy health status and the risk of preterm delivery. Arch Pediatr Adolesc Med 159:89–90.

Goldenberg RL, Goepfert AR, and Ramsey PS. 2005. Biochemical markers for the prediction of preterm birth. Am J Obstet Gynecol 192:S36–46.

Goldenberg RL, Culhane JF, Iams JD, and Romero R. 2008. Epidemiology and causes of preterm birth. Lancet. 371:75–84.

Golightly E, Jabbour HN, and Norman JE. 2011. Endocrine immune interactions in human parturition. Mol Cell Endocrinol 335:52-59.

Gondos B. 1985. Development of the Reproductive Organs. Ann Clin Lab Sci 15:363-373.

Gray DJ, Robinson HB, Malone J, and Thomson RB. 1992. Adverse outcome in pregnancy following amniotic fluid isolation of Ureaplasma urealyticum. Prenat Diagn 12:111-117.

Griendling KK, Sorescu D, and Ushio-Fukai M. 2000. NAD(P)H oxidase: role in cardiovascular biology and disease. Circ Res 86:494–501.

Gupta S, Agarwal A, Banerjee J, and Alvarez J. 2007. The role of oxidative stress in spontaneous abortion and recurrent pregnancy loss: a systematic review. Obstet Gynecol Surv 62:335-347.

Hadi T, Bardou M, Mace G, Sicard P, Wendremaire M, Barrichon M, Richaud S, Demidov O, Sagot P, Garrido C, and Lirussi F. 2015. Glutathione prevents preterm parturition and fetal death by targeting macrophage induced reactive oxygen species production in the myometrium. FASEB J 29:2653–2666.

Hahn LA. 2018. The Influence of Pro-Inflammatory Conditions on Heat Shock Protein Expression in Human Myometrial Cells. BSc Honour Thesis, Department of Physiology. University of Saskatchewan.

Hakuno F and Takahashi SI. 2018. 40 Years of IGF1:IGF1 receptor signaling pathways. J Mol Endocrinol 61:T69-T86.

Halgunset J, Johnsen H, Kjollesdal AM, Qvigstad E, Espevik T, and Austgulen R. 1994. Cytokine levels in amniotic fluid and inflammatory changes in the placenta from normal deliveries at term. Eur J Obstet Gynecol Reprod Biol 56:153-160.

Handayaningsih AE, Iguchi G, Fukuoka H, Nishizawa H, Takahashi M, Yamamoto M, Herningtyas EH, Okimura Y, Kaji H, Chihara K, Seino S, and Takahashi Y. 2011. Reactive Oxygen Species Play and Essential Role in IGF-I Signaling and IGF-I-Induced Myocyte Hypertrophy in C2C12 Myocytes. Endocrinology 153:912-921.

Hanks SK, and Polte TR. 1997. Signaling through focal adhesion kinase. Bioessays 19:137-145.

Hanna IR, Hilenski LL, Dikalova A, Taniyama Y, Dikalov S, Lyle A, Quinn MT, Lassegue B, and Griendling KK. 2004. Functional Association of Nox1 with p22phox in Vascular Smooth Muscle Cells. Free Radic Biol Med 37:1542-1549.

Hanna J, Goldman-Wohl D, Hamani Y, Avraham I, Greenfield C, Natanson-Yaron S, Prus D, Cohen-Daniel L, Arnon TI, Manaster I, Gazit R, Yutkin V, Benharroch D, Porgador A, Keshet E, Yagel S, and Mandelboim O. 2006. Decidual NK cells regulate key developmental processes at human fetal-maternal interface. Nat Med 12:1065-1074.

Harder T, and Simons K. 1997. Caveolae, DIGs, and the dynamics of sphingolipid-cholesterol microdomains. Curr Opin Cell Biol 9:534–542.

Hendler I, Goldenberg R, Mercer B, Iams J, Meis P, Moawad A, MacPherson C, Caritis S, Miodovnik M, MenardK, Thurnau G, and Sorokin Y. 2005. The Preterm Prediction study: Association between maternal body mass index and spontaneous and indicated preterm birth. Am J Obstet Gynecol 192:882-886.

Higashi M, Shimokawa H, Hattori T, Hiroki J, Mukai Y, Morlkawa K, Ichiki T, Takahashi S, and Takeshita A. 2003. Long-Term Inhibition of Rho-Kinase Suppresses Angiotensis II-Induced Cardiovascular Hypertrophy in Rats In Vivo. Circ Res 93:767-775.

Hilenski LL, Clempus RE, Quinn MT, Lambeth JD, and Griendling KK. 2004. Distinct subcellular localizations of Nox1 and Nox4 in vascular smooth muscle cells. Arterioscler Thromb Vasc Biol 24:677–683.

Holterman CE, Thibodeau JF, Towaij C, Gutsol A, Montezano AC, Parks RJ, Cooper ME, Touyz RM, and Kennedy CRJ. 2014. Nephropathy and elevated BP in mice with podocyte-specific NADPH oxidase 5 expression. J Am Soc Nephrol 25:784-797.

Hynes RO. 1992. Integrins: versatility, modulation, and signaling in cell adhesion. Cell 69:11-25.

Ikeda S, Yamaoka-Tojo M, Hilenski L, Patrushev NA, Anwar GM, Quinn MT, and Ushio-Fukai M. 2005. IQGAP1 regulates reactive oxygen species-dependent endothelial cell migration through interacting with Nox2. Arterioscler Thromb Vasc Biol 25:2295-2300.

Insel PA, Head BP, Ostrom RS, Patel HH, Swaney JS, Tang CM, and Roth DM. 2005. G Protein–Coupled Receptor Signaling Microdomains in Cardiac Myocytes. Ann NY Acad Sci 1047:166-172.

Jauniaux E, Watson AL, Hempstock J, Bao YP, Skepper JK, and Burton GJ. 2000. Onset of maternal arterial blood flow and placental oxidative stress. A possible factor in human early pregnancy failure. Am J Pathol 157:2111–2122

Jauniaux E, Greenwold N, Hempstock J, and Burton GJ. 2003. Comparison of ultrasonographic and Doppler mapping of the intervillous circulation in normal and abnormal early pregnancies. Fertil Steril 79:100–106

Javeshghani D, Magder SA, Barreiro E, Quinn MT, and Hussain SN. 2002. Molecular characterization of a superoxide-generating NAD(P)H oxidase in the ventilatory muscles. Am J Respir Crit Care Med 165:412–418.

Jones JI, and Clemmons DR. 1995. Insulin-like growth factors and their binding proteins: biological actions. Endocr Rev 16:3–34.

Jones SA, O'Donnell VB, Wood JD, Broughton JP, Hughes EJ, and Jones OT. 1996. Expression of phagocyte NADPH oxidase components in human endothelial cells. Am J Physiol 271:H1626-H1634.

Katagiri S, Moon Y, and Yuen B. 1996. The role for the uterine insulin-like growth factor I in early embryonic loss after superovulation in the rat. Fertil Steril 65:426-436.

Kawahara T, Ritsick D, Cheng G, and Lambeth JD. 2005. Point mutations in the proline-rich region of p22phox are dominant inhibitors of Nox1- and Nox2-dependent reactive oxygen generation. J Biol Chem 280:31859–31869.

Keelan J. 2016. Intrauterine inflammatory activation, functional progesterone withdrawal, and the timing of term and preterm birth. J Reprod Immunol 125:89-99.

Kiss PJ, Knisz J, Zhang Y, Baltrusaitis J, Sigmund CD, Thalmann R, Smith RJH, Verpy E, and Banfi B. 2006. Inactivation of NADPH oxidase organizer 1 Results in Severe Imbalance. Curr Biol 16:208-213.

Lassegue B, Sorescu D, Szocs K, Yin Q, Akers M, Zhang Y, Grant S, Lambeth D, and Griendling K. 2001. Novel gp91phox homologues in vascular smooth muscle cells: nox1 mediates angiotensin II-induced superoxide formation and redox-sensitive signaling pathways. Circ Res 88:888–894.

Leto TL, Lomax KJ, Volpp BD, Nunoi H, Sechler JM, Nauseef WM, Clark RA, Gallin JI, and Malech HL. 1990. Cloning of a 67-kD neutrophil oxidase factor with similarity to a noncatalytic region of p60c-src. Science 248:727–730.

Leto TL, Adams AG, and de Mendez I. 1994. Assembly of the phagocyte NADPH oxidase: binding of Src homology 3 domains to proline-rich targets. Proc Natl Acad Sci USA 91: 10650–10654.

Li S, Seitz R, and Lisanti MP. 1996. Phosphorylation of Caveolin by Src Tyrosine Kinases. The alpha-isoform of caveolin is selectively phosphorylated by v-Src in vivo. J Biol Chem 271:3863-3868.

Lim G, Tracey J, Boom N, Karmakar S, Wang J, Berthelot JM, and Heick C. 2009. CIHI survey: hospital costs for preterm and small-for-gestational age babies in Canada. Healthc Q.12:20-40.

Lye SJ, Nicholson BJ, Mascarenhas M, MacKenzie L, and Petrocelli T. 1993. Increased expression of connexin-43 in the rat myometrium during labor is associated with an increase in the plasma estrogen:progesterone ratio. Endocrinology 132:2380-2386.

Lyle AN, Deshpande NN, Taniyama Y, Seidel-Rogol B, Pounkova L, Du P, Papaharalambus C, Lassègue B, Griendling KK. 2009. Poldip2, a novel regulator of Nox4 and cytoskeletal integrity in vascular smooth muscle cells. Circ Res 105:249–259

MacPhee DJ, and Lye SJ. 2000. Focal Adhesion Signaling in the Rat Myometrium Is Abruptly Terminated with the Onset of Labour. Endocrinology 141:274-283.

Martyn KD, Frederick LM, von Loehneysen K, Dinauer MC, and Knaus UG. 2006. Functional analysis of Nox4 reveals unique characteristics compared to other NADPH oxidases. Cell Signal 18:69-82.

McGregor JA, Hastings C, Roberts T, and Barrett J. 1999. Diurnal variation in saliva estriol level during pregnancy: a pilot study. Am J Obstet Gynecol 180:223-225.

McLean M, Bisits A, Davies J, Walters W, Hackshaw A, De Voss K, and Smith R. 1999. Predicting risk of preterm delivery by second trimester measurement of maternal plasma corticotropin-releasing hormone and alpha-fetoprotein concentrations. Am J Obstet Gynecol 181:207-215.

Menon R. 2008. Spontaneous preterm birth, a clinical dilemma: etiologic, pathophysiologic and genetic heterogeneities and racial disparity. Acta Obstet Gynecol Scand 87:590–600.

Menon R, Bonney EA, Condon J, Mesiano S, and Taylor RN. 2016. Novel concepts on pregnancy clocks and alarms: redundancy and synergy in human parturition. Hum Reprod Update 22:535-560.

Mesiano S, Chang EC, Fitter JT, Kwek K, Teo G, ad Smith R. 2002. Progesterone Withdrawal and Estrogen Activation in Human Parturition Are Coordinated by Progesterone Receptor A Expression in the Myometrium. J Clin Endocrinol Metab 87:2924-2930.

Mesiano S, Wang Y, and Norwitz ER. 2011. Progesterone receptors in the human pregnancy uterus: do they hold the key to birth timing?. Reprod Sci 18:6-19.

Mitra SK, Hanson DA, and Schlaepfer DD. 2005. Focal adhesion kinase: in control and command of cell motility. Nat Rev Mol Cell Biol 6:56-68.

Miyano K, Ueno N, Takeya R, and Sumimoto H. 2006. Direct Involvement of the Small GTPase Rac in Activation of the Superoxide-producing NADPH Oxidase Nox1. J Biol Chem 281:21857-21868.

Moe KT, Aulia S, Jiang F, Chua YL, Koh TH, Wong MC, and Dusting GJ. 2006. Differential upregulation of Nox homologues of NADPH oxidase by tumor necrosis factor-alpha in human aortic smooth muscle and embryonic kidney cells. J Cell Mol Med 10: 231–239.

Moore TA, Ahmad IM, and Zimmerman MC. 2018. Oxidative Stress and Preterm Birth: An Integrative Review. Biol Res Nurs 20:497-512.

Mor G, and Koga K. 2008. Macrophages and pregnancy. Reprod. Sci 15:435–436.

Mor G, Cardenas I, Abrahams V, and Guller S. 2011. Inflammation and pregnancy: the role of the immune system at the implantation site. Ann NY Acad Sci 1221:80-87.

Morgan MJ, and Liu ZG. 2011. Crosstalk of reactive oxygen species and NF-κβ signaling. Cell Res 21:103-115.

Nakano Y, Longo-Guess CM, Bergstrom DE, Nauseef WM, Jones SM, and Banfi B. 2008. Mutation of the Cyba gene encoding p22phox causes vestibular and immune defects in mice. J Clin Invest 118:1176-1185.

Nauseef WM. 2004. Assembly of the phagocyte NADPH oxidase. Histochem Cell Biol 122:277–291.

Navot D, Bergh PA, Williams M, Garrisi GJ, Guzman I, Sandler B, Fox J, Schreiner-Engel P, Hofmann GE, and Grunfeld L. 1991 An insight into early reproductive processes through the in vivo model of ovum donation. J Clin Endocr Metab 72:408–414.

Neulen J, and Breckwoldt M. 1994. Placental progesterone, prostaglandins and mechanisms leading to initiation of parturition in the human. Exp Clin Endocrinol 102:195–202.

Oh JH, You SK, Hwang MK, Ahn DS, Kwon SC, Taggart MJ, and Lee YH. 2003. Inhibition of Rho-associated kinase reduces MLC20 phosphorylation and contractility of intact myometrium and attenuates agonist-induced Ca^{2+} sensitization of force in permeabilized rat myometrium. J Vet Med Sci 65:43-50.

Okamoto T, Schlegel A, Scherer PE, and Lisanti MP. 1998. Caveolins, a family of scaffolding proteins for organizing "preassembled signaling complexes" at the plasma membrane. J Biol Chem 273:5419-5422.

Osman I, Young A, Ledingham MA, Thomson AJ, Jordan F, Greer IA, and Norman JE. 2003. Leukocyte density and pro-inflammatory cytokine expression in human fetal membranes, decidua, cervix and myometrium before and during labour at term. Mol Hum Reprod 9:41–45

Ou CW, Orsino A, and Lye SJ. 1997. Expression of Connexin-43 and Connexin-26 in the Rat Myometrium during Pregnancy and Labor Is Differentially Regulated by Mechanical and Hormonal Signals. Endocrinology 138:5398-5407.

Ou CW, Chen ZQ, Qi S, and Lye SJ.1998. Increased expression of the rat myometrial oxytocin receptor messenger ribonucleic acid during labor requires both mechanical and hormonal signals. Biol Reprod 59:1055-1061.

Petry A, Weitneuer M, and Gorlach A. 2010. Receptor activation of NADPH oxidases. Antioxid Redox Signal 13:467-487.

PHAC (Public Health Agency of Canada). 2017. Perinatal health indicators for Canada 2017: a report of the Canadian Perinatal Surveillance System. Ottawa, ON.

Polettini J, Silva MG, Kacerovsky M, Syed TA, Saade G, and Menon R. 2014. Expression profiles of fetal membrane nicotinamide adenine dinucleotide phosphate oxidases (NOX) 2 and 3 differentiates spontaneous preterm birth and pPROM pathophysiologies. Placenta 35:188-194.

Pryor WA. 1986. Oxy-radicals and related species: their formation, lifetimes, and reactions Annu Rev Physiol 48:657-667.

Ramsey PS, and Andrews WW. 2003. Biochemical predictors of preterm labor: fetal fibronectin and salivary estriol. Clin Perinatol 30:701-733.

Riley M, Wu X, Baker PN, and Taggart MJ. 2005. Gestational-Dependent Changes in the Expression of Signal Transduction and Contractile Filament-Associated Proteins in Mouse Myometrium. J Soc Gynecol Investig 12:e33-e43.

Romero R, Espinoza J, Goncalves LF, Kusanovic JP, Friel LA, and Nien JK. 2006. Inflammation in preterm and term labour and delivery. Semin Fetal Neonatal Med 11:317-326.

Roy K, Wu Y, Meitzler JL, Juhasz A, Liu H, Jiang G, Lu J, Antony S, and Doroshow JH. 2015. NADPH oxidases and cancer. Clin Sci 128:863-875.

Sabry M, and Al-Hendy A. 2012. Medical Treatment of Uterine Leiomyoma. Reprod Sci 19:339-353.

Saigal S, and Doyle LW. 2008. An overview of mortality and sequelae of preterm birth from infancy to adulthood. Lancet 371:261-269.

Salamonsen LA, and Lathbury LJ. 2000. Endometrial leukocytes and menstruation. Hum Reprod Update 6:16–27.

Schaller MD, Borgman CA, Cobb BS, Vines RR, Reynold AB, and Parsons JT. 1992. PP125FAK, a structurally unique protein tyrosine kinase associated with focal adhesions. Proc Natl Acad Sci USA 89:5192–5196.

Schroder K, Zhang M, Benkhoff S, Mieth A, Pliquett R, Kosowski J, Kruse C, Luedike P, Michaelis UR, Weissmann N, Dimmeler S, Shah AM, and Brandes RP. 2012. Nox4 Is a Protective Reactive Oxygen Species Generating Vascular NADPH Oxidase. Circ Res 110:1217-1225.

Schroder K, Weissmann N, and Brandes RP. 2017. Organizers and activators: Cytosolic Nox proteins impacting on vascular function. Free Radic Biol Med 109:22-32.

Shynlova O, Mitchell JA, Tsampalieros A, Langille BL, and Lye SJ. 2004. Progesterone and gravidity differentially regulate expression of extracellular matrix components in the pregnant rat myometrium. Biol Reprod 70:986–992.

Shynlova O, Oldenhof A, Dorogin A, Xu Q, Mu J, Nashman N, and Lye SJ. 2006. Myometrial apoptosis: activation of the caspase cascade in the pregnant rat myometrium at midgestation. Biol Reprod 74:839–849.

Shynlova O, Tsui P, Dorogin A, Langille BL, and Lye SJ. 2007. Insulin-like growth factors and their binding proteins define specific phases of myometrial differentiation during pregnancy in the rat. Biol Reprod 76:571–578.

Shynlova O, Tsui P, Dorogin A, and Lye SJ. 2008. Monocyte chemoattractant protein-1 (CCL-2) integrates mechanical and endocrine signals that mediate term and preterm labor. J Immunol 181:1470–1479.

Shynlova O, Tsui P, Jaffer S, and Lye SJ. 2009a. Integration of endocrine and mechanical signals in the regulation of myometrial functions during pregnancy and labour. Eur J Obstet Gynecol Reprod Biol 144:2–10.

Shynlova O, Chow M and Lye S. 2009b. Expression and Organization of Basement Membrane and Focal Adhesion Proteins in Pregnant Myometrium is Regulated by Uterine Stretch. Repro Sci 16:960-969.

Shynlova O, Kwong R, and Lye SJ. 2010. Mechanical stretch regulated hypertrophic phenotype of the myometrium during pregnancy. Reproduction 139:247-253.

Shynlova O, Nedd-Roderique T, Li Y, Dorogin A, and Lye SJ. 2013a. Myometrial immune cells contribute to term parturition, preterm labour and post-partum involution in mice. J Cell Mol Med 17:90–102.

Shynlova O, Lee YH, Srikhajon K, and Lye SJ. 2013b. Physiologic uterine inflammation and labor onset: Integration of endocrine and mechanical signals. Reprod Sci 20:154–167.

Shynlova O, Nadeem L, Zhang J, and Dunk C. 2020. Myometrial activation: Novel concepts underlying labor. Placenta 92:28-36.

Smith GC, Pell JP, and Dobbie R. 2003. Interpregnancy interval and risk of preterm birth and neonatal death: retrospective cohort study. BMJ 327:313.

Sturrock A, Cahill B, Norman K, Huecksteadt TP, Hill K, Sanders K, Karwande SV, Stringham JC, Bull DA, Gleich M, Kennedy TP, and Hoidal JR. 2005. Transforming growth factor beta-1 induces Nox 4 NAD(P)H oxidase and reactive oxygen species-dependent proliferation in human pulmonary artery smooth muscle cells. Am J Physiol Lung Cell Mol Physiol 290:L661–L673.

Soares MJ, Chakraborty D, Rumi MAK, Konno T, and Renaud S.J. 2012. Rat placentation: An experimental model for investigating the hemochorial maternal-fetal interface. Placenta 33:233–243.

Statistics Canada. 2009a. Census of Population, 1851 to 2011. Ottawa: Statistics Canada; 2012.

Statistics Canada. 2009b. Geography. Ottawa: Statistics Canada; 2012.

Suh YA, Arnold RS, Lassegue B, Shi J, Xu X, Sorescu D, Chung AB, Griendling KK, and Lambeth JD. 1999. Cell transformation by the superoxide-generating oxidase Mox1. Nature 401:79–82.

Taddei ML, Parri M, Mello T, Catalano A, Levine AD, Raugei G, Ramponi G, and Chiarugi P. 2007. Integrin-mediated cell adhesion and spreading engage different sources of reactive oxygen species. Antioxid Redox Signal 9:469-481.

Takeya R, Ueno N, Kami K, Taura M, Kohjima M, Izaki T, Nunoi H, and Sumimoto H. 2003. Novel human homologues of p47phox and p67phox participate in activation of superoxide-producing NADPH oxidases. J Biol Chem 278:25234–25246.

Tamura T, Goldenberg R, Freeberg L, Cliver S, Cutter G, and Hoffman H. 1992. Maternal serum folate and zinc concentrations and their relationship to pregnancy outcome. Am J Clin Nutr 56:365-370.

Tan H, Yi L, Rote NS, Hurd WW, and Mediano S. 2012. Progesterone receptor-A and -B Have Opposite Effects on Proinflammatory Gene Expression in Human Myometrial Cells: Implications for Progesterone Actions in Human Pregnancy and Parturition. J Clin Endocrinol Metab 97:E719-E730.

Thomson AJ, Telfer JF, Young A, Campbell S, Stewart CJ, Cameron IT, Greer IA, and Norman JE. 1999. Leukocytes infiltrate the myometrium during human parturition: further evidence that labour is an inflammatory process. Hum Reprod 14:229–236.

Tornblom SA, Klimaviciute A, Bystrom B, Chromek M, Brauner A, and Ekamn-Ordeberg G. 2005. Non-infected preterm parturition is related to increased concentrations of IL-6, IL-8 and MCP-1 in human cervix. Reprod Biol Endocr 3:39.

Tucker JM, Goldenberg RL, Davis RO, Copper RL, Winkler CL, and Hauth JC. 1991. Etiologies of preterm birth in an indigent population: is prevention a logical expectation? Obstet Gynecol 77:343–47.

Turi A, Kiss AL, and Mullner N. 2001. Estrogen Downregulated the Number of Caveolae and the Level of Caveolin in Uterine Smooth Muscle. Cell Biol Int 25:785-795.

Ushio-Fukai M, Griendling KK, Becker PL, Hilenski L, Halleran S, and Alexander RW. 2001. Epidermal growth factor receptor transactivation by angiotensin II requires reactive oxygen species in vascular smooth muscle cells. Arterioscler Thromb Vasc Biol 21:489–495.

Ushio-Fukai M. 2009. Compartmentalization of Redox Signaling Through NADPH Oxidase–Derived ROS. Antioxid Redox Signal 11:1289–1299.

Vallet P, Charnay Y, Steger K, Ogier-Denis E, Kovari E, Herrmann F, Michel JP, and Szanto I. 2005. Neuronal expression of the NADPH oxidase NOX4, its regulation in mouse experimental brain ischemia. Neuroscience 132:233–238.

Van Buul JD, Fernandez-Borja M, Anthony EC, and Hordijk PL. 2005. Expression and localization of NOX2 and NOX4 in primary human endothelial cells. Antioxid Redox Signal 7:308–317.

Verguts J, Ameye L, Bourne T, and Timmerman D. 2013. Normative data for uterine size according to age and gravidity and possible role of the classical golden ratio. Obstet Gynecol 4:713-717.

Vilhardt F and van Deurs B. 2004. The phagocyte NADPH oxidase depends on cholesterol-enriched membrane microdomains for assembly. EMBO J 23:739-748.

Wendremaire M, Hadi T, Pezze M, Barrichon M, Lopez T, Neiers F, Sagot P, Garrido C, and Lirussi F. 2020. Macrophage-induced reactive oxygen species promote myometrial contraction and labor-associated mechanisms. Biol Reprod 102:1326-1339.

White BG, Williams SJ, Highmore K, and MacPhee DJ. 2005. Small heat shock protein 27 (Hsp27) expression is highly induced in rat myometrium during late pregnancy and labour. Reproduction 129:115-126.

White BG and MacPhee DJ. 2011. Distension of the uterus induces HspB1 expression in rat uterine smooth muscle. Am J Physiol Regul Integr Comp Physiol 301:R1418-R1426.

WHO. 1977. WHO: recommended definitions, terminology and format for statistical tables related to the perinatal period and use of a new certificate for cause of perinatal deaths. Modifications recommended by FIGO as amended October 14, 1976. Acta Obstet Gynecol Scand 56:247–53.

Williams SJ, White BG, and MacPhee DJ. 2005. Expression of α_5 integrin (Itga5) is elevated in the rat myometrium during late pregnancy and labour: implication for development of a mechanical syncytium. Biol Reprod 72:1114-1124.

Williams PJ, Searle RF, Robson SC, Innes BA, and Bulmer JN. 2009. Decidual leukocyte populations in early to late gestation normal human pregnancy. J Reprod Immunol 82:24-31.

Williams SJ, Shynlova O, Lye SJ, and MacPhee DJ. 2010. Spatiotemporal expression of α_1, α_3, and β_1 integrin subunits is altered in rat myometrium during pregnancy and labour. Reprod Fertil Dev 22:718-732.

Winick M and Noble A. 1965. Quantitative changes in DNA, RNA and protein during prenatal and postnatal growth in the rat. Dev Biol 12:451-466.

Wray S and Arrowsmith S. 2012. Uterine smooth muscle. In: Muscle. Academic Press. Boston, MA, USA. Hill JA and Olson EN. 1207-1216.

Yang D, Elner SG, Bian ZM, Till GO, Petty HR, and Elner VM. 2007. Pro-inflammatory Cytokines Increase Reactive Oxygen Species through Mitochondria and NADPH Oxidase in Cultured RPE Cells. Exp Eye Res 85:462-472.

Yang F, Zheng Q, and Jin L. 2019. Dynamic Function and Composition Changes of Immune Cells During Normal and Pathological Pregnancy at the Maternal-Fetal Interface. Front Immunol 10:2317.

Young A, Thomson AJ, Ledingham M, Jordan F, Greer IA, and Norman JE. 2002. Immunolocalization of proinflammatory cytokines in myometrium, cervix, and fetal membranes during human parturition at term. Biol Reprod 66:445–449.

Young RC. 2007. Myocytes, myometrium, and uterine contractions. Ann NY Acad Sci 1101:72-84.

Zamir E, and Geiger B. 2001. Molecular complexity and dynamics of cell-matric adhesions. J Cell Sci 114:3583-3590.

Zhou S, Yi T, Shen K, Zhang B, Huang F, and Zhao X. 2011. Hypoxia: the driving force of uterine myometrial stem cells differentiation into leiomyoma cells. Med Hypotheses 77:985-986.

Zuo L, Ushio-Fukai M, Hilenski LL, and Alexander RW. 2004. Microtubules regulate angiotensin II type 1 receptor and Rac1 localization in caveolae/lipid rafts: role in re- dox signaling. Arterioscler Thromb Vasc Biol 24:1223–1228.

Zuo L, Ushio-Fukai M, Ikeda S, Hilenski L, Patrushev N, and Alexander RW. 2005. Caveolin-1 is essential for activation of Rac1 and NAD(P)H oxidase after angiotensin II type 1 re-ceptor stimulation in vascular smooth muscle cells: role in redox signaling and vascular hypertrophy. Arterioscler Thromb Vasc Biol 25:1824–1830.